ANALYSIS AND DESIGN OF NON RECURSIVE DIGITAL DIFFERENTIATORS IN FRACTIONAL DOMAIN FOR SIGNAL PROCESSING APPLICATIONS

Thesis submitted
in fulfillment of the requirement for the award of degree
of

DOCTOR OF PHILOSOPHY

Submitted by

SANJAY KUMAR

REG. NO. 950906014

UNDER THE SUPERVISION OF

PROF. (Dr.) RAJIV SAXENA,
JAYPEE UNIVERSITY OF ENGINEERING AND TECHNOLOGY,
RAGHOGARH, GUNA (M.P.).

Dr. KULBIR SINGH,
THAPAR UNIVERSITY,
PATIALA (PUNJAB).

DEPARTMENT OF ELECTRONICS AND COMMUNICATION ENGINEERING
THAPAR UNIVERSITY,
PATIALA-147004

ॐ अज्ञान तिमिरान्धस्य ज्ञानाञ्जनशलाकया।
चक्षुरुन्मीलितं येन तस्मै श्री गुरवे नमः॥

I was born in the darkest ignorance, and my spiritual master opened my eyes with the torch of knowledge. I offer my respectful obeisances unto him.

Bhagavad–Gītā

CERTIFICATE

Certified that the thesis entitled "**Analysis and Design of Non Recursive Digital Differentiators in Fractional Domain for Signal Processing Applications**" being submitted by **Mr. Sanjay Kumar** to the **Department of Electronics and Communication Engineering, Thapar University, Patiala** in fulfillment of the requirements for the award of degree of "**Doctor of Philosophy**" is a record of bonafide research work carried out by him. He has worked under our guidance and supervision and fulfilled the requirements for the submission of this thesis which has reached the requisite standard. The matter presented in this thesis does not incorporate any material previously published or written by any other person except where due reference is made in the text.

The results obtained in this thesis have not been submitted in part or full to any other institute or university for the award of degree or diploma.

(Dr. Rajiv Saxena)
Professor and Head ECED,
Jaypee University of Engineering and Technology,
Guna, Madhya Pradesh, 473 226,
India.

(Dr. Kulbir Singh)
Associate Professor, ECED,
Thapar University,
Patiala, Punjab, 147 001,
India.

ACKNOWLEDGMENTS

First and foremost, I am very thankful to my Almighty *Shri Hari* for *His* blessings, without *Him* I would be helpless and void of energy and intelligence. I am very grateful to *Him* for creating this wonderful and beautiful world and the knowledgeable society. Full of thanks are due, for always keeping an eye on me and protecting me always even if I did not deserve it.

I would like to express my sincere gratitude to my research advisors, Professor Rajiv Saxena and Dr. Kulbir Singh for their support and guidance during the course of my study. They have always being willing to give me insights and pointers to tackle the problems along the way keeping very keen interest in listening to my problems. They were always there when I needed to see them and attentive when I spoke with them. My respect for them grew and will always grow throughout my entire life. As my advisors, they were always there for me and had my best interests at heart. They always pointed me in the right direction when I lost the path and supported me when I was in the right path. In addition to being my mentors, they have also been good friends and nice human beings to me.

I would also like to thank the facilities provided by Thapar University for the successful study. Also my completion of acknowledgment remains void without thanking my head of the department Professor Rajesh Khanna, senior faculty members Professor A. K. Chatterjee, Professor Sanjay Kumar Sharma, Dr. Alpana Agarwal, Mrs. Manu Bansal and my friends in the department and outside department Professor Abhay Mishra, Professor Rajshree Mishra, Dr. Rajesh Kumar Gupta, Ashutosh Kumar Tiwari, Mayank Kumar Rai, Dr. Ashutosh Kumar Singh, Dr. Hem Dutt Joshi, Mr. Krishna Murari, Shirish Tripathi, Deependra Sharma, Pradeep Teotia, Capt. Mohit Khattri, Vineet Khattri, Aashish Sharma for making my time cheerful, funny and enjoyable. I also bow my head in front of Madam Saxena Jee for giving me very kind attention and taking care of me as and when required.

A very special and heartful thanks to Professor Rajiv Saxena. Inspite of very busy schedule, he is very cheerful and encouraging person. As a mentor, he used to share his all experiences with me with very great interest. When I used to have a telephonic conversation with

him, I have always felt very delighted to talk with him. I have not seen such a person in my life who is very easy in the technical discussions via telephone. One very important and nice thing I want to share about him with you all is that you will get the feeling that you are in the hand of a very careful and fatherly person. By listening to his voice, you'll feel very energetic and full of energy and confidence that you can solve every problem in life and research with ease. I am also very thankful to Dr. Kulbir Singh, who made me introduce to Professor Saxena. He had inspired me in every segment of my study. Lastly, I would like to add that my mentors are such persons that are willing to take the bullet for me when things don't work out.

I am also thankful to various researchers of the world who are engaged in sharing their experienced knowledge in the web communities of ResearchGate, LinkedIn, Academia.edu, and others.

Lastly, I would like to thank my family for their love, encouragement and support. For my dearest parents who raised me with a love of science and supported me in all my pursuits. They always wanted me to study more and more and do best for the society. The presence of my parents–in–law, brothers and sisters in every endeavor of my life is also very supporting and loving.

The best outcome from these striving years is finding my best friend, soul–mate and wife. She is the only person who can appreciate my quirkiness and sense of humor. She has been very true, supportive and faithful during my best and worst times. When I did not have faith in me, she was there to instrument my confidence. Thank you so much to all my dearest.

♫ *When writing the Story of Your Life, don't Let anyone else hold the pen* ♫

!! *Jai Shri Radhe Radhe* !!

Sanjay Kumar
Thapar University, Patiala
2013

ABSTRACT

There is a universe of mathematics lying in between

the complete differentiations and integrations.

— O. Heaviside.

THE PURPOSE OF THE REPORTED WORK is to provide a comprehensive and unified introduction to the principles and applications of the differentiation property in the fractional Fourier transform domain. The fractional Fourier transform (FrFT) is a generalized definition of the classical Fourier transform (FT). The FrFT has proved to be a powerful tool for the analysis of time–varying signals by representing rotation of a signal in the time–frequency plane. In the areas where FT and the frequency domain concepts are used, the performance can be enhanced through the use of FrFT. In addition, it has a close relationship with other signal transforms like wavelet, linear canonical transform.

The well–known properties of the FrFT have been established in many of the rich literatures, which have many applications in the signal and image processing fields. In the reported work, the concept of fractional order differentiation property in the FrFT domain is established.

Keeping an eye on the aspects of the *fractional order calculus*, the proposed work is carried out. The fractional order calculus (FOC) is a branch of mathematics is as old as the classical Newtonian calculus, and deals with the theory of differential and integral operators of non–integer order and to the differential equations containing such operators.

The origin of the FOC theory can be traced back to the end of the seventeenth century, the time when Newton and Leibniz developed the foundation of the differential and integral calculus. Even though the concept of the FOC theory is established long back, yet the subject came practically over the last few decades. The new models of the systems have been developed

by engineers and scientists based on the fractional differential equations approach. These models have been successfully applied in various research fields such as, mechanics (theory of viscoelasticity), electrical engineering (transmission of ultrasound waves), medicine (modeling of human tissue under mechanical loads) and the list continues.

The applications of the FOC theory are limited in the fields of electronics and communication engineering and an attempt has been made to incorporate the concept of FOC theory in the signal and image processing regimes.

In the proposed study, an idea of amalgamation comes into picture. To achieve the fractional order differentiation property in the FrFT domain, the concept of FOC is amalgamated with the FrFT theory and it exhibits two degrees of freedom. In the case of the traditional differentiation property in the FrFT domain, there is only one degree of freedom thus, having single varying parameter of interest. Due to two degrees of freedom in the reported work, now there are two varying parameters and thus, more design flexibility can be achieved.

In order to be self–contained, the fundamentals of FrFT, FOC have been thoroughly studied before coming to the main theme of the subject. A particular goal of this reported work is to provide a solid foundation that may later be used for the construction of the efficient and reliable numerical methods of the results. We strongly believe that a successful development and a thorough understanding of such numerical schemes are not possible without such analytical background.

Before laying down the foundations of the fractional order differentiation in the FrFT domain, the integer order differentiation is considered in the FrFT domain. The closed–form analytical expression of the integer–order differentiator is established in the FrFT domain the design method of window based technique.

The window functions are successfully been used in diverse areas of filtering, beamforming, communication and signal processing therefore, its role is quite impressive and economical from the point of view of computational complexity and ease associated with its application. Thus, an attempt is made to analyze the window functions in the FrFT domain by establishing the closed–form analytical expression which shows its behavior with varying fractional Fourier transform (FrFT) parameter. The study of main side lobe level, half main lobe width and side–lobe fall–off rate is also done for different values of the FrFT parameter.

The analytical aspects of establishing the fractional order differentiation property in the FrFT domain is well–considered. Based on the fractional differintegral definitions of FOC theory namely, Riemann–Liouville (RL), Grünwald–Letnikov (GL) and Caputo, the approach begins. Thus, the formulation is established that has two varying parameters namely, the fractional derivative order parameter (μ) related to the FOC approach and the fractional Fourier transform parameter (φ) of the FrFT theory.

The fractional order differentiating filter is designed based on the popular and familiar definitions of FOC and FrFT theories. Following the established analytical results, the one–dimensional and the two–dimensional applications are discussed. The signal filtering application is considered that utilizes the fractional order differentiation property in the FrFT domain based on the FOC concept. The signal of interest is made to corrupt with the high–frequency chirp noise and it is shown that the fractional order differentiating filter performs better to eliminate the noise as compared to the time–domain and the frequency–domain filtering. Thereby, the comparative understanding is also developed between the fractional order calculus differintegral definitions based on the example considered. Furthermore, the understanding so developed is in conformity with the already established mathematical results available in most of the mathematics literatures.

The established analytical result is used for the two–dimensional signal processing application of edge detection on an image. Based on the FOC definitions, the fractional differential mask is used for the edge detection operation in the FrFT domain. Thus, the design flexibility of two varying parameters, μ and φ performs the edge detection operation in the FrFT domain. As stated in the rich literatures, the traditional approach of edge detection that utilizes various edge detection operators like Roberts, Prewitt, Sobel and second–derivative Laplacian method underperforms in the case of noisy environment. So, the study shows that by utilizing the fractional differential mask in the FrFT domain, the edge detection operation performs well in the noisy environment. The performance is judged through qualitative (visual perception) and quantitative analysis (performance metric parameters of peak signal to noise ratio and mean square error). Thus, the edge detection operation utilizing the fractional order operators exhibits good noise immunity and effective performance that opens up the horizon in the future image processing applications.

Finally, this study has multidimensional facets in various research areas of electronics and communication engineering. The fractional order calculus has inherent advantages, therefore by amalgamating the concept of fractional order calculus with the signal processing transforms, many great future developments could come up that would lead to many suitable applications in various fields. We believe that the researchers, both new and old cannot remain within the boundaries of the integral order calculus and that too exhibiting only one degree of freedom for applications. So the need arises for the viable mathematical tool that will accomplish future endeavors of engineering developments and that the fractional order calculus is the future for the signal processing society. Thus, an era has come up that opens up the horizon of generalizing various science and engineering problems to get better results and opening a new paradigm of *FRACTIONAL ORDER SIGNAL PROCESSING* and the era of *FRACTIONAL ORDER CALCULUS* is the calculus of *21st CENTURY.*

LIST OF PUBLICATIONS

[P.1] "Caputo–Based Fractional Derivative in Fractional Fourier Transform Domain," ***IEEE Journal on Emerging and Selected Topics in Circuits and Systems***, vol. 3, no. 3, pp. 330–337, **2013**.

[P.2] "Closed–Form Analytical Expression of Fractional Order Differentiation in Fractional Fourier Transform Domain," ***Springer—Circuits, Systems, and Signal Processing***, vol. 32, no. 4, pp. 1875–1889, **2013**.

[P.3] "Kummer Confluent Hypergeometric Function and Fractional Fourier transform Based Fractional Order Calculus," ***International Conference on Special Functions and Their Applications***, Annual Conference of Society for Special Functions and Their Applications, National Institute of Technology, Surat, Gujarat, India, June 27–29, **2012**.

[P.4] "Analysis of Dirichlet and Generalized "Hamming" Window Functions in the Fractional Fourier Transform Domains," ***Elsevier—Signal Processing***, vol. 91, no. 3, pp. 600–606, **2011**.

ACRONYMS AND ABBREVIATIONS

1D	One–Dimensional.
2D	Two–Dimensional.
CFrFT	Continuous Fractional Fourier Transform.
CHF	Confluent Hypergeometric Function.
DD	Digital Differentiator.
DFrFT	Discrete Fractional Fourier Transform.
DSP	Digital Signal Processing.
ECG	Electrocardiograph.
FIR	Finite–Impulse Response.
FOC	Fractional–Order Calculus.
FODD	Fractional–Order Digital Differentiator.
FrFT	Fractional Fourier Transform.
FrFTD	Fractional Fourier Transform Domain.
FT	Fourier Transform.
FTD	Fourier Transform Domain.
GL	Grünwald–Letnikov.
HMLW	Half Main Lobe Width.
IIR	Infinite–Impulse Response.

IODD	Integer–Order Digital Differentiator.
$\boldsymbol{MSE}$	Mean Square Error.
MSLL	Maximum Side Lobe Level.
PID	Proportional Integral Derivative.
$\boldsymbol{PSNR}$	Peak Signal to Noise Ratio.
RL	Riemann–Liouville.
$\boldsymbol{RMSE}$	Root Mean Square Error.
SLFOR	Side–Lobe Fall–Off Rate.

GLOSSARY OF SYMBOLS

$\boldsymbol{a}$	Fractional Fourier Order Parameter.
$\boldsymbol{\mu}$	Fractional Derivative Order Parameter.
$\boldsymbol{\varphi}$	Fractional Fourier Transform Parameter.
$\boldsymbol{\Gamma}$	Gamma Function.
${}_1\boldsymbol{F}_1$	Confluent Hypergeometric Function of the First Kind.
$\boldsymbol{\Im}$	Fourier Transform Operator.
$\boldsymbol{\psi_n(t)}$	Hermite Orthonormal Function.
$\Omega(\boldsymbol{n})$	High–Frequency Chirp Noise.
$\boldsymbol{\nabla}$	Gradient Operator.
$\boldsymbol{\nabla^2}$	Laplacian Operator.
$\boldsymbol{D_+^{\mu}}$	Left Riemann–Liouville Fractional Derivative.
$\boldsymbol{D_-^{\mu}}$	Right Riemann–Liouville Fractional Derivative.
${}_l^C\boldsymbol{D_t^{\mu}}$	Caputo Fractional Derivative Operator.
$\mathbf{erf}$	Error Function.
$\mathbf{erfc}$	Complementary Error Function.
$\mathbf{erfi}$	Imaginary Error Function.
$\boldsymbol{H^{\mu}(u_{\varphi})}$	Fractional Order Impulse Response Filter
$\boldsymbol{H_n(t)}$	Hermite Function.
$\mathrm{T}_{\mathcal{F}}^{\varphi}(\cdot)$	Fractional Fourier Transform Operator.
$\boldsymbol{u_{\varphi}}$	Fractional Fourier Transform Domain.

LIST OF FIGURES

Figure–6.16 Variation of Peak Signal to Noise Ratio ($PSNR$) (in dB) versus fractional Fourier order parameter, a for different mask operators and the fractional differential mask μ using FrFT.

LIST OF TABLES

TABLE OF CONTENTS

CHAPTER 1

INTRODUCTION

Science is a way of thinking much more than it is a body of knowledge. Science may set limits to knowledge, but should not set limits to imagination.

— Anonymous.

1.1 GENERAL

FILTERING IS THE MOST USEFUL FORM OF SIGNAL PROCESSING operation incorporated in all applications, to remove the frequencies in certain parts and to improve the magnitude, phase, or group delay in some other part(s) of the spectrum of a signal. The operation of filtering can be classified into many different ways in the present scenario. There exists no hierarchical classification as such to classify filters. Its classification can be visualized pictorially as in Figure-1.1.

The demand of today's digital world is based on digital filtering schemes as compared to its analog counterpart. Due to increasing speed, less cost and decreased size of the microelectronic digital components, digital filtering prevails over analog filtering. Digital filtering is the process of spectrum shaping using digital hardware as the basic building block. Thus the aim of digital filtering is the same as those of continuous filtering, but the physical realization is different. Linear digital filter theory is based on the well–known linear difference equations with constant coefficients, as against the linear differential equations used for linear continuous filter theory **[45]**. Real–time digital filters exhibit several advantages over continuous filters. A greater degree of accuracy is attained for its realization. No special components are needed to realize filters with time–varying coefficients. Aggregates of digital filters are

economic in the very low frequency band (0.01 to 1 Hz) where the size of analog components becomes appreciable.

The choice of filters for general applications was based on three broad criteria that is, filters should: (a) provide as little distortion as possible to the signal; (b) be as flat as possible in the pass–band, and; (c) exhibit attenuation characteristics of better than –90 dB (~$3x10^{-5}$ in absolute terms) in the stopband. Other desirable characteristics include short filter length, short frequency transition beyond the cutoff point, and possibly the ability to manipulate the attenuation in the stopband. These conditions are believed to be consistent with a wide range of general applications where one can make no assumptions about the end use of the filters. **[85]**

The conditions (a) to (c) as stated in the previous paragraph are usually satisfied by linear phase filters. This class of filters is most easily designed using finite impulse response (FIR) techniques with appropriate windowing, known as the window technique. However, the main advantages are that FIR filters are always stable and they are least susceptible to round–off arithmetic errors as can occur in some shorter recursive filter types. More importantly, phase linearity is guaranteed in FIR filters, thereby avoiding signal distortion.

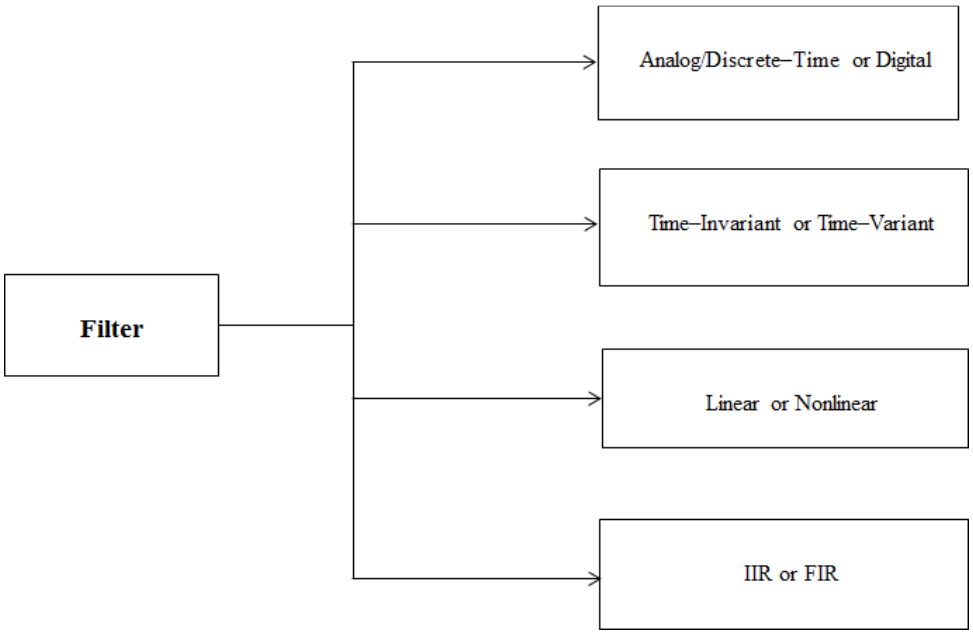

Figure–1.1: Suggested Classification of Filter.

1.2 HISTORICAL DEVELOPMENTS OF FRACTIONAL FOURIER TRANSFORM

In mathematics and in signal processing, the term 'transform' or more specifically, the *signal transform* is a mathematical transform with many applications in sciences and engineering. It is a tool that transforms a mathematical function of time into a new function whose argument is frequency with units of cycles/s (hertz) or radians per second. The signal transforms play key role in signal processing. It is used in all processing stages, from signal representation to signal restoration and data recovery, to signal encoding for storage and transmission, to feature extraction and decision–making.

Since its inception in the signal processing regime in the very beginning of 1920–1940s, the integral transforms, specifically, convolution and Fourier and Laplace integral transforms, have been used in the engineering discipline.

Generally, signal transformations are mapping in signal space; they define how one signal is converted into another. For continuous signals, the signal transforms are mathematically modeled as integral transforms,

$$q(\xi) = \int p(x)\, \mathbb{K}(x, \xi)\, dx \qquad \textbf{(1.1)}$$

where $p(x)$ and $q(\xi)$ are input and output signals of the transform in their respective coordinates (x) and (ξ) and the function $\mathbb{K}(x, \xi)$ specifies the particular transform; it is called the *transform kernel*. In the signal processing jargon, transforms are associated with signal processing systems and the transform kernel is called the system *point spread function*. **[103]**

Different transforms were reported based on various definitions of kernel functions. Each transform has its own set of properties and therefore is suited to a particular category of signal only. Examples include Fourier transform, Laplace transform, z–transform, and so on. The other direction of development is to find new transforms that have some special capabilities to meet new requirements for current and future applications. It is often found that some of the transforms, when applied to solve complex problems, have their inherent shortcomings in dealing with certain types of signals.

For example, the Fourier transform often fails to provide meaningful information for time–varying signals which contain frequency components that change with time. Time–varying (or non–stationary) signals have been extensively used to describe many natural phenomena. It is easily understood that Fourier–related transforms were not capable of dealing with non–stationary signals because the kernel functions do not have any facility to describe the changes of frequencies in time. **[58]**

A number of time–frequency transforms are reported to analyze and/or synthesize various signals in both time and frequency domains simultaneously. According to the ways of accommodating the nature of varying frequency, some time–frequency transforms can be loosely classified into the window–based category. Typical examples are the short–time Fourier transform and a few of the modified Wigner distributions, such as the pseudo Wigner distribution and smoothed Wigner distribution. Although the window functions are used under different assumptions and for different purposes, these functions all have the shortcoming of undesirable effects on the useful signal components in the time–frequency distribution. The resolution in time and/or frequency is often reduced because the window unavoidably suppresses a part of the information in the signal. Based on the uncertainty principle, it seems difficult to solve the problem associated with the window–based time–frequency transform. **[152]**

In the other category, the time–frequency transforms have their kernel functions that inherently describe the time–varying nature of the signal. One example is the fractional Fourier transform whose kernel function has a variable φ to rotate the time–frequency distribution in the time–frequency plane. The idea of fractional powers of the Fourier operator appears in the mathematical literature as early as 1929. With its rapid progress in the research community, it finds its place in quantum mechanics **[6, 154]**, optics, and signal processing **[65]**. A lot of research work started in the early Nineties which lead to many scientific publications and patent **[48, 56]** and is heading with a very rapid pace. It is to be noted that not only the Fourier transform is fractionalized, but the term fractional or fractal finds its place in almost every research areas of optics, signal processing, numerical analysis, calculus, geometry, and so on.

Thus, for the signal transform to be completely defined, it has to satisfy some basic properties including linearity, scaling, translation, modulation, conjugation, differentiation,

integration, multiplication with time, division by time, similarity, uncertainty principle, etc. **[65]**. All the properties have been well–established in the classic works of literature.

The need arises for the differentiation property of fractional order in the fractional Fourier transform framework. So, one gets the flexibility of two varying parameters: fractional derivative order parameter μ for the fractional order differentiation and the fractional Fourier transform parameter φ for the FrFT, that will lead to many interesting results in the significant applications of signal and image processing.

1.3 HISTORICAL DEVELOPMENTS OF FRACTIONAL ORDER CALCULUS

The fractional order calculus (FOC) is a natural extension of the traditional Newtonian calculus. Most of the mathematicians and researchers of FOC regard September 30th, 1695 as its birthday. The intuitive idea of FOC is as old as integer–order calculus, as mentioned in a letter written by Leibniz to L'Hôpital. Leibniz, when asked about what if n were $1/2$ in $d^n y/dx^n$, said: "It will lead to a paradox". But he added prophetically, "From this apparent paradox, one day useful consequences will be drawn". **[27]**

In the last decades, it became an area of intense research and development. It started from some speculations of G. W. Leibniz (1695, 1697) and L. Euler (1730), and it has developed progressively up to now. Various mathematicians and researchers who have contributed a lot for the development of the FOC concept in science and engineering arenas includes, P. S. Laplace (1812), S. F. Lacroix (1819), J. B. J. Fourier (1822), N. H. Abel (1823–1826), J. Liouville (1832–1873), B. Riemann (1847), H. Holmgren (1865–1867), A. K. Grunwald (1867–1872), A. V. Letnikov (1868–1872), H. Laurent (1884), P. A. Nekrassov (1888), A. Krug (1890), J. Hadamard (1892), O. Heaviside (1892–1912), S. Pincherle (1902), G. H. Hardy and J. E. Littlewood (1917–1928), H. Weyl (1917), P. Lvy (1923), A. Marchaud (1927), H.T. Davis (1924–1936), E. L. Post (1930), A. Zygmund (1935–1945), E. R. Love (1938–1996), A. Erdelyi (1939–1965), H. Kober (1940), D. V. Widder (1941), M. Riesz (1949), W. Feller (1952). **[110]**

The standard mathematical models of integer–order derivatives do not adequately define the real life physical processes which are nonlinear in nature. So the fractional order calculus has

been used to model many physical and engineering processes that are best described by the fractional order differential equations. Many fractional order derivative definitions exist to define the FOC concept and each has their advantages and disadvantages. In recent years, many applications of FOC played a pivotal role in various fields such as economics, chemistry to fractional filters and fractals.

In the engineering discipline, most of the research work of fractional order differ–integrals is dedicated in the modeling of the fractional order control systems, fractional Brownian motion and fractional order circuits and systems. Very less research have come up in the signal and image processing domains. So, an attention is paid in the signal and image processing applications utilizing the fractional order calculus concept.

1.4 FRACTIONAL ORDER DIGITAL DIFFERENTIATOR

The development of FOC for modeling physical systems has been widely considered in last decades. It has found use in the studies of viscoelasticity and damping, diffusion and wave propagation to many other application areas in engineering including electrical networks, electromagnetic field and transmission line theory, microwave engineering, as a mathematical tool in control theory, signal processing, modeling and identification and chaos and fractals.

Fractional systems or non–integer order systems can be considered as a generalization of integer order systems that rely on the mathematical tool of fractional order calculus. FOC is a generalization of differentiation and integration to non–integer order fundamental operator ${}_aD_t{}^{\mu}$, where a and t are the limits of operation and $\mu \in \mathbb{R}$ **[89]**. There exist many equivalent definitions that are most frequently used for the general fractional differ–integral. Namely, the Riemann–Liouville (RL) definition, Weyl definition, Riesz definition, Marchaud–Hadamard definition, Grünwald–Letnikov (GL) definition, the Caputo definition, which will be dealt later in the chapters.

The concept of fractional order differentiation and integration could be explained in a lucid language as follows: Since everyone is very familiar with the elementary calculus that was studied in the school days. To say, for instance, if a function $f(x) = x^2$, then if we integrate it to

first order, then the result would be $\int f(x)\,dx = (1/3)\,x^3 + C_1$ and integrating the same function to the second order yields $\int\{\int f(x)\,dx\}\,dx = (1/12)\,x^4 + C_1\,x + C_2$ where C_1 and C_2 are arbitrary constants of integration. Similarly, $\frac{d}{dx}\,f(x) = 2x$, and $\frac{d^2}{dx^2}\,f(x) = 2$. However, if one asks to integrate the function $f(x)$ to its half–order, or to find its half–order derivative, then how could we define these operations?

Based on this very simple principle of fractional order differentiation and integration, the conversation between Leibniz and L'Hôpital gave birth to what is known as 'Fractional Order Calculus'.

Based on the concept of fractional order differentiation, the fractional order differentiator could be designed for suitable signal and image processing applications. The fractional order differentiator is concerned with estimating the fractional order derivatives of a signal or an unknown signal from its noisy observed data. It finds usage in fractional order control systems, signal processing, chaos and fractals, electrical networks, electromagnetic field theory. In signal processing, the fractional order differentiator proves to be an important mathematical tool that can give more peculiar characteristics as compared to the integer order differentiator. Furthermore, if the fractional order differentiator is designed to work in the fractional Fourier transform domain, then more suitable applications could be established in the world of sciences and engineering.

1.5 ORGANIZATION OF THESIS

This thesis is organized into seven chapters. The chapter wise flow is summarized below:

Chapter 2: Literature Survey

This chapter presents an in–depth literature survey for the research work. It presents the preliminaries of digital differentiator, fractional order calculus and the fractional Fourier transform. It also contains the explanation of various mathematical functions required in the proposed work.

Chapter 3: Integer–Order Digital Differentiator (IODD) in FrFT Domain (FrFTD)

Following the conclusions drawn in Chapter 2, the design of integer–order digital differentiator in the fractional Fourier transform domain is proposed. A brief review of its configurations and classifications is also mentioned followed by the comparative analysis between the finite impulse response and the infinite impulse response digital differentiator configurations. The main focus is made in the finite impulse response digital differentiator, which is classified into two namely; integer–order digital differentiator and the fractional–order digital differentiator. Also, various design methods for the design of the finite impulse response digital differentiator are briefly explained with their advantages and limitations. The window based design method is chosen for its designing with the reason mentioned therein, followed by the derivation of the closed–form analytical expression of various window functions and shows its behavior in the fractional Fourier transform domain. Lastly presented is the detailed mathematical analysis of designing the differentiator in the fractional Fourier transform domain with the simulation results.

Chapter 4: Fractional–Order Digital Differentiator (FODD) in FrFT Domain (FrFTD)

In this chapter, the mathematical foundation of the fractional order digital differentiator is investigated that behaves in the FrFT domain. The mathematical tool of the fractional order calculus proves to be beneficial for this investigation. The most popular and familiar definitions of the fractional order differ–integrals are used for deriving the closed–form analytical expression of the fractional–order differentiation in the FrFT domain, followed by the uniqueness of the fractional–order differentiator in the FrFT domain.

Chapter 5: Filtering Application of FODD in FrFTD

This chapter focuses on the filtering application of the proposed fractional order differentiator in the FrFT domain. The role of fractional order differentiator as an optimal filter in the FrFT domain is also explained. The design is proposed for the low–pass finite impulse response fractional order differentiator in the FrFT domain, based on the definitions of the Riemann–Liouville (RL) and Caputo based fractional order derivative definitions. Finally, the simulation

results are presented for the proposed differentiator, followed by the comparative analysis between RL and Caputo based design.

Chapter 6: Edge Detection on Images

The application of the proposed differentiator in image processing is discussed in this chapter. The application of the edge detection on images is investigated. First of all, basic edge detection concept is explained followed by various edge detection operators, including Roberts, Prewitt, Sobel and second derivative Laplacian method. Thereafter, the analytical aspects concerning the edge detection operation based on the fractional order differentiation in the FrFT domain is explained. Based on the Grünwald–Letnikov (GL) fractional order derivative definition, a fractional differential mask is used along with the two–dimensional fractional Fourier transform definition to propose the edge detection in the FrFT domain. Finally, the performance of the established edge detection operators and the proposed edge detection fractional order operator are investigated in the FrFT domain. The performance parameters that are paid attention to are peak signal to noise ratio and mean square error and they are presented in tabular form for an image of interest. The simulation results and the fruitful discussion of the proposed edge detection operation also add up to the completion of this chapter.

Chapter 7: Conclusions and Future Scope of Work

Finally, the conclusion of the study along with the future scope of the work is presented and discussed in this chapter.

CHAPTER 2

LITERATURE SURVEY

A researcher cannot perform significant research without first understanding the literature in the field.

— Boote and Beile, 2005.

A THOROUGH, SOPHISTICATED LITERATURE REVIEW is the foundation and inspiration for substantial and useful research. Conducting a literature review is a means of demonstrating an author's knowledge about a particular field of study, including vocabulary, theories, key variables and phenomena, and its methods and history.

2.1 PRELIMINARIES OF DIGITAL DIFFERENTIATOR (DD)

Differentiators or differentiating filters are used in many digital systems to find the time–derivative of the incoming signal. They are used in almost all applications of sciences and engineering. For instance, it is used in communication, control and radar systems, biomedical applications and audio and video processing applications, and other fields of engineering. The advantages of digital filters are based on the fact that the performance of the applied algorithms is always predictable. There is no dependence on the tolerances and adjustment of the electrical components as in analog counterpart which allows for the interference–proof and long–term stable system implementation.

For the past decades, several techniques have been proposed to design digital differentiators. The design methods for designing integer–order digital differentiator (IODD) and fractional–order digital differentiator (FODD) are mentioned in the next section.

2.1.1 Design Methods of DD

There exists several design techniques for designing IODD and FODD for widespread applications. The design methods of DD are surveyed for both IODD and FODD.

2.1.1.1 Integer–order DD (IODD)

A DD or IODD forms an integral part of many practical signal processing systems because the time derivative of signals is sometimes required for further use or analysis. A DD, which can be used to simulate the behavior of an analog differentiator, is a processor whose output pulse sequence is obtained by approximating the derivative of a continuous–time signal from the samples of that signal. First– and second–derivative DDs have been used in the design of compensators for control systems, for monitoring electrocardiograph (ECG) signals, in the study of velocity and acceleration in human locomotion **[150]** and for the calculation of geometric moments in optical systems **[29]**.

Rabiner and Steiglitz **[100]** have presented the design of recursive and nonrecursive DD. For the design of nonrecursive DD, the frequency sampling technique was used. The coefficients for the recursive DD were optimally chosen to minimize a square–error criterion based on the magnitude of the frequency response. It has been found that the frequency response characteristics of the recursive DD had small magnitude errors but significant phase errors as compared to the nonrecursive DD, which exhibits no phase errors. Also, the delay of the recursive DDs was small compared to the delay of the nonrecursive DD.

DD can be designed using two approaches, namely, the time–domain approach and the frequency–domain approach. In the time–domain approach, first–derivative FIR DD can be designed using classical numerical differentiation algorithms such as the Newton, Bessel, Everett, Stirling, and Lagrange formulas **[107]**. The underlying principle of these algorithms is to fit a continuous–time interpolation polynomial to a given input pulse sequence. Sampling the continuous–time polynomial by a DD at the discrete time yields the output pulse sequence, which effectively approximates the true derivative of a continuous–time signal. The magnitude responses of DD generally approximate the ideal magnitude response reasonably well over the

lower frequency band (i.e., $0 \leq \omega T/(2\pi) \leq 1/4$, where T is the sampling period and ω the angular frequency). These differentiators are normally referred to as narrow–band DDs.

In the frequency–domain approach, first– and higher–derivative FIR DD satisfying prescribed specifications of the ideal frequency response can be designed using the minimax method **[101]**, the Fourier series method in conjunction with the Kaiser window function **[1, 3]**, the Fourier series method in conjunction with accuracy constraints, the eigenfilter method **[134]**, quadratic programming method **[156]**, the least–squares methods **[148]**, Taylor series method **[75]** and genetic algorithm **[149]**.

Because of the constraints imposed on the frequency responses, they are normally referred to as frequency–selective differentiating filters which, in addition to performing signal differentiation, can pass and reject certain frequency components of the signal. That is, they can be designed to have a narrow–band, mid–band **[21–23]**, or wide–band **[99]** magnitude response depending on the application **[119]**.

2.1.1.2 Fractional–order DD (FODD)

The design methods of FODD are divided into two classes: continuous–time (CT) model and discrete–time (DT) model. **[74]**

For the continuous–time model, Podlubny *et al.* **[74]** presented an approach to design fractional order systems and fractional–order controllers based on the concepts of continued–fraction expansion (CFE) approach.

Other CT model methods include:

(i) Carlson's method **[59]**, where Carlson proposed an iterative approximation of the n–th root using a regular Newton process.

(ii) Roy's method **[130]** for the realization of fractional circuits using distributed circuit model that composes passive elements such as resistors and capacitors.

(iii) Charef's method **[8]** to study the dynamic behavior of the fractal system or fractional power pole. A method of singularity function is presented which consists of cascaded

branches of a number of pole–zero (negative real) pairs or simple resistance–capacitance (RC) section.

(iv) Matsuda's method **[94]** based on the approximation of an irrational function by a rational one, obtained via CFE and thereby fitting the original function in a set of logarithmically spaced points.

(v) Oustaloup's method **[13]** where discretization is carried out in two steps, i.e., first frequency domain fitting in continuous time domain is performed followed by discretizing the fit s–transfer function.

For the discrete–time model, the design methods of FODD include the following:

(i) Fractional differencing formulas **[111]**.

(ii) Tustin method **[25]**.

(iii) Direct power series expansion (PSE) method of the Euler operator **[77]**.

(iv) CFE method of the Tustin operator **[25]**.

(v) Al–Alaoui operator, a new established mixed scheme of Euler and Tustin operators **[104]**.

(vi) CFE of Al–Alaoui operator **[25]**.

(vii) Numerical integration method **[77]** and

(viii) Newton's method **[18]**.

2.1.2 Applications of DD

Digital differentiator is an important component in the engineering discipline including communication, control engineering and biomedical applications. This section deals with the one–dimensional and the two–dimensional applications of digital differentiators.

2.1.2.1 One–dimensional (1D) applications

The 1D practical applications of DD as a signal processing system is mentioned below:

(a) *QRS detection in ECG signal*:

Electrocardiogram (ECG) represents electrical activity of human heart. The main problem of digitized signal is interference with other noisy signals like power supply network, 50 Hz frequency and breathing muscle artefacts. These noisy elements have to be removed before the signal is used for next data processing like heart rate frequency detection. Digital filters and signal processing should be designed very effective for next real–time applications in embedded devices. Various algorithms have been developed as in **[141]** for its processing.

(b) *Power system measurement*:

Parameter measurement is an important task in digital power metering and digital protection relaying. Many of well–proven techniques have been used for this purpose. One of shortcomings of these techniques is that they need at least two and half cycle (50 ms) or more time for frequency estimation and other parameter measurement. At the same time these techniques always include much more computation for measurement process. This shortcoming will influence application of these techniques in real–time cases. Many algorithms have been developed **[83]** based on a numerical differentiation and digital FIR filter based algorithm for parameter measurement of non–sinusoidal signals of power systems.

(c) *Parameter estimation of fractional noise process*:

Fractional noise process or fractionally differenced Gaussian noise (fdGn) is a discrete time equivalent of fractional Brownian noise. Filtered versions of such processes are ideally suited for modeling signals with different short–term and long–term correlation structure.

The fractional noise process $r(n)$ can be modeled as the output of a fractional order integrator with frequency response $1/(j\omega)^{\beta}$ driven by a white noise $\zeta(n)$ with zero mean and variance ${\sigma_r}^2$ **[112]**. So, the power spectral density of the fractional noise process $r(n)$ is given by: $S_r(\omega) = \frac{{\sigma_r}^2}{\omega^{2\beta}}$. Thus the fractional order digital differentiator can be used to estimate the

parameters β and ${\sigma_r}^2$ from the observation data when $r(n)$ passes through the ideal fractional order digital differentiator **[34]**.

(d) ***Estimation of the fractional order derivative of the contaminated signal*****:**

Recently, Chen *et al.* **[49]** proposed a novel digital fractional order Savitzky–Golay differentiator (DFOSGD) to estimate the fractional order derivative of the noise–free and the noisy signal. It uses the polynomial least–squares method and the Riemann–Liouville fractional order derivative definition. So it gets the advantage of amalgamating the fractional order calculus concept with the Savitzky–Golay filter, to accurately and easily estimate the fractional order derivative of the contaminated signal.

2.1.2.2 Two–dimensional (2D) applications

The 2D applications of DD are reviewed as below:

(a) ***Edge detection in images*****:**

Edge detection consists of a set of mathematical methods which aim at identifying points in a digital image at which the image brightness changes sharply or has discontinuities. The points at which image brightness changes sharply are typically organized into a set of curved line segments termed *edges*. Most of the existing analytic approaches to edge detection are based on the concept of differentiation **[10]**. The FIR edge detectors **[44]** are designed such that they have the ability to differentiate the edges and to smooth the noise in a noisy image simultaneously.

(b) ***Digital image sharpening*****:**

Image sharpening refers to any enhancement technique that highlights the edges and fine details in an image or to enhance details that has been blurred, either in error or as a natural effect of a particular method of image acquisition. Its usage varies and includes the applications like electronic printing, medical imaging, industrial inspection and autonomous target detection in smart weapons for increasing the local contrast and sharpening the images.

The sharpening is usually accomplished by spatial filters based on the derivative filters. Differentiation can be expected to have the opposite effect of averaging, which tends to blur detail in an image, and thus sharpen an image and be able to detect edges. The most common method of differentiation in image processing applications is the gradient. The details can be found in **[34, 123]**.

2.2 PRELIMINARIES OF FOC

The theory of fractional order calculus (FOC) has a quite long and prominent history; in fact one may trace it back to the very origins of classical Newtonian calculus itself. Interest in FOC became evident almost as soon as the ideas of classical calculus were known. The systematic studies of FOC were undertaken during the first half of the 19th century. Euler, Lagrange, and Fourier mentioned the concept of derivatives of arbitrary order earlier in their studies without contemplating any specific application **[89]**. Notable contributions have been made to both the theory and applications of FOC during the 20th century when some rather special, but natural, properties of differintegrals (i.e., derivatives of arbitrary order) were examined with respect to arbitrary functions.

The term fractional order calculus is more than 300 years old topic i.e., it is as old as the integer one although up to recently its application was exclusively in mathematics. It is a generalization of the ordinary differentiation and integration to non–integer (arbitrary) order. In a letter to L'Hôpital in 1695, Leibniz raised the following question "Can the meaning of derivatives with integer order be generalized to derivatives with non–integer orders?" The story goes that L'Hôpital was somewhat curious about that question and replied by another question to Leibniz, "What if the order will be $1/2$?" Leibniz replied in a letter dated September 30, 1695: "It will lead to a paradox, from which one day useful consequences will be drawn." The question raised by Leibniz for a fractional derivative was an ongoing topic in the last 300 years. Several mathematicians and researchers like Liouville, Riemann, and Weyl made major contributions to the theory of fractional order calculus **[89, 91]** . This contribution was continued from Fourier, Abel, Leibniz, Grünwald and Letnikov.

Many real systems are better described with FOC differential equations known as fractional–order differential equations, as it is well–suited tool to analyze and characterize problems with long–term 'memory' and chaotic behavior. Thus, it becomes a tool used in almost every area of science and has been found to be useful in various unrelated fields including diffusion theory, electrochemistry, rheology **[57]**, theory of transmission lines, elasticity **[7]**, the theory of differential equations **[78]**, fluid mechanics and moments of probability distribution functions **[89]**. There are also associated logical and mathematical concepts namely, alphabet coding, Fourier transform, fractional Fourier transform and fractional order calculus for the analysis of the deoxyribonucleic acid data of different chromosomes **[153]**.

Few years ago, the concept of FOC was unexplored in engineering, because of its inherent complexity, the apparent self–sufficiency of the classical integer order calculus, and the fact that it does not have a fully acceptable geometrical or physical interpretation **[71]**. Nevertheless, the application of FOC just emerged in the last two decades, due to the progress in the area of chaos and nonlinear dynamics. In the field of dynamical systems theory, some work is carried out but the proposed models and algorithms are still in a preliminary stage of its establishment. Its adoption in many scientific areas verified that the fractional–order models capture phenomena and properties that the classical integer–order simply neglects. **[89]**

The most popular and familiar definitions of the fractional differintegrals are Riemann–Liouville, Grünwald–Letnikov and Caputo, which are elaborated below and will be used for the future course of the study.

2.2.1 Riemann–Liouville (RL) Definition

The concept of non–integer or fractional order integration can be traced back to the genesis of the differential calculus itself. For $t > 0$,

$$ {}^{RL}J^{\mu}x(t) = \frac{1}{\Gamma(\mu)}\int_0^t (t-\tau)^{\mu-1}\, x(\tau)\, d\tau \qquad \textbf{(2.2.1)} $$

is called the Riemann–Liouville fractional integral of the function $x(t)$ of order μ with $Re(\mu) > 0$. **[73]**

The Riemann–Liouville differential operator of FOC of order μ is defined as:

$$ {}^{RL}D^{\mu}\, x(t) = \begin{cases} \frac{1}{\Gamma(n-\mu)}\, \frac{d^n}{dt^n} \int_0^t \frac{x(\tau)}{(t-\tau)^{\mu+1-n}}\, d\tau, & n-1 < \mu < n \in \mathbb{N}, \\ \frac{d^n}{dt^n}\, x(t), & \mu = n \in \mathbb{N}, \end{cases} \quad \textbf{(2.2.2)} $$

where $\mu > 0$, $t > 0$.

2.2.2 Grünwald–Letnikov (GL) Definition

It is one of the familiar definitions of the fractional differintegrals, introduced by Anton Karl Grünwald (1838–1920) from Prague, in 1867, and by Aleksey Vasilievich Letnikov (1837–1888) in Moscow in 1868. The Grünwald–Letnikov μth order fractional derivative of a function $x(t)$ with respect to t is defined as **[73]**:

$$ {}^{GL}D^{\mu}\, x(t) = \lim_{h\to 0} h^{-\mu} \sum_{j=0}^{N} (-1)^j \binom{\mu}{j} x(t-jh) \quad \textbf{(2.2.3)} $$

where $\mu > 0$, D^{μ} denotes the fractional derivative, $N = t/h$, h is the step size, and

$$ \binom{\mu}{j} = \frac{\mu(\mu-1)(\mu-2)\cdots(\mu-k+1)}{k!} = \frac{\Gamma(\mu+1)}{k!\,\Gamma(\mu-k+1)}, \quad \textbf{(2.2.4)} $$

$$ {}^{GL}D^{\mu}\, x(t) = \lim_{h\to 0} h^{-\mu} \sum_{j=0}^{t/h} (-1)^j \left(\frac{\Gamma(\mu+1)}{k!\,\Gamma(\mu-k+1)}\right) x(t-jh) \quad \textbf{(2.2.5)} $$

where Γ is the gamma function defined by the Euler limit expression

$$ \Gamma(\xi) = \lim_{n\to\infty} \frac{n!\, n^{\xi}}{\xi(\xi+1)\cdots(\xi+n)} \quad \textbf{(2.2.6)} $$

where $\xi > 0$, or the so–called Euler integral definition:

$$ \Gamma(\xi) = \int_0^{\infty} t^{\xi-1} \exp(-t)\, dt \ (\xi > 0), \quad \textbf{(2.2.7)} $$

$$ {}^{GL}D^{\mu}\, x(t) = \lim_{h\to 0} h^{-\mu} \sum_{j=0}^{t/h} (-1)^j\, b_j\, x(t-jh) \quad \textbf{(2.2.8)} $$

where the weighing coefficients b_j can be calculated recursively by the following formulae:

$$b_0 = 1,\ b_j = \left(1 - \frac{1+\mu}{j}\right)\ b_{j-1},\ j \geq 1 \qquad \textbf{(2.2.9)}$$

It implies, $b_1 = (-\mu)\ b_0 = -\mu,\ b_2 = \frac{(1-\mu)}{2}\ b_1 = \frac{(-\mu)(1-\mu)}{2}, \cdots$ **(2.2.10)**

In general, $b_n = \frac{1}{n!}\ (-\mu)(1-\mu)(2-\mu)\cdots\big((n-1)-\mu\big),\ n = 0, 1, 2, \cdots$ **(2.2.11)**

2.2.3 Caputo Definition

There is another option for computing fractional derivatives; the Caputo fractional derivative. It was introduced by M. Caputo in his 1967 paper **[109]** and is defined as:

$$ {}^{c}D^{\mu}\ x(t) = \begin{cases} \frac{1}{\Gamma(n-\mu)}\ \int_0^t \frac{x^{(n)}(\tau)}{(t-\tau)^{\mu+1-n}}\ d\tau, & n-1 < \mu < n\ \in\ \mathbb{N}, \\ \frac{d^n}{dt^n}\ x(t), & \mu = n\ \in\ \mathbb{N}, \end{cases} \qquad \textbf{(2.2.12)}$$

is called the Caputo fractional derivative or Caputo differential operator of fractional calculus of order μ.

It is to be noted that the RL derivatives have certain disadvantages when trying to model the real–world phenomena with fractional differential equations. **[90]**

2.3 SPECIAL MATHEMATICAL FUNCTIONS

Many mathematical functions have been emerged out in the field of engineering mathematics and mathematical physics that deserves attention for finding the best solution to a given problem. In fact, there is no real definition of which functions are to be regarded as “special functions” **[14]**. Yet there are wide range of books and courses on them which heavily use them in engineering mathematics, analytical number theory and in mathematical physics.

During the course of this study, we came across some of the special mathematical functions that find wide applicability in the study. These are discussed below.

2.3.1 Hermite Function

Hermite function and indeed Hermite polynomials are not new. In mathematics, the Hermite polynomials $H_n(t)$ are a classical orthogonal polynomial sequence that arise in probability, combinatorics and in physics. It has been used in a number of important applications, including those for multiscale analysis and communication systems and signal processing **[17, 97]**. It has many interesting properties, including their relation to Gaussian and their property of being eigenfunctions of the Fourier transform. In signal processing, the Hermite function plays a vital role as the eigenfunctions of Fourier transform and fractional Fourier transform **[154]**. The Hermite functions with scaling operation and chirp multiplication can also be the eigenfunctions of the linear canonical transform **[137]**. The Hermite function, $H_n(t)$ is a set of orthogonal polynomial over the domain $(-\infty, \infty)$ with weighting function e^{-t^2}, as illustrated in Figure-2.1 for $n = 1, 2, 3$ and 4.

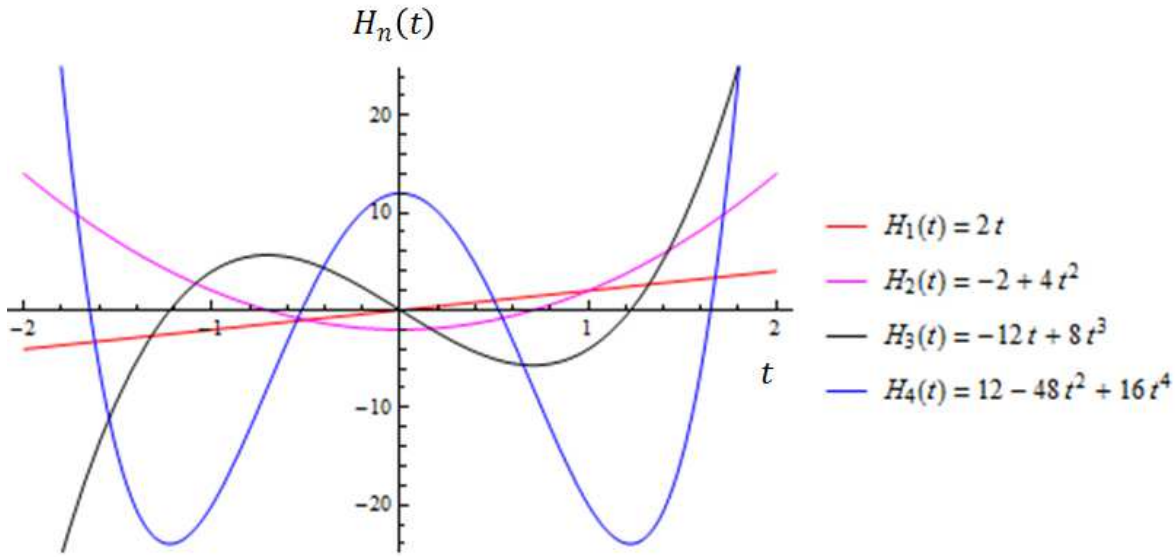

Figure–2.1: Plot of Hermite function for various values of $n = 1, 2, 3, 4$.

The Hermite polynomials $H_n(z)$ can be defined by the contour integral:

$$H_n(z) = \frac{n!}{2\pi j} \oint e^{-t^2+2\,t\,z}\, t^{-n-1} dt, \qquad \textbf{(2.3.1)}$$

where the contour encloses the origin and is traversed in a counterclockwise direction. **[157]**

The Hermite polynomials are defined either by:

$$H_n(t) = (-1)^n e^{t^2/2} \frac{d^n}{dt^n} e^{-t^2/2},\ n = 0, 1, 2, \cdots \text{ and } -\infty < t < \infty \qquad \textbf{(2.3.2)}$$

known as *probabilists' Hermite polynomials*, or by:

$$H_n(t) = (-1)^n e^{t^2} \frac{d^n}{dt^n} e^{-t^2},\ n = 0, 1, 2, \cdots \text{ and } -\infty < t < \infty \qquad \textbf{(2.3.3)}$$

known as *physicists' Hermite polynomials*.

These polynomials form a set of orthogonal polynomials on the real line $\mathbb{R}$ with respect to the Gaussian weighting function **[107]** $m(t) = e^{-t^2}$ as:

$$\int_{-\infty}^{\infty} H_l(t)\, H_m(t)\, e^{-t^2} dt = 2^l\, l!\, \sqrt{\pi}\, \delta_{l-m} \qquad \textbf{(2.3.4)}$$

From these polynomials, one can construct the Hermite orthonormal function $\psi_n(t)$, which are related to the Hermite polynomials $H_n(t)$ by:

$$\psi_n(t) = \frac{H_n(t)\, e^{-t^2/2}}{\sqrt{2^n\, n!\, \sqrt{\pi}}} \qquad \textbf{(2.3.5)}$$

whose graphical plot is shown in Figure-2.2.

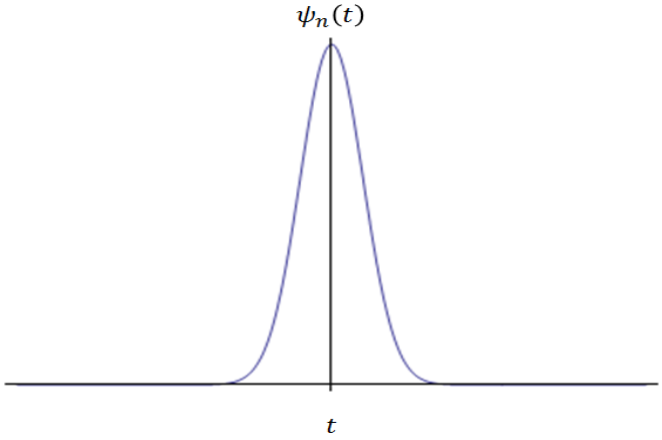

(a)

Figure–2.2: First four Hermite functions. (a) $\psi_0(t)$, (b) $\psi_1(t)$, (c) $\psi_2(t)$, (d) $\psi_3(t)$.

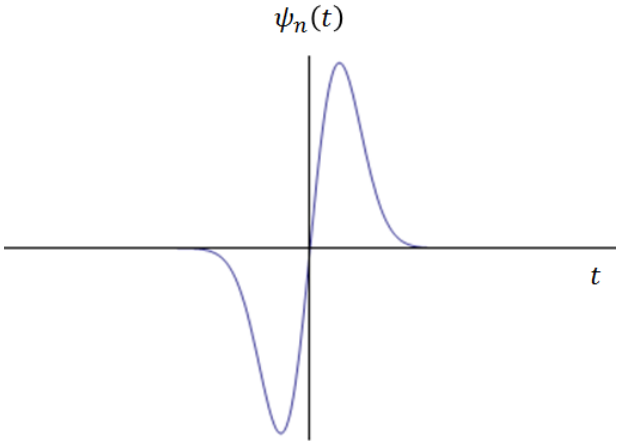

(b)

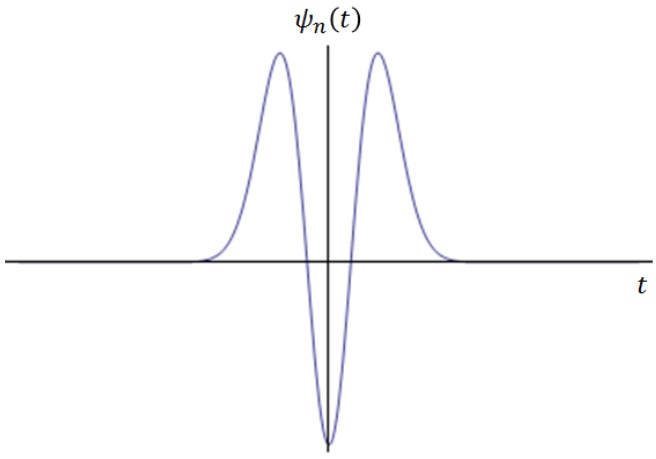

(c)

Figure–2.2 (*Continued*)

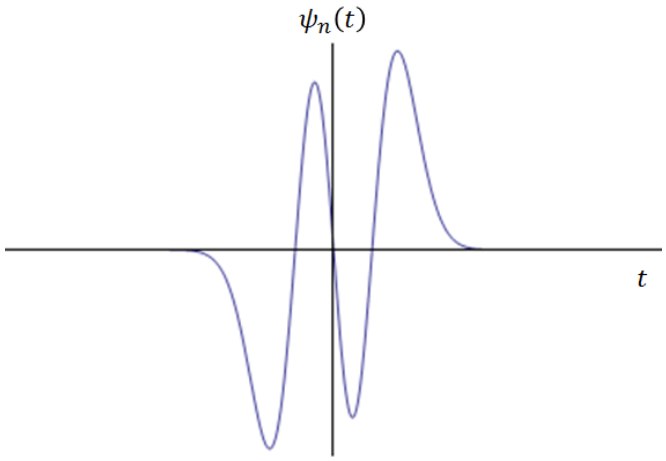

(d)

Figure–2.2 (*Continued*)

The first few Hermite polynomials are given as:

$$H_0(t) = 1 \quad \textbf{(2.3.6a)}$$

$$H_1(t) = 2t \quad \textbf{(2.3.6b)}$$

$$H_2(t) = 4t^2 - 2 \quad \textbf{(2.3.6c)}$$

$$H_3(t) = 8t^3 - 12t \quad \textbf{(2.3.6d)}$$

$$H_4(t) = 16t^4 - 48t + 12 \quad \textbf{(2.3.6e)}$$

$$H_5(t) = 32t^5 - 160t^3 + 120t \quad \textbf{(2.3.6f)}$$

$$H_{n+1}(t) = 2t\, H_n(t) - 2n\, H_{n-1}(t) \;\; n \geq 1 \quad \textbf{(2.3.6g)}$$

The Hermite polynomials $H_n(t)$ can be recursively obtained by the formula given by (2.3.6g).

2.3.2 Error Function

In the field of mathematics, the error function, also known as the Gauss error function is a special function of sigmoid shape which occurs in probability, statistics and partial differential

equations. The error function and the complementary error function are important special functions which appear in the solutions of diffusion problems in heat, mass and momentum transfer and in digital communication and signal processing areas. It is defined as **[107]**:

$$\text{erf}\,(x) = \frac{2}{\sqrt{\pi}} \int_0^x \exp(-t^2)\, dt \qquad \textbf{(2.3.7)}$$

A series approximation for small value of x of this function is given by:

$$\text{erf}\ (x) = \frac{2}{\sqrt{\pi}} \left(x - \frac{x^3}{3 \cdot 1!} + \frac{x^5}{5 \cdot 2!} - \frac{x^7}{7 \cdot 3!} + \cdots \right) \qquad \textbf{(2.3.8)}$$

while an approximate expression for large values of x can be obtained from:

$$\text{erf}\ (x) \cong 1 - \frac{\exp(-x^2)}{\sqrt{\pi}\, x} \left(1 - \frac{1}{2\, x^2} + \frac{1 \cdot 3}{(2\, x^2)^2} - \frac{1 \cdot 3 \cdot 5}{(2\, x^2)^3} + \cdots \right) \qquad \textbf{(2.3.9)}$$

Some properties related to erf function are:

(i) $\text{erf}\,(-\infty) = -1,$

(ii) $\text{erf}\ (+\infty) = 1,$

(iii) $\text{erf}\ (0) = 0,$

(iv) $\text{erf}\ (-x) = -\,\text{erf}\ (x),$

(v) $\text{erf}\ (x^*) = [\text{erf}\ (x)]^*$

(vi) $\frac{d}{dx}(\text{erf}\ (x)) = \frac{2\exp(-x^2)}{\sqrt{\pi}},$

(vii) $\int \text{erf}\ (x)\, dx = x\,\text{erf}\ (x) + \frac{\exp(-x^2)}{\sqrt{\pi}} + \text{constant}$

(viii) $\lim_{x \to -\infty} \text{erf}\ (x) = -1$

(ix) $\lim_{x \to \infty} \text{erf}\ (x) = 1$

(x) In general, $\frac{d^{n+1}}{dx^{n+1}}\text{erf}\ (x) = (-1)^n\, \frac{2}{\sqrt{\pi}}\, H_n\,(x) \exp(-x^2)\ (n = 0, 1, 2, \cdots)$

where $H_n(x)$ are the Hermite polynomials.

In addition to the error function, two other functions related to it are also in use by the research community. They are:

(i) the complementary error function, erfc is defined as:

$\text{erfc}\,(x) = 1 - \text{erf}\ (x)$

or, $\text{erfc}\,(x) = \frac{2}{\sqrt{\pi}} \int_x^{\infty} \exp(-t^2)$ **(2.3.10)**

which combined with the series expansion of the error function, $\text{erf}\,(x)$, provides the approximate expressions for small and large values of x as:

$$\text{erfc}\,(x) = 1 - \frac{2}{\sqrt{\pi}} \left(x - \frac{x^3}{3 \cdot 1!} + \frac{x^5}{5 \cdot 2!} - \frac{x^7}{7 \cdot 3!} + \cdots \right) \quad \textbf{(2.3.11)}$$

$$\text{erfc}\,(x) \cong \frac{\exp(-x^2)}{\sqrt{\pi}\, x} \left(1 - \frac{1}{2\, x^2} + \frac{1 \cdot 3}{(2\, x^2)^2} - \frac{1 \cdot 3 \cdot 5}{(2\, x^2)^3} + \cdots \right) \quad \textbf{(2.3.12)}$$

(ii) The imaginary error function, erfi defined as:

$$\text{erfi}\,(z) = -j\, \text{erf}\,(jz) \quad \textbf{(2.3.13)}$$

for $j = \sqrt{-1}$

Some properties related to erfc function are:

(i) $\text{erfc}\,(-x) = 2 - \text{erfc}\,(x)$

(ii) $\text{erfc}\,(-\infty) = 2$

(iii) $\text{erfc}\,(\infty) = 0$

(iv) $\text{erfc}\,(0) = 1$

(v) $\frac{d}{dx}\, \text{erfc}\,(x) = -\frac{2 \exp(-x^2)}{\sqrt{\pi}}$

(vi) $\int \text{erfc}\,(x)\, dx = x\, \text{erfc}\,(x) - \frac{\exp(-x^2)}{\sqrt{\pi}} + \text{constant}$

(vii) $\lim_{x \to -\infty} \text{erfc}\,(x) = 2$

(viii) $\lim_{x \to \infty} \text{erfc}\,(x) = 0$

(ix) $\int_0^{\infty} \text{erfc}\,(x)\, dx = 1/\sqrt{\pi}$

(x) $\int_0^{\infty} \text{erfc}^2\,(x)\, dx = \left(2 - \sqrt{2}\right)/\sqrt{\pi}$

2.3.3 Kummer Confluent Hypergeometric Function

The Kummer confluent hypergeometric function (CHF) belongs to an important class of special functions of mathematical physics with a large number of applications in different branches of quantum mechanics, atomic physics, acoustics, optics, electromagnetic theory, and in microwave engineering. It also finds wide applicability in digital communication and signal processing fields **[152]**. For example, CHF can be used to obtain a statistical description of the signal

parameter estimator. It also helps in the detection of a binary phase–modulated carrier which has been transmitted along with noise and demodulated by cross correlation and sampling at the receiver. In principle, the CHF function may be computed as a power series, an integral of a function, or a solution to a differential equation.

The confluent hypergeometric function of the first kind **[107]** is defined by the absolutely convergent infinite power series:

$$ {}_1F_1(a;b;z) = \sum_{n=0}^{\infty} \frac{a_n}{b_n} \frac{z^n}{n!} \quad \textbf{(2.3.14)} $$

where $\{a, b\}$ are parameters and $\{a_n, b_n\}$ are rising factorials. It is analytic, regular at zero entire single–valued transcendental function of all a, b, z (real and complex) except $b = 0, -1, -2, -3, \cdots$, for which it has simple poles For $a, b > 0$, it is represented by the following integral:

$$ {}_1F_1(a;b;z) = \frac{\Gamma(b)}{\Gamma(b-a)\,\Gamma(a)} \int_0^1 p^{a-1}\,(1-p)^{b-a-1} \exp(zv)\, dv \quad \textbf{(2.3.15)} $$

where $\Gamma(\cdot)$ is the gamma function. The CHF ${}_1F_1(a;b;z)$ can be obtained as the result of a limit process applied to the hypergeometric function ${}_2F_1(a,b;c;z)$. The hypergeometric function ${}_pF_q$ is defined in **[107]** as follows for $a_1, \cdots a_p, b_1, \cdots b_q, z \in \mathbb{C}$:

$$ {}_pF_q\left(a_1, \cdots a_p;\ b_1, \cdots b_q;\ z\right) = \sum_{j=0}^{\infty} \frac{(a_1)_j \cdots (a_p)_j}{(b_1)_j \cdots (b_q)_j} \frac{z^j}{j!} \quad \textbf{(2.3.16)} $$

where for some parameter σ, the Pochhammer symbol $(\sigma)_j$ is defined as:

$$ (\sigma)_0 = 1,\ (\sigma)_j = \sigma(\sigma+1)\cdots(\sigma+j-1), j = 1, 2, \cdots \quad \textbf{(2.3.17)} $$

The CHF is related to various elementary and special functions as follows:

$$ {}_1F_1(a;a;z) = \exp(z) \quad \textbf{(2.3.18)} $$

$$ {}_1F_1\left(\frac{1}{2};\frac{3}{2};-z^2\right) = \frac{\sqrt{\pi}}{2\,z}\operatorname{erf}(z) \quad \textbf{(2.3.19)} $$

The CHF function also contains other functions as special cases, including many that are widely used in mathematical physics. Special cases include the Bessel functions, the incomplete gamma

(and hence further special cases including error functions and Fresnel integrals), Laguerre polynomials, Hermite polynomials, Coulomb wave functions, and parabolic cylinder functions.

2.3.4 Gamma Function and Related Function

A transcendental function — the Gamma function, extends the values of the factorial $z!$ to any complex number z. It was introduced in 1729 by L. Euler in a letter to Ch. Goldbach, using the infinite product **[107]**:

$$\Gamma(z) = \lim_{n\to\infty} \frac{n!\, n^z}{z(z+1)\cdots(z+n)} = \lim_{n\to\infty} \frac{n^z}{z(1+z/2)\cdots(1+z/n)}, \quad \textbf{(2.3.20)}$$

which was used by L. Euler to obtain the integral representation (Euler integral of the second kind):

$$\Gamma(z) = \int_0^\infty \exp(-t)\, t^{z-1}\, dt \quad \textbf{(2.3.21)}$$

which converges in the right half of the complex plane $Re(z) > 0$. Indeed, we have

$$\Gamma(x+jy) = \int_0^\infty \exp(-t)\, t^{x-1+jy}\, dt = \int_0^\infty \exp(-t)\, t^{x-1} \exp(jy\log(t))\, dt \quad \textbf{(2.3.22)}$$

$$= \int_0^\infty \exp(-t)\, t^{x-1} [\cos(y\log(t)) + j\, \sin(y\log(t))]\, dt \quad \textbf{(2.3.23)}$$

The expression in the square brackets in (2.3.23) is bounded for all t; convergence at infinity is provided by $\exp(-t)$, and for the convergence at $t = 0$ we must have $x = Re(z) > 1$.

2.3.4.1 Fundamental relations and properties of Gamma function

(1) Euler's functional equation:

$z\,\Gamma(z) = \Gamma(z+1)$,

or $\Gamma(z) = \frac{1}{z\cdots(z+n)}\,\Gamma(z+n+1)$;

$\Gamma(1) = 1$, $\Gamma(n+1) = n!$ if n is an integer; it is assumed that $0! = \Gamma(1) = 1$.

(2) Euler's completion formula:

$\Gamma(z)\,\Gamma(1-z) = \frac{\pi}{\sin(\pi z)}$

In particular, $\Gamma(1/2) = \sqrt{\pi}$;

$\Gamma\left(n+\frac{1}{2}\right) = \frac{1\cdot 3\cdots(2n-1)}{2^n}\sqrt{\pi}$

If $n > 0$ is an integer;

$\left|\Gamma\left(\frac{1}{2}+jy\right)\right|^2 = \frac{\pi}{\cosh(y\pi)}$, where y is real.

(3) Gauss' multiplication formula:

$\prod_{k=0}^{m-1}\Gamma\left(z+\frac{k}{m}\right) = (2\pi)^{(m-1)/2}\, m^{(1/2)-mz}\,\Gamma(mz),\ m = 2, 3, \cdots$

If $m = 2$, this is the Legendre duplication formula.

2.4 PRELIMINARIES OF FRACTIONAL FOURIER TRANSFORM (FrFT)

The Fourier transform (FT) is one of the most widely and frequently used signal processing tool for signal analysis. The generalization of the classical Fourier transform—the fractional Fourier transform (FrFT)—has a long history dating back to the 1930s **[65]**. For the first time, Namias in 1980s employed it to solve differential and partial differential equations in quantum mechanics from classical quadratic Hamiltonians **[154]**. Later, McBride and Kerr improved the former results **[6]** to develop operational calculus to define the FrFT.

The continuous fractional Fourier transform (FrFT) performs the spectrum rotation of the signal in the entire time–frequency plane, and is becoming an important signal processing tool for time–varying signal analysis.

In recent years, the FrFT has attracted a considerable amount of attention, resulting in main applications in the areas of optics and signal processing. The FrFT has proved to be a suitable potential candidate in the signal processing community, with diverse applications ranging from optical signal processing, time–variant filtering and multiplexing **[65, 124]**, swept–frequency filters **[95]**, radar and sonar signal processing **[126, 128]**, communication **[114]**,

correlation **[11, 121, 127]**, pattern recognition, time–frequency signal processing, multiplexing **[64, 93, 98, 162]**, digital watermarking **[61, 116, 143]**, and image encryption **[65]**, beamforming for the mobile antennas **[120]** and also in video encryption algorithm **[47]** and to name a few. In addition, **[147]** proposed an uncertainty relation on the product of the signal representations in the two FrFT domains for the real signals.

2.4.1 Mathematical Properties of FrFT

The FrFT is the generalized formula for the Fourier transform that transforms a function into an intermediate domain between time and frequency. It can also be interpreted as a rotation of the time–frequency plane. The fractional Fourier transform is also called *rotational Fourier transform* or *angular Fourier transform* in some of the rich literature.

The traditional Fourier transform decomposes a signal into sinusoids, whereas the FrFT expresses the signal in terms of the orthonormal basis functions formed by chirps that is, to say the FrFT is a time–frequency transform, which uses a chirp as a basis function **[65]**. It is also suitable for the analysis of linear chirp signals. It can perform pulse compression, similar to the matched filter, when the transform order is matched to the chirp rate of the signal.

The FrFT can be understood as a Fourier transform to the ath power where, a is not required to be an integer. The signals with significant overlap in both the time and frequency domain may have a little or no overlap in the fractional Fourier transform domain (FrFTD). **[65]**

The FrFT of order a of an arbitrary function $x(t)$ and its inverse with an angle φ are defined as **[95]**:

$$X^{\varphi}(u_{\varphi}) = \mathrm{T}_{\mathcal{F}}{}^{\varphi}[x(t)] = \int_{-\infty}^{\infty} K_a(u_{\varphi}, t)\, x(t)\, dt \qquad \textbf{(2.4.1)}$$

$$x(t) = \int_{-\infty}^{\infty} K_{-a}(u_{\varphi}, t) X^{\varphi}(u_{\varphi})\, du_{\varphi} \qquad \textbf{(2.4.2)}$$

where a is the fractional Fourier transformation order corresponding to the rotation angle $\varphi = a\pi/2$ with $a \in \mathbb{R}$ and $\mathrm{T}_{\mathcal{F}}{}^{\varphi}(\cdot)$ denotes the FrFT operator. The u_{φ} axis is regarded as the fractional Fourier domain, and the variable u_{φ} is the fractional Fourier frequency and $K_a(u_{\varphi}, t)$ is the FrFT kernel. The kernel of the FrFT is defined by the following equation:

$$K_a\left(u_\varphi, t\right) =$$

$$\begin{cases} \sqrt{\frac{1-i\cot\varphi}{2\pi}}\exp\left[i\left(\frac{t^2+{u_\varphi}^2}{2}\right)\cot\varphi - i\,u_\varphi\,t\,\csc\varphi\right] & \text{if } \varphi \text{ is not a multiple of } \pi, \\ \delta\left(t-u_\varphi\right) & \text{if } \varphi \text{ is a multiple of } 2\pi, \\ \delta\left(t+u_\varphi\right) & \text{if } \varphi+\pi \text{ is a multiple of } 2\pi. \end{cases} \quad \textbf{(2.4.3)}$$

and the FrFT is defined by means of the transformation kernel:

$$\mathrm{T}_{\mathcal{F}}{}^{\varphi}[x(t)] = X^{\varphi}\left(u_\varphi\right) = \int_{-\infty}^{\infty} x(t)\,K_a\left(u_\varphi, t\right)dt \quad \textbf{(2.4.4)}$$

$$= \begin{cases} \sqrt{\frac{1-i\cot\varphi}{2\pi}}\int_{-\infty}^{\infty} x(t)\exp\left[i\left(\frac{t^2+{u_\varphi}^2}{2}\right)\cot\varphi - i\,u_\varphi\,t\,\csc\varphi\right] & \text{if } \varphi \text{ is not a multiple of } \pi, \\ \delta(t) & \text{if } \varphi \text{ is a multiple of } 2\pi, \\ \delta(-t) & \text{if } \varphi \text{ is a multiple of } 2\pi, \end{cases}$$

Thus, the FrFT reduces to the conventional FT for $\varphi = \pi/2$. Hence, if we substitute $\varphi = \pi/2$ in the properties of the FrFT, we obtain the properties of the conventional FT.

2.4.1.1 Properties satisfied by the kernel of the FrFT

The transformation kernel (2.4.3) can be thought of as a sequence of following operations:

(i) Multiplication by a chirp in the reference domain;
(ii) A conventional Fourier transform;
(iii) Frequency scaling by a factor $\csc\varphi$;
(iv) Multiplication by a chirp in the transformed domain followed by an amplitude scaling.

The conventional Fourier transform is a decomposition of the signal into harmonics (sinusoids). The FrFT is a decomposition of the signal into linear chirps having fixed sweep rate $\frac{1}{2}\cot\varphi$, distinguished by a time shift and phase factor such that,

$$K_a\left(u_\varphi, t\right) = e^{-j\frac{{u_\varphi}^2}{2}\tan\varphi}K_a\left(t-u_\varphi\csc\varphi, 0\right) \quad \textbf{(2.4.5)}$$

Here, $K_a\left(u_\varphi, t\right)$ is the FrFT kernel which holds the following properties:

Orthogonal:

$$\int_{-\infty}^{\infty} K_a(u_\varphi, t)\ K_a{}^*(v_\varphi, t)dt = \delta(u_\varphi - v_\varphi) \quad \textbf{(2.4.6)}$$

Additive:

$$\int_{-\infty}^{\infty} K_a(u_\varphi, t)\, K_p(m, u_\varphi)du_\varphi = K_{a+p}(m, t) \quad \textbf{(2.4.7)}$$

Unitary:

$$K_{-\beta}(u_\varphi, t) = K_\beta{}^*(u_\varphi, t) \quad \textbf{(2.4.8)}$$

where the asterisk $*$ represents the complex conjugate.

2.4.1.2 FrFT as a tool in time–frequency plane

Time and frequency represent the two fundamental physical variables for signal analysis and processing. The most widely and extensively used Fourier transform (FT) provides a mapping between the time domain and the frequency domain **[65]**. The classical continuous–time Fourier transform $X(\omega)$ of a time domain signal $x(t)$ is defined as:

$$(\Im x)(\omega) = X(\omega) = \frac{1}{\sqrt{2\pi}}\int_{-\infty}^{\infty} x(t)\ e^{-j\omega t}\, dt \quad \textbf{(2.4.9)}$$

where $\Im$ denotes the FT operator.

The inverse Fourier transform (IFT) is defined as:

$$x(t) = \frac{1}{\sqrt{2\pi}}\int_{-\infty}^{\infty} e^{j\omega t}\ X(\omega)\ d\omega \quad \textbf{(2.4.10)}$$

It is very well–known that the signal can be transformed from the time domain to the frequency domain by performing the FT. To perform the FT two times cannot transform the signal back to the time domain and it will become a time reverse operation. Also the operation of performing the FT four times is the same as the identity operation, and one can get back the signal from the frequency domain to the time domain by performing the FT three times.

Thus, performing the Fourier transformation can transform the signal to the frequency domain. We obtain the fractional Fourier transform by doing the FT φ times, where φ is not an

integer number as is shown in Figure-2.3. This operation is defined as the *fractional Fourier transform* (FrFT). Thus, the FrFT can be viewed as the generalization of FT. So many properties associated with the FT can be generalized by using the FrFT.

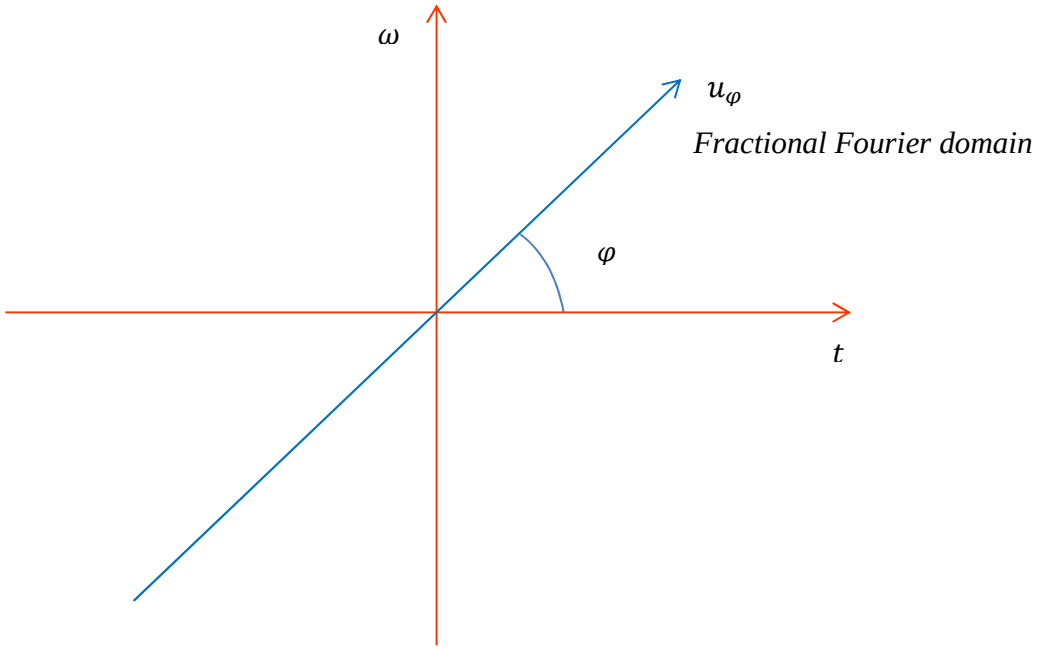

Figure–2.3: Fractional Fourier domain u_φ of the time–frequency plane associated with the transform angle φ.

Thus, FrFT is viewed as a very powerful tool for signal processing, and it exhibits potential signal processing and image processing applications in the research community.

2.4.1.3 Properties of FrFT

Some of the essential properties of FrFT are listed below **[65]**:

(i) The fractional Fourier transform operator is linear.

(ii) The fractional Fourier transform operator satisfies inverse property, $(\mathfrak{T}_{\mathcal{F}}{}^{\varphi})^{-1} = \mathfrak{T}_{\mathcal{F}}{}^{-\varphi}$.

(iii) The first–order transform $\mathfrak{T}_{\mathcal{F}}{}^{1}$ corresponds to the classical Fourier transform $\mathfrak{I}$ and the

zeroth–order transform $\mathrm{T}_{\mathcal{F}}{}^{0}$ means doing no transform.

(iv) The fractional Fourier transform operator satisfies periodicity property, $\mathrm{T}_{\mathcal{F}}{}^{\varphi}\big(x(t)\big) = \mathrm{T}_{\mathcal{F}}{}^{\varphi+2N\pi}\big(x(t)\big)$, where N is an integer.

(v) The fractional operator is additive, $\mathrm{T}_{\mathcal{F}}{}^{\gamma}\mathrm{T}_{\mathcal{F}}{}^{\theta} = \mathrm{T}_{\mathcal{F}}{}^{\gamma+\theta}$.

Table 2.1 presents some important and useful properties of the FrFT, which are the extensions of the corresponding properties of the FT. The property 10 shows the parity property: If $x(t)$ is even, then $X^{\varphi}\big(u_{\varphi}\big)$ is even; if $x(t)$ is odd, then $X^{\varphi}\big(u_{\varphi}\big)$ is odd. **[65]**

TABLE 2.1

PROPERTIES OF FrFT

	Property Description	**Signal**	**φth order FrFT**
1.	Linearity	$ax(t) + by(t)$	$aX^{\varphi}\big(u_{\varphi}\big) + bY^{\varphi}\big(u_{\varphi}\big)$
2.	Time shift	$x(t-\tau)$	$X^{\varphi}\big(u_{\varphi} - \tau\cos\varphi\big)e^{j\frac{\tau^2}{2}\sin\varphi\cos\varphi - ju_{\varphi}\tau\sin\varphi}$
3.	Modulation	$x(t)e^{jqt}$	$X^{\varphi}\big(u_{\varphi} - q\sin\varphi\big)e^{-j\frac{q^2}{2}\sin\varphi\cos\varphi + ju_{\varphi}q\cos\varphi}$
4.	Time scaling	$x(ct)$	$\sqrt{\frac{1-j\cot\varphi}{c^2-j\cot\varphi}}\,e^{j\frac{u_{\varphi}{}^2}{2}\cot\varphi\left(1-\frac{\cos^2\varphi}{\cos^2\gamma}\right)}X^{\gamma}\left(u_{\varphi}\frac{\sin\gamma}{c\sin\varphi}\right)$ for $\gamma = \arctan(c^2\tan\varphi)$
5.	Chirp multiplication	$x(t)e^{-j\pi rt^2}$	$\sqrt{\frac{1-j\cot\varphi}{1-j\cot\beta}}\,e^{j\pi u_{\varphi}{}^2\left(1-\frac{\sin\beta\cos\beta}{\sin\varphi\cos\varphi}\right)}X^{\beta}\left(u_{\varphi}\frac{\sin\beta}{\sin\varphi}\right)$ where $\cot\beta = \cot\varphi - r$.

6.	Chirp convolution	$x(t)$ $* e^{-j\frac{\pi}{4}}\sqrt{\frac{1}{r}}\exp\left(\frac{j\pi t^2}{r}\right)$	$\sqrt{\frac{1+j\tan\varphi}{1-j\cot\beta}}\exp\left[-j\pi {u_\varphi}^2\tan\varphi\left(1+\frac{\sin\beta\cos\beta}{\sin\varphi\cos\varphi}\right)\right]X^\beta\left(-u_\varphi\frac{\sin\beta}{\cos\varphi}\right)$ where, $\cot\beta=-\tan\varphi-r$ and $'*'$ denotes the convolution operation.
7.	Differentiation	$\frac{dx(t)}{dt}$	$X^{\varphi\prime}(u_\varphi)\cos\varphi+ju_\varphi X^\varphi(u_\varphi)\sin\varphi$ where, $X^{\varphi\prime}(u_\varphi)=\frac{dX^\varphi(u_\varphi)}{du_\varphi}$
8.	Integration	$\int_k^t x(t')dt'$	$\sec\varphi\, e^{-j\frac{{u_\varphi}^2}{2}\tan\varphi}\int_k^{u_\varphi}X^\varphi(z)e^{j\frac{z^2}{2}\tan\varphi}\,dz,$ $\forall\ \varphi\neq(n+1)\frac{\pi}{2}$
9.	Multiplication by t	$tx(t)$	$u_\varphi X^\varphi(u_\varphi)\cos\varphi+jX^{\varphi\prime}(u_\varphi)\sin\varphi$
10.	Parity	$x(-t)$	$X^\varphi(-u_\varphi)$
11.	Division by t	$\frac{x(t)}{t}$	$-j\sec\varphi\ e^{j\frac{{u_\varphi}^2}{2}\cot\varphi}\int_{-\infty}^{u_\varphi}X^\varphi(z)e^{-j\frac{z^2}{2}\cot\varphi}dz,$ $\forall\ \varphi\neq n\pi$
12.	Parseval's Relation	$\int_{-\infty}^{\infty}x(t)y^*(t)\,dt$ $\int_{-\infty}^{\infty}\lvert x(t)\rvert^2dt$	$\int_{-\infty}^{\infty}X^\varphi(u_\varphi)\,Y^{\varphi*}(u_\varphi)du_\varphi$ $\int_{-\infty}^{\infty}\lvert X^\varphi(u_\varphi)\rvert^2\,du_\varphi$

$\left|X^{\varphi}(u_{\varphi})\right|^2$ is the fractional energy spectrum of the signal $x(t)$, with an angle φ. If $x(t)$ is real, we can get one property which is related with $X^{\varphi}(u_{\varphi})$ as:

$$X^{-\varphi}(u_{\varphi}) = X^{\varphi *}(u_{\varphi}) \qquad \textbf{(2.4.11)}$$

where the notation $*$ denotes the complex conjugate.

Table 2.2 provides the transform results for some common functions. **[65]**

TABLE 2.2

TRANSFORMS OF SOME COMMON WELL–KNOWN FUNCTIONS

	Signal	**φth order FrFT**	**Condition**
1.	$\delta(t-\tau)$	$\sqrt{\frac{1-j\cot\varphi}{2\pi}}\, e^{j\frac{{u_\varphi}^2+\tau^2}{2}\cot\varphi - ju_\varphi\tau\csc\varphi}$	if φ is not a multiple of π.
2.	1	$\sqrt{1+j\tan\varphi}\, e^{-j\frac{{u_\varphi}^2}{2}\tan\varphi}$	if $\varphi-\pi/2$ is not a multiple of π.
3.	e^{jqt}	$\sqrt{1+j\tan\varphi}\, e^{-j\frac{{u_\varphi}^2+q^2}{2}\tan\varphi + ju_\varphi q\sec\varphi}$	if $\varphi-\pi/2$ is not a multiple of π.
4.	$e^{jc\frac{t^2}{2}}$	$\sqrt{\frac{1+j\tan\varphi}{1+c\tan\varphi}}\, e^{j\frac{{u_\varphi}^2}{2}\frac{c-\tan\varphi}{1+c\tan\varphi}}$	if $\varphi-\arctan(c)-\pi/2$ is not a multiple of π.
5.	$e^{-\frac{t^2}{2}}$	$e^{-\frac{{u_\varphi}^2}{2}}$	

6.	$H_n(t)\, e^{-\frac{t^2}{2}}$ (H_n: Hermite polynomial)	$e^{-jn\varphi}\, H_n(u_\varphi)\, e^{-\frac{{u_\varphi}^2}{2}}$	
7.	$e^{-p\frac{t^2}{2}}$	$\sqrt{\frac{1-j\cot\varphi}{p-j\cot\varphi}}\, e^{j\frac{{u_\varphi}^2}{2}\frac{(p^2-1)\cot\varphi}{(p^2+\cot^2\varphi)}}\, e^{-\frac{{u_\varphi}^2}{2}\frac{p\csc^2\varphi}{(p^2+\cot^2\varphi)}}$	
8.	$e^{\pm\frac{j}{2}(at^2+bt)}$	$\sqrt{\frac{1+j\tan\varphi}{1\pm a\tan\varphi}}\, e^{j\frac{{u_\varphi}^2(a\mp\tan\varphi)+2u_\varphi b\sec\varphi\mp b^2\tan\varphi}{2(a\tan\varphi\pm1)}}$ for $\cot\varphi \neq \pm a$	

2.4.2 Discrete FrFT (DFrFT)

The FrFT is a generalization of the conventional Fourier transform, and has aroused wide attention in recent years, and has found many important applications in the areas of optics, quantum mechanics, image processing, signal processing, etc.

The FrFT is interpreted as a counter–clockwise rotation of the time–frequency plane and has been proven to relate to other time varying signal analysis tools, such as, Wigner–Ville distribution (WVD), short–time Fourier transform (STFT), wavelet transform, and so on **[65]**.

From many years, the research community was in search of the efficient discrete computational method, which plays a vital role for the application of the FrFT to signal processing. However, the satisfactory definition of the discrete FrFT (DFrFT) that is fully consistent with the continuous FrFT was lacking, but still many prominent scientists and researchers have contributed a lot in this direction and provided a variety of approaches for its

digital computation. The basic instinct to establish the discrete version of the FrFT definition should follow the same relation as the discrete Fourier transform (DFT) has with the classical Fourier transform. The ideal DFrFT will be a generalization of the DFT that obeys the rotation rules as the continuous FrFT and provides similar results as the FrFT. **[65]**

The discrete version or implementation of the FrFT should obey the properties of unitarity, index additivity, reduction to DFT when $\varphi = \pi/2$, and approximation of the continuous FrFT.

Several publications have appeared in the research community proposing the discretization of the continuous FrFT. **[28, 31, 39, 66, 84, 135, 139]**

In **[133]**, Pei *et al*. have proposed a new type of DFrFT algorithm, which has the *advantage* of unitary, additivity, and flexibility and the added advantage of obtaining the closed–form analytic expression. The performance of this algorithm is very similar to the continuous FrFT and is efficiently calculated by fast Fourier transform.

The authors of **[133]** presented a good review of the DFrFT algorithms along with their advantages and disadvantages. For the proposed study, the DFrFT algorithm of **[133]** is used as it exhibits many of the important properties of the continuous FrFT.

2.5 APPLICATIONS OF FODD IN FILTERING AND EDGE DETECTION

The FODD finds numerous applications in one–dimensional and two–dimensional applications of signal and image processing. It includes the signal filtering operation and the edge detection operation. Vast amount of literature are available in the research community that come up for these applications.

Samadi *et al*. **[146]** proposed a discrete–time fractional–order differentiator to obtain the fractional order derivatives of Riemann–Liouville type for a uniformly sampled polynomial signal. The approach is in the time domain, where the input signal is represented in continuous time using the Newton series. The closed–form expressions for the coefficients of both the integer and the fractional–order differentiators of arbitrary order are also obtained. Also, it is

mathematically proved that the frequency response of a system with integer values of fractional derivative order parameter is a Hermite approximation to the ideal response at the origin.

Zhao *et al*. **[70]** presented a novel method of designing the fractional order FIR differentiators in the frequency domain. A novel method is proposed for designing digital FIR fractional order differentiator using the frequency response approximation. The FIR filter is chosen to approximate to the ideal digital fractional order differentiator under the weighting mean square error sense of the frequency response. It is shown through simulations that the designed FIR fractional order differentiator can accurately calculate the fractional derivative of given digital signal and thus the definition of the fractional order differentiator in the frequency domain is tunable and the design approach is effective.

Tseng *et al*. **[34]** investigated the design of fractional order differentiator based on the radial basis function interpolation method. It gets the advantage that the design error can be reduced by suitably choosing the shape parameter of the radial basis function. The radial basis function based non–integer delay sample estimation method is applied to obtain the transfer function of the fractional order differentiator. Finally, the applications in digital image sharpening and parameter estimation of fractional noise processes are studied to demonstrate the usefulness of the design approach. Also, a second order microwave differentiator is also implemented by using microstrip transmission lines. In particular, the *z*–domain formulations of scattering characteristics of nonuniform transmission lines facilitate the implementation of discrete domain differentiator in microwave circuits **[19]**.

Tseng *et al*. **[36]** presented the design of fractional order differentiator based on the discrete Fourier transform (DFT) interpolation method. The initial studies shows that the DFT interpolation and the fractional order differentiator design are two independent research topics and they have attempted to combine the two ideas to get a new kind of fractional order differentiating filter in the signal processing area.

Chen *et al*. **[49]** proposed the new design method for digital fractional order Savitzky–Golay (SG) differentiator. It generalizes the SG filter from an integer order to the fractional order for estimating the fractional order derivative of the contaminated signal. It uses the polynomial

least–squares method and the Riemann–Liouville fractional derivative definition to estimate the fractional order derivative of the noise–free signal and the noisy signal.

Tseng *et al*. **[37]** proposed the design of fractional order differentiator using discrete cosine transform. It is different from other design methods of the researchers in the sense that it uses the discrete cosine transform–based interpolation method, to compute the fractional derivative of a given signal. It also get the advantage of having the closed–form design.

Mathieu *et al*. **[26]** demonstrates the edge detection operation based on non–integer (fractional) order differentiation. It improves the criterion of thin detection, or detection selectivity in the case of parabolic luminance transitions, and the criterion of immunity to noise, which can be interpreted in terms of robustness to noise in general.

Yang *et al*. **[69]** proposes a new edge detection operator that adopts fractional differentiation and integration. Its performance in terms of detection accuracy and noise immunity of the operator are compared with those of the traditional operators through examples. It eliminates the smoothing preprocessing and provides a new approach to tune the compromise between noise immunity and detection accuracy.

Chen *et al*. **[158]** proposes the fractional differential method for edge detection operation. It mainly discusses how to use the advantages of the fractional differential method to improve the shortcomings of Roberts edge detection operator. So it puts forward a new method based on the combination of fractional differential and Roberts operator and gets the advantage to detect edges with high accuracy, more details, fine distinction and has good noise immunity.

2.6 MOTIVATION

As inferred from the study of available literature in the research community, a vast amount of research work has been carried out in the areas of integer–order and fractional–order digital differentiators. Various applications have also been carried out using them in the signal and image processing domains. The insightful concept of FrFT has also been applied for different applications in the engineering disciplines. But that amounts to be in isolation with only one variable parameter as the degree of freedom.

So an interest urged to incorporate the concept of fractional order calculus for designing the fractional order differentiators, which has a variable parameter known as the fractional derivative order parameter. Thereby, amalgamating the two different concepts of FOC and FrFT, a new kind of differentiator could be proposed. So, the proposed differentiator will perform in the time–frequency plane of the fractional Fourier transform. Thus, there is the advantage of having two degrees of freedom, as against the individual parameter of the FrFT.

Thus interestingly, based on the relevant facts and the rich literature, an attempt is made to outline the gaps in the study and to design the statement of problems for the proposed work.

2.6.1 Gaps in the Study

The most of the literature available mainly focuses on the work done on DD, FODD and FrFT in isolation. Still a lot of work has to be carried out for the design of DD in the fractional domain.

There is a scope of research motivation for the design of DD in the fractional domain. A new mathematical analysis has to be carried out to design DD in the fractional domain. It may be either FOC approach or FrFT approach.

Simultaneously, a new analytical method could be developed to analyze window functions such as, Dirichlet, Generalized “Hamming” etc. in the fractional domain and to investigate their various parameters like maximum side lobe level (MSLL), half main lobe width (HMLW), side–lobe fall–off rate (SLFOR) through simulations. The advantage that is obtained from FrFT is that it contains an adjustable parameter with which the various window parameters can be controlled and much better results can be obtained as compared to the classical Fourier transformation techniques. Thus, an attempt can be made to design DD using window method in the fractional Fourier transform domain and to analyze its behavior in the time–frequency plane.

The research focus can also be extended for the one–dimensional application of signal filtering operation and the two–dimensional application of the edge detection on images by utilizing the designed fractional order differentiator in the fractional Fourier transform domain.

These are some of the gaps as they are identified during the course of literature survey.

2.6.2 Statement of Problems

Based on the initial studies, literature survey reported and the understanding established, the following statement of problems are undertaken in this course of study:

(i) The areas of FOC, FrFT and DD will be reviewed in depth and design methods for implementing DD will be studied and simulated accordingly.

(ii) A detailed analysis and design of DD in the fractional domain will be done.

(iii) The one-dimensional application of DD and its comparative study with the existing techniques will be studied.

(iv) The two-dimensional application of DD in images will be studied.

The above mentioned problems are dealt with detailed mathematical analysis, appropriate applications and simulation studies in the following Chapters.

2.7 RESEARCH METHODOLOGY

The design of fractional order differentiating filter is important for various engineering applications. In this research work, the study of FOC, FrFT and DD will be considered in greater detail. Consequently, the design of DD based on FOC and FrFT theory will also be analyzed in depth. All the requisite mathematical equations governing the design of DD in the fractional domain (that is, fractional order differentiator in the fractional Fourier transform domain) will be examined broadly. The design of DD in the fractional domain using the window functions will also be considered, both analytically and through simulations. Then the benefits of utilizing DD in the fractional domain will be revealed in various applications of one–dimensional and two–dimensional forms as in filtering operation and edge detection on images.

The proposed work model describing the fractional order differentiation in the fractional Fourier transform domain has been simulated on the platform of Wolfram Mathematica® software (version 8.0) on a system having configuration Pentium 4, with an Intel® CPU 1.8 GHz processor having 1 GB RAM.

CHAPTER 3

INTEGER–ORDER DIGITAL DIFFERENTIATOR IN FrFTD

THE FILTERING OF THE DIGITIZED DATA is the oldest research discipline in the field of digital signal processing (DSP). Its origin goes back to forty years and today there has been a considerable interest in the field of digital filtering that the quantity of rich literature pertaining to it exceeds to that of any other research field in the digital signal processing regime **[52]**. Many researchers have contributed a lot in the designing of digital differentiator (DD) or differentiating filter in the Fourier transform domain. Following this, an attempt is made to design the digital differentiator in the fractional Fourier transform domain both analytically and through simulations.

3.1 DIGITAL DIFFERENTIATOR AT A GLANCE

Filtering is the processing of time–domain signal resulting in some change in the signal's original spectral content. The change is usually the reduction or filtering out, of some unwanted input spectral components; that is, filters allow certain frequencies to pass while attenuating other frequencies. **[125]**

An ideal discrete–time differentiator is a linear system in which, when samples of a band–limited continuous signal are used as input, the output samples represent the derivative of the continuous signal **[131]**. More precisely, given a continuous–time signal $x_a(t)$ band–limited to $[-\pi/T\,,\pi/T)$, when its corresponding sampled version $x(n) = x_a(nT)$ is input to an ideal differentiator, it produces the output signal $y(n)$ such that:

$$y(n) = \frac{dx_a(t)}{dt}\Big|_{t=nT} \quad \textbf{(3.1.1)}$$

If the Fourier transform of the continuous–time signal is denoted by $X_a(j\Omega)$, then the Fourier transform of its derivative can be deduced as $j\Omega X_a(j\Omega)$ **[53]**. Therefore, an ideal discrete–time differentiator is characterized by a frequency response $H(e^{j\omega})$ of the following form:

$$H(e^{j\omega}) = j\omega, \text{ for } -\pi \leq \omega \leq \pi \quad \textbf{(3.1.2)}$$

The magnitude and phase responses of a differentiator are depicted in Figure-3.1.

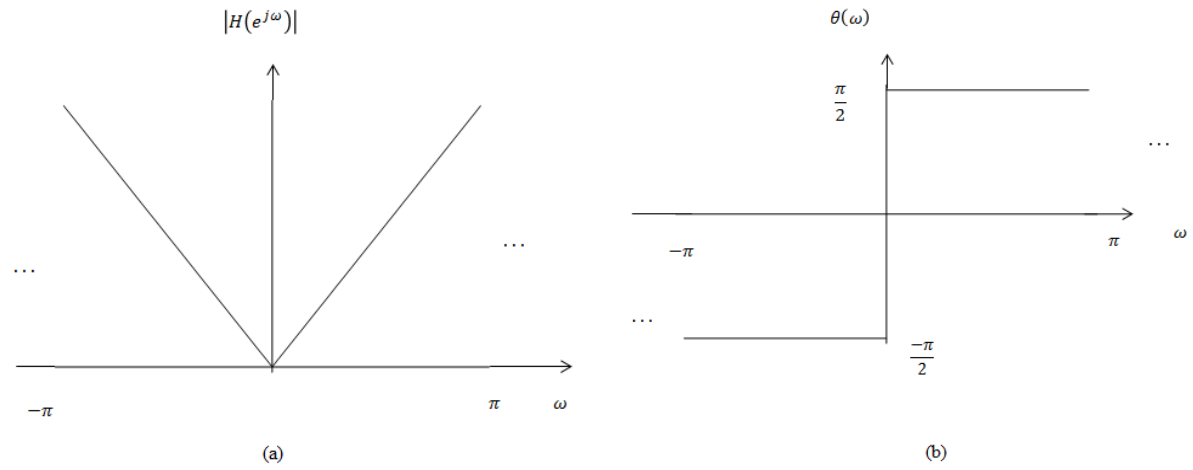

Figure–3.1: Magnitude and phase responses of digital differentiator.

Using the relationship between $H(e^{j\omega})$ and $h(n)$ as:

$$H(e^{j\omega}) = \sum_{n=-\infty}^{\infty} h(n)e^{-j\omega n} \quad \textbf{(3.1.3)}$$

$$h(n) = \frac{1}{2\pi}\int_{-\pi}^{\pi} H(e^{j\omega})e^{j\omega n}d\omega \quad \textbf{(3.1.4)}$$

The corresponding impulse response $h(n)$ of the differentiator is given by:

$$h(n) = \frac{1}{2\pi}\int_{-\pi}^{\pi} j\omega e^{j\omega n}d\omega = \begin{cases} 0 & \text{for } n = 0 \\ \frac{1}{2\pi}e^{j\omega n}\left(\frac{\omega}{n} - \frac{1}{jn^2}\right)\Big|_{-\pi}^{\pi} = \frac{(-1)^n}{n} & \text{for } n \neq 0 \end{cases} \quad \textbf{(3.1.5)}$$

The design of an FIR differentiator can be considered as the problem of designing an Nth order causal linear phase FIR filter with the impulse response $h(n)$ of length $N+1$ and transfer function $H(z)$, defined as:

$$H(z) = \sum_{n=0}^{N} h(n) z^{-n} \quad \textbf{(3.1.6)}$$

The frequency response $H\left(e^{j\omega T}\right)$ approximates the desired frequency function $D\left(e^{j\omega T}\right)$ given by:

$$D\left(e^{j\omega T}\right) = e^{-jN\omega T/2}(j\omega T)^{K} \quad \textbf{(3.1.7)}$$

in the frequency region $\omega T \in [0, \omega_c T]$, $\omega_c T \leq \pi$. The desired function in (3.1.7) corresponds to a causal digital Kth degree differentiator. **[164]**

The frequency response of linear phase FIR filters can be rewritten as:

$$H\left(e^{j\omega T}\right) = \begin{cases} e^{-jN\omega T/2} H_R(\omega T), \text{Type I, II} \\ j e^{-jN\omega T/2} H_R(\omega T) \text{ Type III, IV} \end{cases} \quad \textbf{(3.1.8)}$$

where $H_R(\omega T)$ is a real–valued zero–phase frequency response. It can be inferred from the above equations that a Type I or II filter must be used when K is even whereas, a Type III or IV filter must be used when K is odd. Various characteristics of FIR differentiators depending upon FIR filter types is summarized as in Table 3.1.

TABLE 3.1

FIR DIFFERENTIATOR CHARACTERISTICS

Type	**Number of distinct coefficients**	***K***	**Full bandwidth**
I	$(N/2)+1$	Even	Feasible
II	$(N+1)/2$	Even	Infeasible
III	$N/2$	Odd	Infeasible
IV	$(N+1)/2$	Odd	Feasible

With the increasing trend towards digital simulation of physical systems, optimal techniques for designing DDs are being more widely investigated. Kaiser **[81]** has presented a review of various techniques for designing both nonrecursive and recursive differentiators.

3.2 CONFIGURATIONS OF DD

The DDs are available in two configurations as illustrated below.

3.2.1 Finite Impulse Response DD (FIR–DD)

Finite impulse response (FIR) digital differentiators with linear phase characteristics are designed using various techniques for low–frequency **[20, 24, 76]**, midband frequency [**22**], high–frequency **[23]** and wideband **[134, 136, 148]** operations. Some of the commonly used design procedures include window based designs **[1]**, minimax designs **[2]**, eigenfilter approach **[134]**, optimization techniques, the weighted least squares techniques **[148]**, optimum noise attenuation **[122]**, Taylor series **[75]**.

3.2.2 Infinite Impulse Response DD (IIR–DD)

The infinite impulse response (IIR) digital differentiators are obtained by inversion and magnitude stabilization of the existing digital integrators. The commonly used digital integrators are backward or rectangular integrator, Tustin or trapezoidal integrator **[104]**. Thus, it is observed that the magnitude response of an ideal integrator lies between rectangular and trapezoidal integrators and also between trapezoidal and Simpsons integrators. Various techniques have been and are currently been used to design the IIR digital differentiators utilizing the numerical analysis principles. **[92, 105, 106, 118]**

3.3 COMPARATIVE ANALYSIS OF FIR–DD AND IIR–DD

There exists two configurations of DD namely, FIR–DD and IIR–DD as explained in the Section 3.2. The comparison can be established between the two kinds of differentiating filters. **[1, 52, 53, 81, 85, 96, 99, 125]**

(i) FIR filters are dependent upon linear phase characteristics, whereas IIR filters are used for applications which are not linear.

(ii) FIR is always stable, whereas IIR can be unstable.

(iii) FIR cannot simulate analog filter responses, but IIR is designed to do that accurately.

(iv) IIR filters make polyphase implementation possible, whereas FIR can always be made causal.

(v) FIR filters are helpful to achieve fractional constant delays. The number of multiplications and additions is used as a criterion for an IIR and FIR filter comparison. IIR filters require more number of multiplications and additions when compared to FIR, because FIR is of a higher order in comparison to IIR, which is of lower order and uses polyphase structures.

(vi) FIR's delay characteristics are much better, but they require more memory. On the other hand, IIR filters are dependent on both input and output, but FIR is dependent upon input only. IIR filters consist of zeros and poles and require less memory than FIR filters, whereas FIR only consists of zeros.

(vii) IIR filters can become difficult to implement and also delay and distort adjustments can alter the poles and zeros, which make the filters unstable, whereas FIR filters remain stable. FIR filters are used for tapping of a higher–order and IIR filters are better for tapping of lower–orders, since IIR filters may become unstable with tapping higher–orders.

(viii) FIR filters are also preferred over IIR filters because they have a linear phase response and are non–recursive, whereas IIR filters are recursive and feedback is also involved.

3.4 CLASSIFICATION OF FIR–DD

Digital differentiator finds wide applications as in instrumentation and control, biomedical electronics, signal and image processing areas, etc. Different design methods have been proposed by research communities to design the best optimal differentiating filter that best suits the applications. The digital differentiating filters can be divided into two generations: integer–order DD (IODD) and fractional–order DD (FODD), depending on the design flexibility. From the vast literature survey done, it is clear that the fractional order systems tend to have larger design flexibility than the conventional integer order systems.

3.4.1 Integer–Order DD (IODD)

In the area of the digital filter design, the conventional integer order derivative constraints have been successfully used to design various FIR filters. Typical examples include:

(i) In the designing of the low pass filter, the derivative constraints can be used to improve the design accuracy at the prescribed frequency point. **[138]**

(ii) In the notch filter design, the derivative constraints can be used to control the 3–dB rejection bandwidth of notch such that the attenuation of interference can be controlled. **[113, 132]**

(iii) the maximally flat low pass filter and digital differentiator are designed by making the number of derivative constraints equal to the number of filter coefficients. **[96]**

3.4.2 Fractional–Order DD (FODD)

In recent years, the concept of the fractional order calculus has received great attention in science and engineering applications, which includes automatic control systems, electrical network, electromagnetic theory, signal processing and image processing applications.

Due to the success of the integer derivative constraint methods in the FIR filter design, it is interesting to apply the fractional derivative constraints to design the linear phase FIR filter. The fractional derivative can be regarded as an extension of the conventional methods. The

advantage that one gets by utilizing the fractional derivative constraint method for designing is of larger design flexibility as compared to the conventional integer derivative constrained methods. **[35]**

3.5 DESIGN METHODS OF FIR–DD

There exists various design methods to design an FIR–DD. Here the discussion is limited to three of the design methods.

3.5.1 Remez Exchange Algorithm

The Remez algorithm also called Remez exchange algorithm is an application of the Chebyshev alternation theorem that constructs the polynomial of best approximation to certain functions under a number of conditions **[1]**. The Remez algorithm in effect goes a step beyond the minimax approximation algorithm to give a slightly finer solution to an approximation problem.

Parks and McClellan in 1972 observed that a filter of a given length with minimal ripple would have a response with the same relationship to the ideal filter that a polynomial of degree $\leq n$ of best approximation has to a certain function, and so the Remez algorithm could be used to generate the coefficients.

The algorithm is an iterative procedure consisting of two steps: First is the determination of the filter coefficients from the alternation frequencies, which involves solving a set of linear equations. Second is the determination of the alternation frequencies from the filter coefficients.

The algorithm has got the advantage that it is very robust and converges quickly to the optimal solution and is widely used in practice to design filters with optimal response for a given number of taps.

3.5.2 Fourier Series Method

A simple method for the design of FIR filters is through the use of the Fourier series **[1]**. Since the Fourier series coefficients are defined over the range $-\infty < n < \infty$, two problems are associated with the Fourier series method:

(i) The FIR filter obtained is of infinite length.

(ii) The filter is noncausal because the impulse response is nonzero for negative time.

While designing the FIR filter using Fourier series method, it is found that the amplitude response of the filter (magnitude of the frequency response) exhibits oscillations in the passband as well as the stopband, which are known as Gibbs' oscillations. They are caused by the truncation of the Fourier series. As the filter length is increased, the frequency of the oscillations increases but the amplitude stays constant. In other words, it doesn't seem to be able to reduce the passband and stopband errors below a certain limit by increasing the filter length. Therefore, the filters that can be designed with the Fourier series method are of little practical usefulness.

3.5.3 Window Based Method

The standard technique for the reduction of Gibbs' oscillations is to truncate the infinite impulse response through the use of a discrete–time window function. The truncation involves the use of a window function which is multiplied with the impulse response. Multiplication in the time–domain maps into frequency–domain convolution and the spectral characteristics of the window function affect the design. The detailed analysis can be found in **[1]**. It is found that the steepness of the transition characteristic of the filter obtained depends on the main–lobe width of the window and the amplitudes of the passband and stopband ripples depend on the ripple ratio of the window. The window method uses the Fourier series in conjunction with a class of functions known as window functions.

The major advantages of using the window method is their relative simplicity as compared to the other methods, closed–form method, easy to apply and the design entails a relatively insignificant amount of computation. There are some of the problems associated with the window based design method as this method is applicable only if the desired magnitude

response is absolutely integrable. If it is complicated or cannot be put into a closed–form analytical expression, then the evaluation of the desired impulse response becomes difficult, a higher–order filter is needed to satisfy the required specifications and a higher–order filter means more computations per sample, which implies that these filters are slower and less efficient in real–time applications.

In the fractional Fourier transform domain, the window based design method proves to a suitable candidate for the FIR filter design, as against the Remez exchange method which is a logical algorithmic method.

3.6 Analytical Aspects of Window Functions in FrFTD

Window functions (also known as an apodization or tapering function) are used in harmonic analysis to reduce the undesirable effects related to the spectral leakage. In signal processing, a window function is mathematical function that is zero–valued outside of some chosen interval. They affect many attributes of a harmonic processor which include detestability, resolution, dynamic range, confidence and ease of implementation **[1]**. Several standard windows are also used to optimize the requirements of a particular application in signal processing.

Window functions have been successfully used in various areas of signal processing and communications such as, spectrum estimation, speech processing, digital filter design, and in other related fields such as, beamforming. A complete review of many window functions and their properties was presented by Harris **[55]** and described in signal processing text books **[1, 53, 99, 125]**. In addition, other window functions with interesting properties are described in **[55, 161]**. All window functions are designed to reduce the side lobes of the spectral output of Fast Fourier transform (FFT) routines. Whilst applying the window function reduces the side lobe leakage, it causes the main lobe to broaden thus, reducing the resolution. This is a trade-off that has to be made, one should choose the window function, which best suites the application.

Window properties are determined by its spectrum $W(e^{j\omega})$ that consists of the main lobe, which is the highest peak in the spectrum and the sidelobes. The characteristic features of the window functions are as:

The *main lobe* of the window should be as narrow as possible, and the *sidelobes* should be as low as possible. Narrow main lobe improves frequency resolution of the DFT analysis, while low sidelobes reduce spectral leakage.

For example, the Dirichlet window is the one with the narrowest main lobe, which is an advantage and the highest sidelobes which is a disadvantage. All the other window functions reduce sidelobes, and thus spectral leakage, by the cost of widening main lobe i.e., reducing frequency resolution. It is also known that rectangular window has the best noise immunity although systematic errors caused by leakage may be dominant for signal containing small number of cycles **[144]**. As a rectangular window has large spectral sidelobes, there is a large spectral leakage. This could pose a problem in applications where the power spectral density (PSD) of the transmit signal is required to have a large rolloff in certain frequency bands. For example, in some wired transmission application, the PSD of the downstream transmit signal needs to fall below a threshold in the frequency bands of upstream transmission to avoid interference. The PSD should also be attenuated in amateur radio bands to reduce interference.

Recently, the fractional Fourier transform (FrFT) has been developed and utilized by a number of researchers, and being used in almost all applications where Fourier transforms were used. For example, the FrFT has been applied to optimal Wiener filtering and matched filtering **[65]**. Applications of FrFT have also been described by Bailey *et al*. **[50]**. Stankovic *et al*. have used windowed FrFT for the analysis of non–stationary signals [**102]**. Also, Sharma *et al*. **[145]** have carried out Kaiser and Parzen–$\cos^6(\pi t)$ (PC6) window function analysis in fractional Fourier transform domain to show the dependence of window main–lobe width on the order of FrFT and also an alternate methodology is described to tune FIR filter transition bandwidth based on FrFT.

This section of the chapter presents the FrFT analysis of Dirichlet and Generalized "Hamming" window functions. The analysis has been carried out for different values of the fractional Fourier transform parameter φ or fractional Fourier order parameter a, both of which are related by the relation $\varphi = a\,\pi/2$.

An attempt has also been made to study the variations of the following parameters: Half Main Lobe Width (HMLW), Maximum Side Lobe Level (MSLL) and Side–lobe fall-off rate

(SLFOR) of these window functions with the variation of the parameter φ or a. It is found that with the adjustment of the parameter φ or a to different values, these window functions can attain a maximum main lobe width and SLFOR.

3.6.1 Dirichlet Window Function

The mathematical analyses of Dirichlet window function in the fractional Fourier transform domain is carried in the following section. Without loss of generality, let $w(t)$ be unity at the origin, and time–limited to the interval $|t| \leq \frac{1}{2}$, i.e.,

$$w(t) = \begin{cases} 1 & |t| \leq 1/2 \\ 0 & \text{elsewhere} \end{cases} \quad \textbf{(3.6.1)}$$

Therefore, the FrFT of $w(t)$ i.e., $\mathrm{F}_{\mathcal{F}}{}^{\varphi}[w(t)] = W^{\varphi}(u_{\varphi})$ can be written as:

$$W^{\varphi}(u_{\varphi}) = \sqrt{\frac{1-j\cot\varphi}{2\pi}} \exp\left(j\frac{{u_{\varphi}}^2}{2}\cot\varphi\right) \int_{-1/2}^{1/2} 1 \cdot \exp\left[j\frac{t^2}{2}\cot\varphi - ju_{\varphi}t\csc\varphi\right] dt \quad \textbf{(3.6.2)}$$

Now, rewriting the integral of (3.6.2):

$$W^{\varphi}(u_{\varphi}) =$$

$$\sqrt{\frac{1-j\cot\varphi}{2\pi}} \exp\left(j\frac{{u_{\varphi}}^2}{2}\cot\varphi\right) \int_{-1/2}^{1/2} \exp\left[\frac{j}{2}\cot\varphi\left\{\left(t-u_{\varphi}\sec\varphi\right)^2 - \left(u_{\varphi}\sec\varphi\right)^2\right\}\right] dt \quad \textbf{(3.6.3)}$$

By substituting $\left(t - u_{\varphi}\sec\varphi\right) = R$ and changing the limits of the integration in (3.6.3):

$$W^{\varphi}(u_{\varphi}) = \sqrt{\frac{1-j\cot\varphi}{2\pi}} \exp\left(-\frac{j}{2}{u_{\varphi}}^2\tan\varphi\right) \int_{-(1/2)-u_{\varphi}\sec\varphi}^{(1/2)-u_{\varphi}\sec\varphi} \exp\left[\left(\frac{j}{2}\cot\varphi\right)R^2\right] dR \quad \textbf{(3.6.4)}$$

Now, solving the integral:

$$\int_{-(1/2)-u_{\varphi}\sec\varphi}^{(1/2)-u_{\varphi}\sec\varphi} \exp\left[\left(\frac{j}{2}\cot\varphi\right)R^2\right] dR$$

the following expression results **[107]**

$$\int_{-(1/2)-u_{\varphi}\sec\varphi}^{(1/2)-u_{\varphi}\sec\varphi} \exp\left[\left(\frac{j}{2}\cot\varphi\right)R^2\right] dR = -\frac{\sqrt{\pi}}{2}\left\{\mathrm{erfi}\left[\frac{(1+j)}{2}\sqrt{\cot\varphi}\left(\frac{1}{2} - u_{\varphi}\sec\varphi\right)\right] - \mathrm{erfi}\left[\frac{(1+j)}{2}\sqrt{\cot\varphi}\left(-\frac{1}{2} - u_{\varphi}\sec\varphi\right)\right]\right\} \quad \textbf{(3.6.5)}$$

where erfi (z) is an entire analytical function of z which is defined in the whole complex z–plane.

By rearranging (3.6.4) and (3.6.5):

$$W^{\varphi}(u_{\varphi}) = -\sqrt{\frac{1-j\cot\varphi}{8}}\exp\left(-\frac{j}{2}{u_{\varphi}}^{2}\right)\left\{\text{erfi}\left[\frac{(1+j)}{2}\sqrt{\cot\varphi}\left(\frac{1}{2}-u_{\varphi}\sec\varphi\right)\right]-\text{erfi}\left[\frac{(1+j)}{2}\sqrt{\cot\varphi}\left(-\frac{1}{2}-u_{\varphi}\sec\varphi\right)\right]\right\} \quad \textbf{(3.6.6)}$$

Thus, from (3.6.6), it can be seen that the FrFT of the Dirichlet window function is directly dependent on the fractional Fourier transform parameter φ.

The various plots of the FrFT of the Dirichlet window function by varying the rotation angles φ, is shown in Figure-3.2 (a) to (f), along with the continuum of the Dirichlet window function shown as the three–dimensional view in Figure-3.2 (g). The real parts of the FrFT are plotted by solid blue lines and the imaginary parts of the FrFT are plotted by solid green lines.

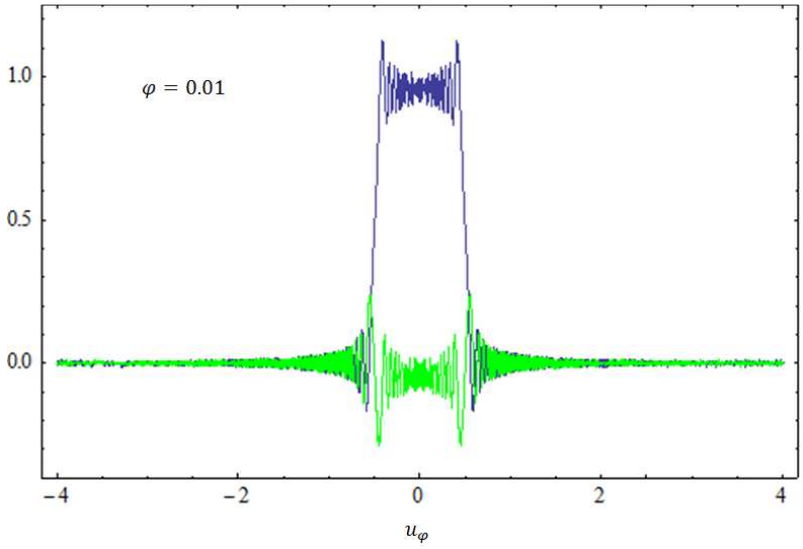

(a)

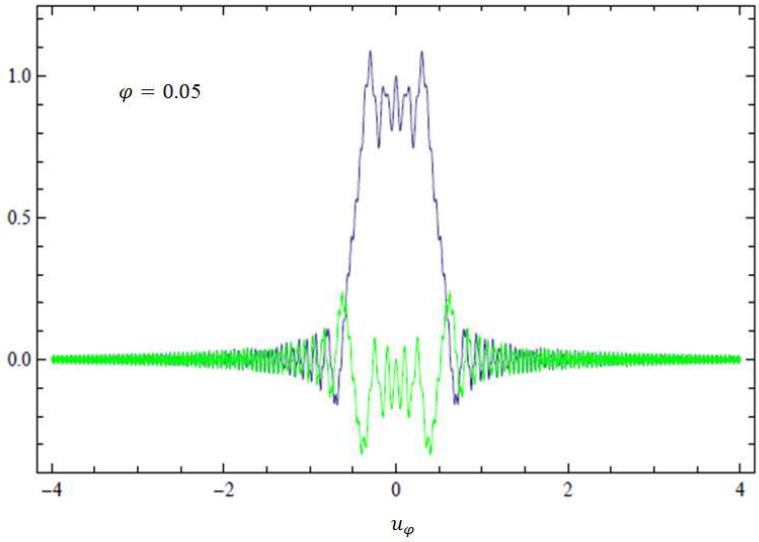

(b)

Figure–3.2: Continuous FrFT of the Dirichlet window function for various rotation angles or fractional Fourier transform parameter, φ:
(a) $\varphi = 0.01$, (b) $\varphi = 0.05$, (c) $\varphi = 0.2$, (d) $\varphi = 0.4$, (e) $\varphi = \pi/4$, (f) $\varphi = \pi/2$, (g) The continuum of the FrFT of the window function, where u_φ is the fractional Fourier transform domain and a is the fractional Fourier order parameter, related by $\varphi = a(\pi/2)$.

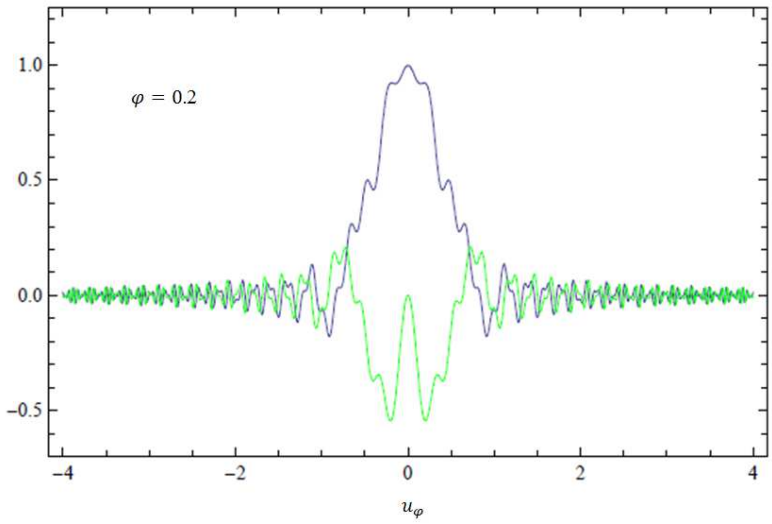

(c)

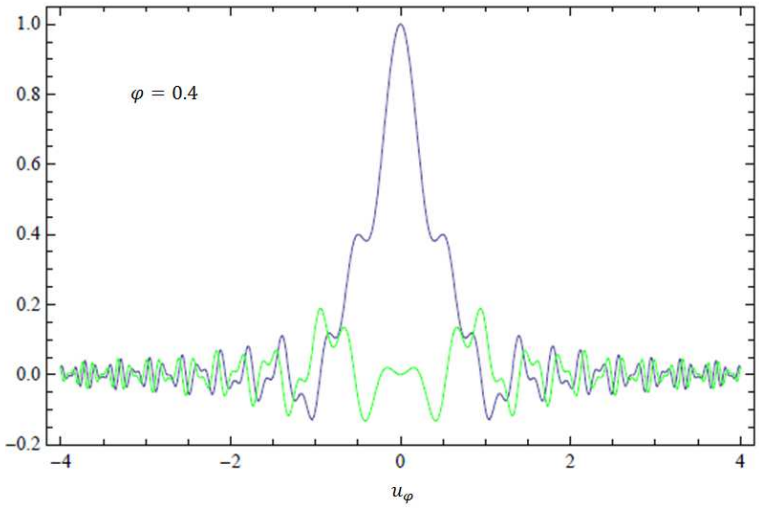

(d)

Figure–3.2 (*Continued*)

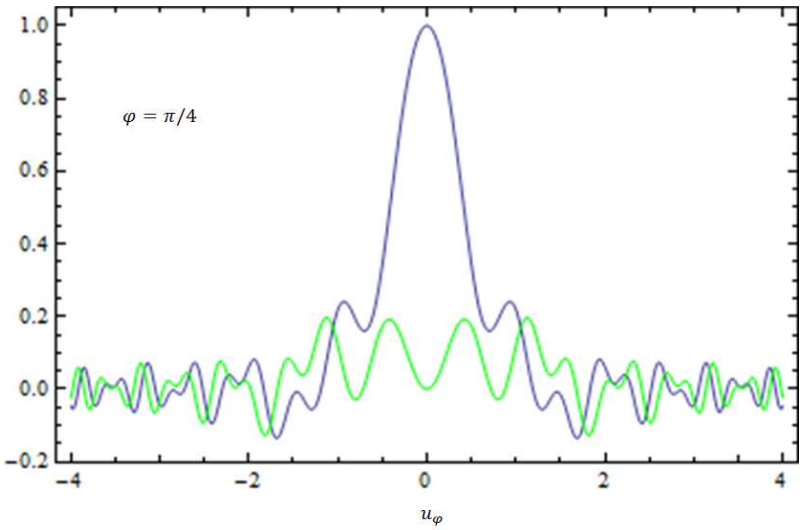

(e)

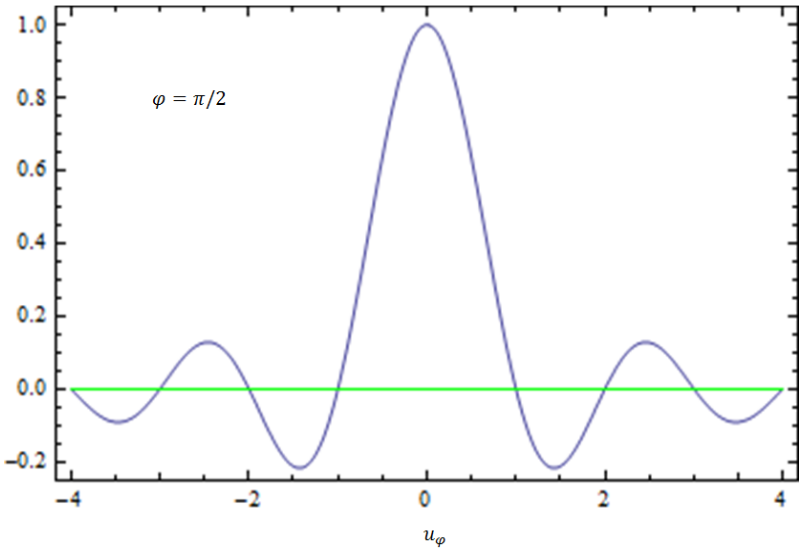

(f)

Figure–3.2 (*Continued*)

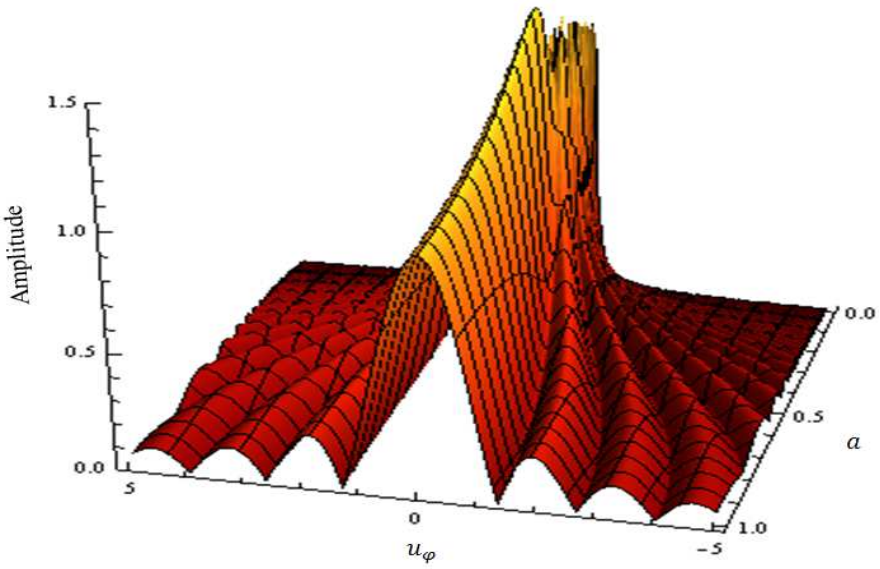

(g)

Figure–3.2 (*Continued*)

3.6.2 Generalized "Hamming" Window Function

The expression for the Generalized "Hamming" Window function in time domain is given as **[99]**:

$$w(t) = \begin{cases} \beta + (1-\beta)\cos(2\pi t) & |t| \le 1/2 \\ 0 & \text{elsewhere} \end{cases} \quad \textbf{(3.6.7)}$$

For $\beta = 0.50$, Hanning window results and for $\beta = 0.54$, one gets Hamming window.

Rewriting (3.6.7) in Euler's form, one get:

$$w(t) = \beta + (1-\beta)\left(\frac{e^{j2\pi t} + e^{-j2\pi t}}{2}\right)$$

or, $w(t) = \beta + \left(\frac{1-\beta}{2}\right)\left(e^{j2\pi t} + e^{-j2\pi t}\right)$ **(3.6.8)**

Now, because $w(t) \overset{\varphi}{\leftrightarrow} W^{\varphi}(u_\varphi)$

Therefore,

$$W^{\varphi}(u_{\varphi}) = \sqrt{\frac{1-j\cot\varphi}{2\pi}}\exp\left(j\frac{{u_{\varphi}}^2}{2}\cot\varphi\right)\int_{-1/2}^{1/2} w(t)\exp\left[j\frac{t^2}{2}\cot\varphi - ju_{\varphi}t\csc\varphi\right]dt \qquad \textbf{(3.6.9)}$$

$$W^{\varphi}(u_{\varphi}) =$$

$$\sqrt{\frac{1-j\cot\varphi}{2\pi}}\exp\left(j\frac{{u_{\varphi}}^2}{2}\cot\varphi\right)\int_{-1/2}^{1/2}\left[\beta + \left(\frac{1-\beta}{2}\right)\left(e^{j2\pi t} + e^{-j2\pi t}\right)\right]\cdot$$

$$\exp\left[j\frac{t^2}{2}\cot\varphi - ju_{\varphi}t\csc\varphi\right]dt \qquad \textbf{(3.6.10)}$$

Rewriting the integral in (3.6.10):

$$W^{\varphi}(u_{\varphi}) =$$

$$\beta\sqrt{\frac{1-j\cot\varphi}{2\pi}}\exp\left(j\frac{{u_{\varphi}}^2}{2}\cot\varphi\right)\int_{-\frac{1}{2}}^{\frac{1}{2}}\exp\left[j\frac{t^2}{2}\cot\varphi - ju_{\varphi}t\csc\varphi\right]dt +$$

$$\frac{(1-\beta)}{2}\sqrt{\frac{1-j\cot\varphi}{2\pi}}\exp\left(j\frac{{u_{\varphi}}^2}{2}\cot\varphi\right)\int_{-\frac{1}{2}}^{\frac{1}{2}}\exp\left[j\frac{t^2}{2}\cot\varphi + jt\left(2\pi - u_{\varphi}\csc\varphi\right)\right]dt +$$

$$\frac{(1-\beta)}{2}\sqrt{\frac{1-j\cot\varphi}{2\pi}}\exp\left(j\frac{{u_{\varphi}}^2}{2}\cot\varphi\right)\int_{-\frac{1}{2}}^{\frac{1}{2}}\exp\left[j\frac{t^2}{2}\cot\varphi - jt\left(2\pi + u_{\varphi}\csc\varphi\right)\right]dt \qquad \textbf{(3.6.11)}$$

Rewriting (3.6.11) as:

$$W^{\varphi}(u_{\varphi}) = I_1 + I_2 + I_3 \qquad \textbf{(3.6.12)}$$

Here,

$$I_1 = \beta\sqrt{\frac{1-j\cot\varphi}{2\pi}}\exp\left(j\frac{{u_{\varphi}}^2}{2}\cot\varphi\right)\int_{-\frac{1}{2}}^{\frac{1}{2}}\exp\left[j\frac{t^2}{2}\cot\varphi - ju_{\varphi}t\csc\varphi\right]dt \qquad \textbf{(3.6.13)}$$

$$I_2 = \frac{(1-\beta)}{2}\sqrt{\frac{1-j\cot\varphi}{2\pi}}\exp\left(j\frac{{u_{\varphi}}^2}{2}\cot\varphi\right)\int_{-\frac{1}{2}}^{\frac{1}{2}}\exp\left[j\frac{t^2}{2}\cot\varphi + jt\left(2\pi - u_{\varphi}\csc\varphi\right)\right]dt \qquad \textbf{(3.6.14)}$$

$$I_{3=}\frac{(1-\beta)}{2}\sqrt{\frac{1-j\cot\varphi}{2\pi}}\exp\left(j\frac{{u_{\varphi}}^2}{2}\cot\varphi\right)\int_{-\frac{1}{2}}^{\frac{1}{2}}\exp\left[j\frac{t^2}{2}\cot\varphi - jt\left(2\pi + u_{\varphi}\csc\varphi\right)\right]dt \qquad \textbf{(3.6.15)}$$

Now, solving (3.6.13) for I_1:

$$I_1 = \beta\sqrt{\frac{1-j\cot\varphi}{2\pi}}\exp\left(j\frac{{u_{\varphi}}^2}{2}\cot\varphi\right)\int_{-\frac{1}{2}}^{\frac{1}{2}}\exp\left[j\frac{t^2}{2}\cot\varphi - ju_{\varphi}t\csc\varphi\right]dt \qquad \textbf{(3.6.16)}$$

Solving (3.6.16) in the same manner as (3.6.4):

$$I_1 = -\beta\sqrt{\frac{1-i\cot\varphi}{8}}\, e^{-\frac{j}{2}u_\varphi{}^2\tan\varphi}\left\{\operatorname{erfi}\left[\frac{(1+j)}{2}\sqrt{\cot\varphi}\left(\frac{1}{2}-u_\varphi\sec\varphi\right)\right]-\operatorname{erfi}\left[\frac{(1+j)}{2}\sqrt{\cot\varphi}\left(-\frac{1}{2}-u_\varphi\sec\varphi\right)\right]\right\} \quad \textbf{(3.6.17)}$$

Now, solving (3.614) for I_2:

$$I_2 = \frac{(1-\beta)}{2}\sqrt{\frac{1-j\cot\varphi}{2\pi}}\exp\left(j\frac{u_\varphi{}^2}{2}\cot\varphi\right)\int_{-\frac{1}{2}}^{\frac{1}{2}}\exp\left[j\frac{t^2}{2}\cot\varphi+jt\left(2\pi-u_\varphi\csc\varphi\right)\right]dt \quad \textbf{(3.6.18)}$$

$$I_2 = \frac{(1-\beta)}{2}\sqrt{\frac{1-j\cot\varphi}{2\pi}}\, e^{\frac{j}{2}\cot\varphi\left[u_\varphi{}^2-\left\{2\pi\tan\varphi-u_\varphi\sec\varphi\right\}^2\right]}\int_{-\frac{1}{2}}^{\frac{1}{2}} e^{\frac{j}{2}\cot\varphi\left[t+\left\{2\pi\tan\varphi-u_\varphi\sec\varphi\right\}\right]^2}dt$$

Solving the integral $\int_{-\frac{1}{2}}^{\frac{1}{2}} e^{\frac{j}{2}\cot\varphi\left[t+\left\{2\pi\tan\varphi-u_\varphi\sec\varphi\right\}\right]^2}dt$, following expression results:

$$\int_{-\frac{1}{2}}^{\frac{1}{2}} e^{\frac{j}{2}\cot\varphi\left[t+\left\{2\pi\tan\varphi-u_\varphi\sec\varphi\right\}\right]^2}dt = -\frac{\sqrt{\pi}}{2}\left\{\operatorname{erfi}\left[\frac{j}{2}\sqrt{\cot\varphi}\left(\frac{1}{2}+2\pi\tan\varphi-u_\varphi\sec\varphi\right)\right]-\operatorname{erfi}\left[\frac{(1+j)}{2}\sqrt{\cot\varphi}\left(-\frac{1}{2}+2\pi\tan\varphi-u_\varphi\sec\varphi\right)\right]\right\} \quad \textbf{(3.6.19)}$$

Now rearranging (3.6.18) and (3.6.19):

$$I_2 = -(1-\beta)\sqrt{\frac{1-j\cot\varphi}{32}}\, e^{\frac{j}{2}\cot\varphi\left[u_\varphi{}^2-\left\{2\pi\tan\varphi-u_\varphi\sec\varphi\right\}^2\right]}\left\{\operatorname{erfi}\left[\frac{(1+j)}{2}\sqrt{\cot\varphi}\left(\frac{1}{2}+2\pi\tan\varphi-u_\varphi\sec\varphi\right)\right]-\operatorname{erfi}\left[\frac{(1+j)}{2}\sqrt{\cot\varphi}\left(-\frac{1}{2}+2\pi\tan\varphi-u_\varphi\sec\varphi\right)\right]\right\} \quad \textbf{(3.6.20)}$$

Now solving (3.6.15) for I_3:

$$I_{3=}\frac{(1-\beta)}{2}\sqrt{\frac{1-j\cot\varphi}{2\pi}}\exp\left(j\frac{u_\varphi{}^2}{2}\cot\varphi\right)\int_{-\frac{1}{2}}^{\frac{1}{2}}\exp\left[j\frac{t^2}{2}\cot\varphi-jt\left(2\pi+u_\varphi\csc\varphi\right)\right]dt \quad \textbf{(3.6.21)}$$

$$I_3 = \frac{(1-\beta)}{2}\sqrt{\frac{1-j\cot\varphi}{2\pi}}\, e^{\frac{j}{2}\cot\varphi\left[u_\varphi{}^2-\left\{2\pi\tan\varphi+u_\varphi\sec\varphi\right\}^2\right]}\int_{-\frac{1}{2}}^{\frac{1}{2}} e^{\frac{j}{2}\cot\varphi\left[t-\left\{2\pi\tan\varphi+u_\varphi\sec\varphi\right\}\right]^2}dt$$

Solving the integral $\int_{-\frac{1}{2}}^{\frac{1}{2}} e^{\frac{j}{2}\cot\varphi\left[t-\left\{2\pi\tan\varphi+u_\varphi\sec\varphi\right\}\right]^2}dt$, following expression results:

$$\int_{-\frac{1}{2}}^{\frac{1}{2}} e^{\frac{j}{2}\cot\varphi\left[t-\{2\pi\tan\varphi+u_\varphi\sec\varphi\}\right]^2} dt =$$

$$-\frac{\sqrt{\pi}}{2}\left\{\text{erfi}\left[\frac{(1+j)}{2}\sqrt{\cot\varphi}\left(\frac{1}{2}-2\pi\tan\varphi-u_\varphi\sec\varphi\right)\right]-\text{erfi}\left[\frac{(1+j)}{2}\sqrt{\cot\varphi}\left(-\frac{1}{2}-2\pi\tan\varphi-u_\varphi\sec\varphi\right)\right]\right\} \quad \textbf{(3.6.22)}$$

Now rearranging (3.6.21) and (3.6.22):

$$I_3 = -(1-\beta)\sqrt{\frac{1-j\cot\varphi}{32}}\, e^{\frac{j}{2}\cot\varphi\left[u_\varphi{}^2-\{2\pi\tan\varphi+u_\varphi\sec\varphi\}^2\right]}\left\{\text{erfi}\left[\frac{(1+j)}{2}\sqrt{\cot\varphi}\left(\frac{1}{2}-2\pi\tan\varphi-u_\varphi\sec\varphi\right)\right]-\text{erfi}\left[\frac{(1+j)}{2}\sqrt{\cot\varphi}\left(-\frac{1}{2}-2\pi\tan\varphi-u_\varphi\sec\varphi\right)\right]\right\} \quad \textbf{(3.6.23)}$$

Thus, the FrFT of the Generalized "Hamming" window function can be obtained by summing (3.6.17), (3.6.20) and (3.6.23) as:

$$W^\varphi(u_\varphi) =$$

$$-\beta\sqrt{\frac{1-j\cot\varphi}{8}}\, e^{-\frac{j}{2}u_\varphi{}^2\tan\varphi}\left\{\text{erfi}\left[\frac{(1+j)}{2}\sqrt{\cot\varphi}\left(\frac{1}{2}-u_\varphi\sec\varphi\right)\right]-\text{erfi}\left[\frac{(1+j)}{2}\sqrt{\cot\varphi}\left(-\frac{1}{2}-u_\varphi\sec\varphi\right)\right]-(1-\beta)\sqrt{\frac{1-j\cot\varphi}{32}}\, e^{\frac{j}{2}\cot\varphi\left[u_\varphi{}^2-\{2\pi\tan\varphi-u_\varphi\sec\varphi\}^2\right]}\right\}\left\{\text{erfi}\left[\frac{(1+j)}{2}\sqrt{\cot\varphi}\left(\frac{1}{2}+2\pi\tan\varphi-u_\varphi\sec\varphi\right)\right]-\text{erfi}\left[\frac{(1+j)}{2}\sqrt{\cot\varphi}\left(-\frac{1}{2}+2\pi\tan\varphi-u_\varphi\sec\varphi\right)\right]\right\}-(1-\beta)\sqrt{\frac{1-j\cot\varphi}{32}}\, e^{\frac{j}{2}\cot\varphi\left[u_\varphi{}^2-\{2\pi\tan\varphi+u_\varphi\sec\varphi\}^2\right]}\left\{\text{erfi}\left[\frac{(1+j)}{2}\sqrt{\cot\varphi}\left(\frac{1}{2}-2\pi\tan\varphi-u_\varphi\sec\varphi\right)\right]-\text{erfi}\left[\frac{(1+j)}{2}\sqrt{\cot\varphi}\left(-\frac{1}{2}-2\pi\tan\varphi-u_\varphi\sec\varphi\right)\right]\right\} \quad \textbf{(3.6.24)}$$

Thus, the FrFT of the Generalized "Hamming" window function, as given by (3.6.24) contains two parameters of interest:

(a) the fractional Fourier transform parameter φ, and
(b) the controlling parameter β, which determines the shape of the window that is, for $\beta = 0.54$, one obtains the Hamming window function and, for $\beta = 0.50$, Hanning window is obtained.

Therefore, by setting the parameter β in (3.6.24) and by varying the different rotation angles φ, one obtains the FrFT of both Hamming and Hanning window function.

The various plots of the FrFT of Hanning and Hamming window functions with the variation of rotation angles φ, is shown in Figure-3.3 (a) to (f) and Figure-3.4 (a) to (f), along with the continuum of the Hanning and Hamming window functions shown as the three–dimensional view in Figure-3.3 (g) and Figure-3.4 (g), respectively. The real parts of the FrFT are plotted by solid blue lines and the imaginary parts of the FrFT are plotted by solid green lines.

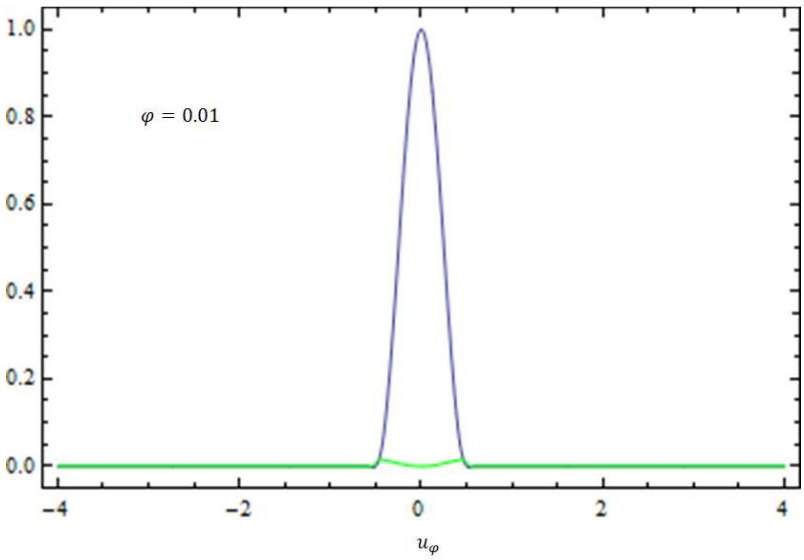

(a)

Figure–3.3: Continuous FrFT of the Hanning window function for various rotation angles or fractional Fourier transform parameter, φ:
(a) $\varphi = 0.01$, (b) $\varphi = 0.05$, (c) $\varphi = 0.2$, (d) $\varphi = 0.4$, (e) $\varphi = \pi/4$, (f) $\varphi = \pi/2$, (g) The continuum of the FrFT of the window function, where u_φ is the fractional Fourier domain and a is the fractional Fourier order parameter, related by $\varphi = a(\pi/2)$.

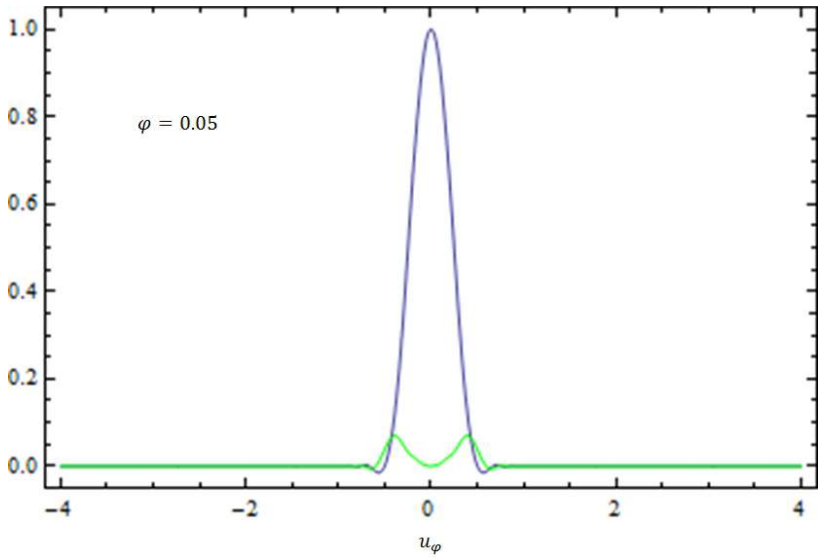

(b)

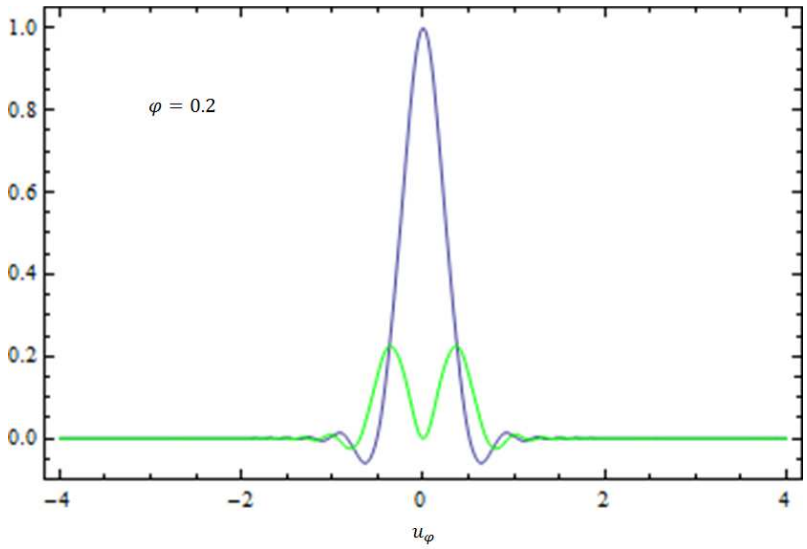

(c)

Figure–3.3 (*Continued*)

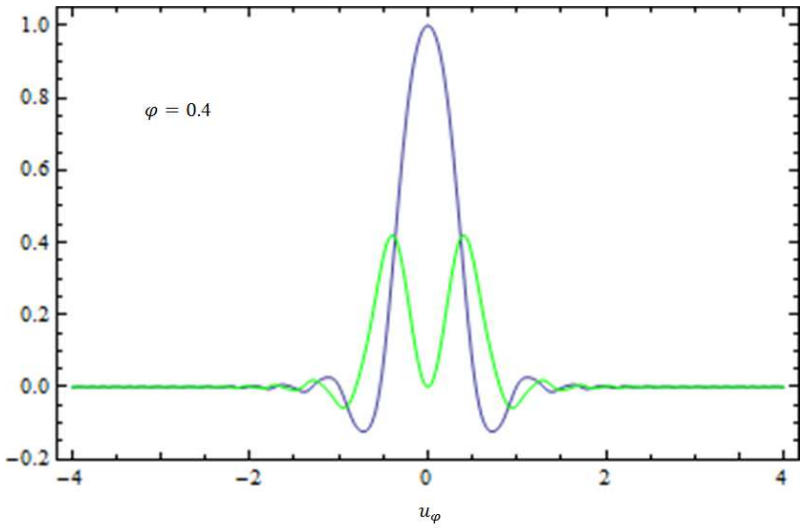

(d)

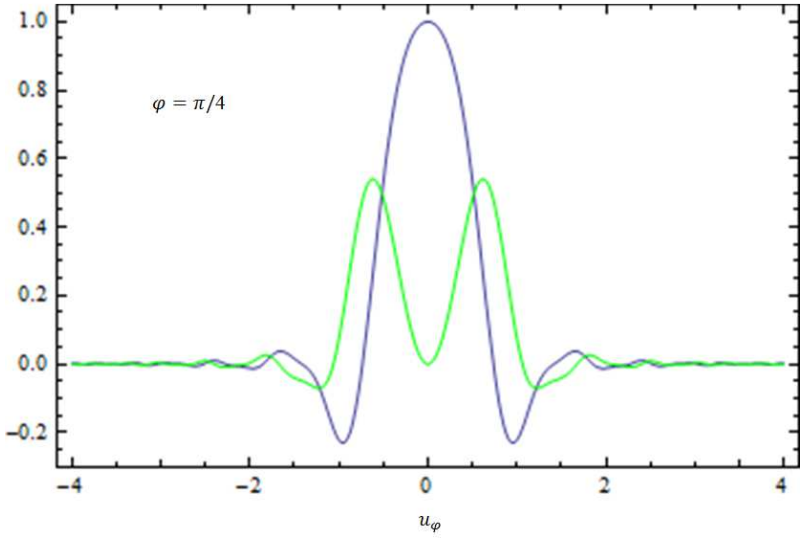

(e)

Figure–3.3 (*Continued*)

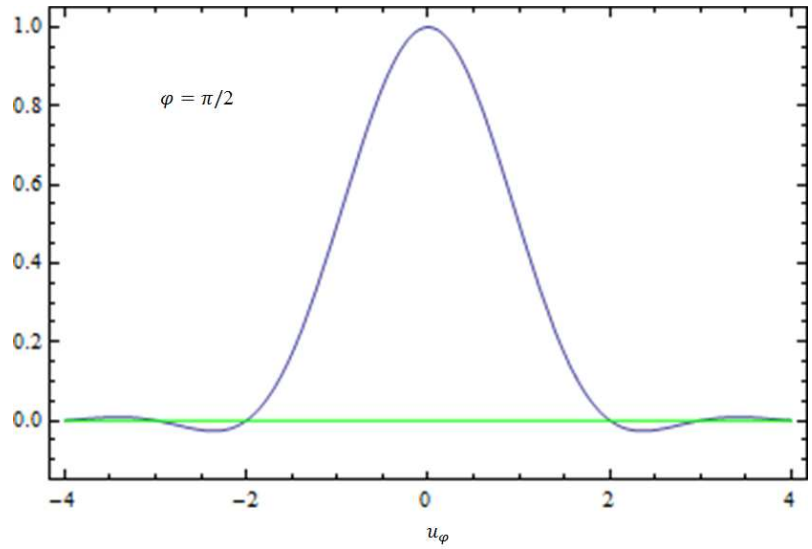

(f)

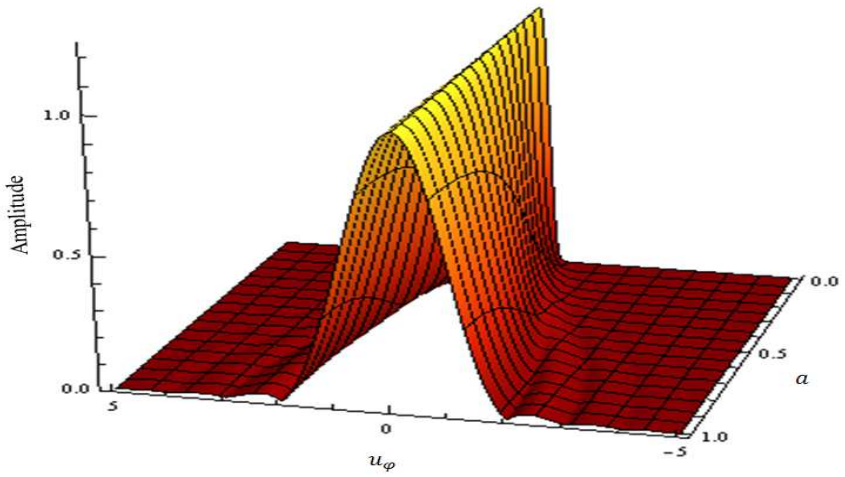

(g)

Figure–3.3 (*Continued*)

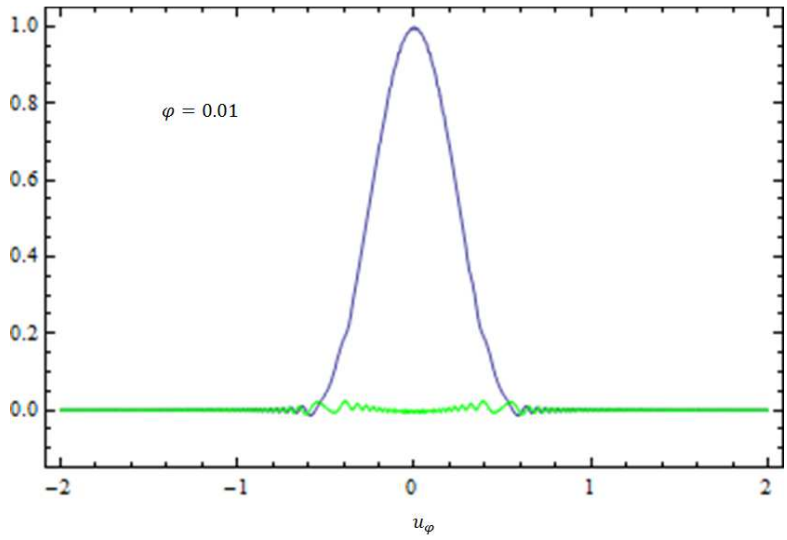

(a)

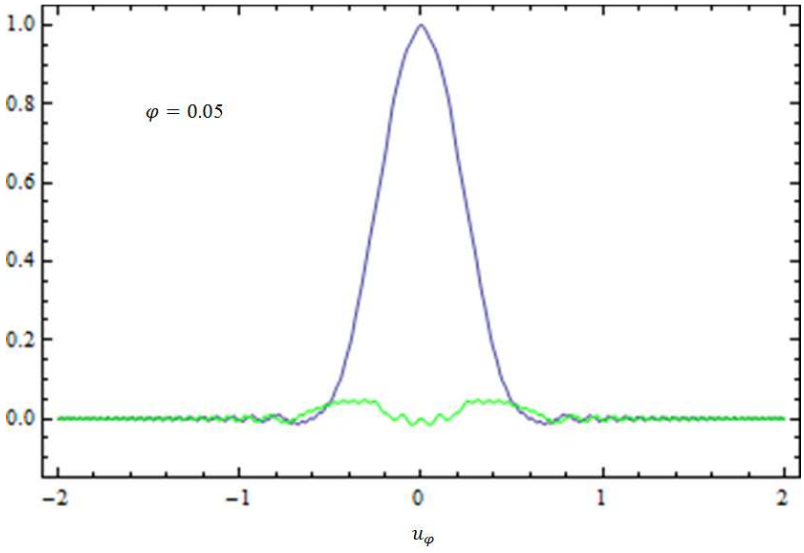

(b)

Figure–3.4: Continuous FrFT of the Hamming window function for various rotation angles or fractional Fourier transform parameter, φ:
(a) $\varphi = 0.01$, (b) $\varphi = 0.05$, (c) $\varphi = 0.2$, (d) $\varphi = 0.4$, (e) $\varphi = \pi/4$, (f) $\varphi = \pi/2$, (g) The continuum of the FrFT of the window function, where u_φ is the fractional Fourier domain and a is the fractional Fourier order parameter, related by $\varphi = a(\pi/2)$.

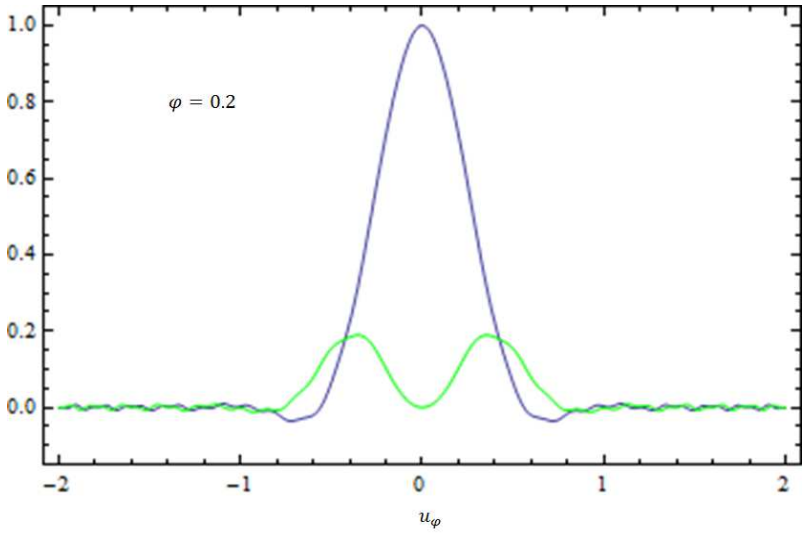

(c)

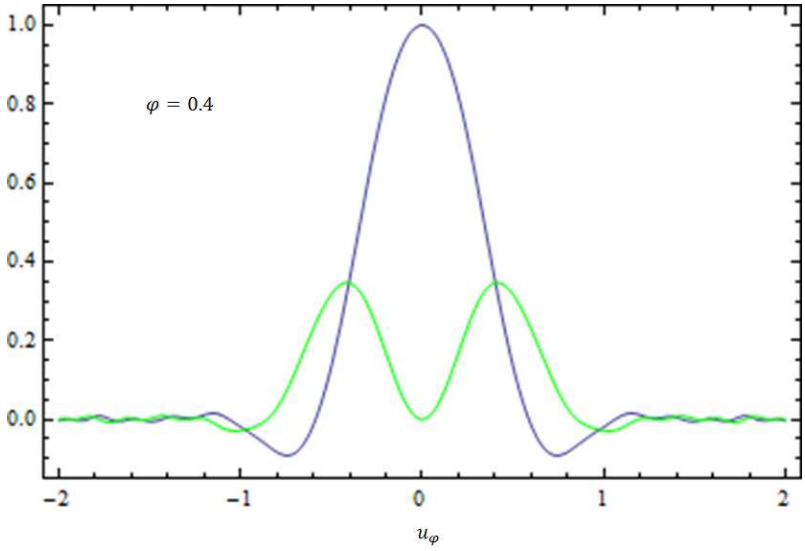

(d)

Figure–3.4 (*Continued*)

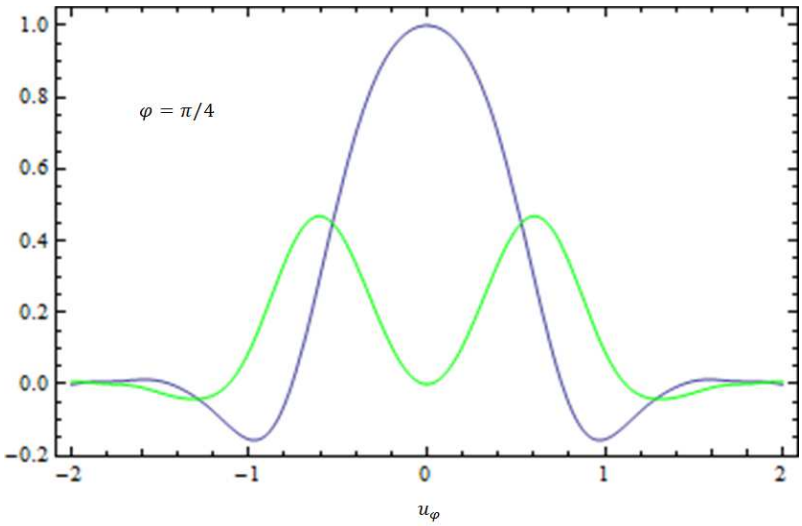

(e)

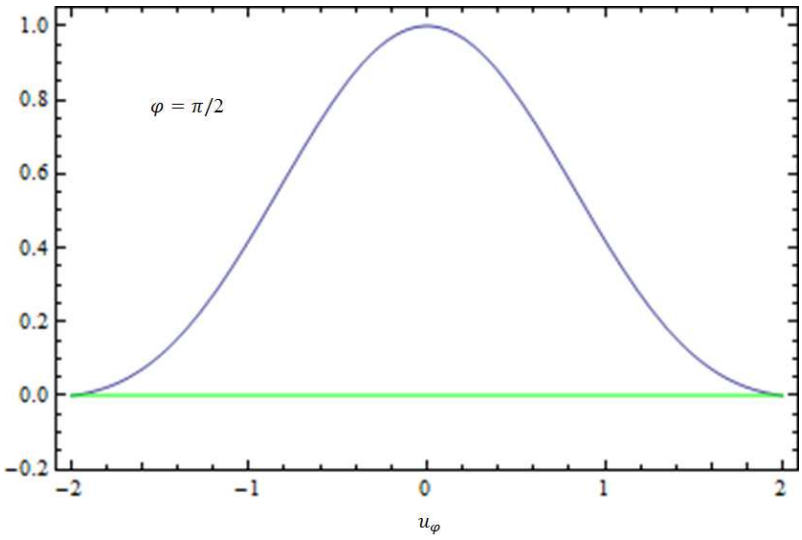

(f)

Figure–3.4 (*Continued*)

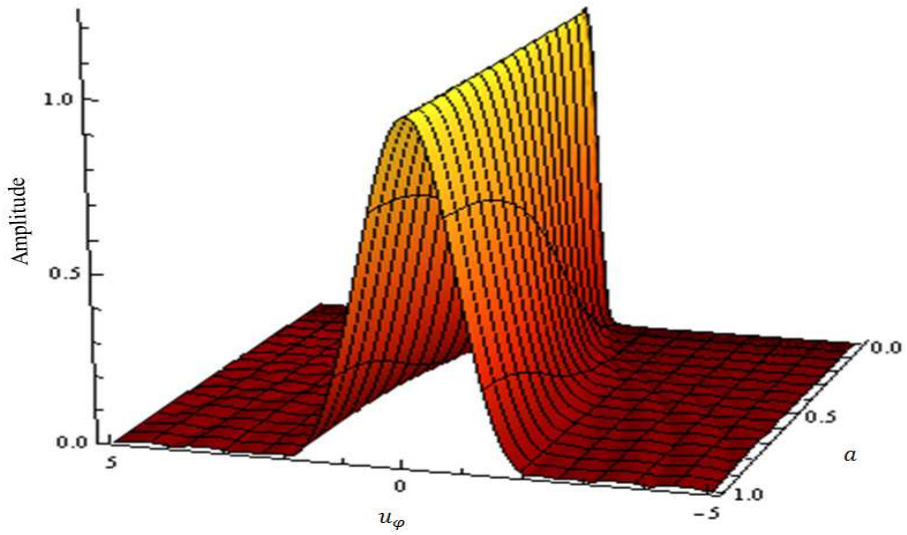

(g)

Figure–3.4 (*Continued*)

Furthermore, as the fractional Fourier order parameter a is varied from 0 to 1, the continuum of Dirichlet, Hanning and Hamming window function converges to Sinc pulse, as shown in Figure-3.2 (g), 3.3 (g) and 3.4 (g), respectively. The values of maximum side lobe level (MSLL), side–lobe fall–off rate (SLFOR) and half main lobe width (HMLW) for Dirichlet and Hanning window functions are tabulated in Table-3.2 and Table-3.3, respectively for various values of the parameter *a*.

TABLE 3.2

PARAMETERS OF DIRICHLET WINDOW FUNCTION WITH VARIATIONS IN PARAMETER *a*

S. No.	*a*	MSLL (dB)	HMLW (bins)	SLFOR (dB/octave)
1.	1.0	-13.0	0.81	-6.00
2.	0.9	-12.9	0.80	-6.20
3.	0.8	-12.8	0.78	-6.20
4.	0.7	-12.7	0.76	-6.25
5.	0.6	-12.5	0.75	-6.29
6.	0.5	-11.9	0.74	-6.54
7.	0.4	-11.7	0.72	-6.69
8.	0.3	-11.3	0.70	-6.75
9.	0.2	-11.2	0.65	-10.30

TABLE 3.3

PARAMETERS OF HANNING WINDOW FUNCTION WITH VARIATIONS IN PARAMETER *a*

S. No.	*a*	MSLL (dB)	HMLW (bins)	SLFOR (dB/octave)
1.	1.0	-32.0	1.87	-18.00
2.	0.9	-30.7	1.77	-18.00
3.	0.8	-30.5	1.71	-18.10
4.	0.7	-30.5	1.61	-18.17
5.	0.6	-30.4	1.51	-18.20
6.	0.5	-30.2	1.50	-18.30
7.	0.4	-29.9	1.44	-18.32
8.	0.3	-29.6	1.36	-18.35
9.	0.2	-40.5	1.22	-17.03

From the Table-3.2 and 3.3, it is clear that for $a = 1$ or $\varphi = \pi/2$, the MSLL of Dirichlet window function is -13 dB down from the main lobe peak and the SLFOR is -6 dB/octave whereas, for Hanning window function, it is -32 dB down from the main lobe peak and the SLFOR is -18 dB/octave as in the case of Fourier transform.

Thus, it is observed that for Dirichlet window function, as the value of the parameter a decreases from 1 to 0, the MSLL starts increasing upto -11.2 dB at $a = 0.2$, HMLW decreases from 0.81 bins to 0.65 bins and SLFOR decreases from -6 dB/octave to -10.3 dB/octave, whereas, in the case of Hanning window function (for $\beta = 0.50$), as the value of the parameter a decreases from 1 to 0, the MSLL starts increasing upto -40.50 dB at $a = 0.2$, HMLW decreases from 1.87 bins to 1.22 bins and SLFOR decreases from -18 dB/octave to-17.03 dB/octave.

3.7 CLOSED–FORM ANALYTICAL EXPRESSION OF IODD IN FrFTD

This section derives the closed–form analytical expression of IODD that behaves in the FrFT domain. We start with the known desired frequency response of IODD in FrFT domain as in (3.7.1),

$$H_d(u_\varphi) = \begin{cases} ju_\varphi, & -\pi \sin\varphi \le u_\varphi \le \pi \sin\varphi; \\ 0, & \text{elsewhere.} \end{cases} \quad \textbf{(3.7.1)}$$

where $H_d(u_\varphi)$ is the of desired frequency response of the IODD in the FrFT domain and φ is the rotation angle in the FrFT domain.

Therefore, the ideal impulse response of the IODD using the inverse FrFT **[133]** is given by:

$$h_d(n) = \sqrt{\frac{1+j\cot\varphi}{2\pi}} \int_{-\pi \sin\varphi}^{\pi \sin\varphi} H_d(u_\varphi) \exp\left[-\frac{j}{2}\left(n^2 + {u_\varphi}^2\right)\cot\varphi + j\, n\, u_\varphi \csc\varphi\right] du_\varphi \quad \textbf{(3.7.2)}$$

Solving (3.7.2), one gets

$$h_d(n) = \sqrt{\frac{1+j\cot\varphi}{2\pi}} \int_{-\pi \sin\varphi}^{\pi \sin\varphi} ju_\varphi \exp\left[-\frac{j}{2}\left(n^2 + {u_\varphi}^2\right)\cot\varphi + j\, n\, u_\varphi \csc\varphi\right] du_\varphi \quad \textbf{(3.7.3)}$$

$$h_d(n) = \sqrt{\frac{1+j\ \cot\varphi}{2\pi}} \exp\left[-\frac{j}{2}\ n^2\ \cot\varphi\right] \int_{-\pi\ \sin\varphi}^{\pi\ \sin\varphi} j \exp\left[-\frac{j}{2}\ {u_\varphi}^2\ \cot\varphi + j\ n\ u_\varphi\ \csc\varphi\right] du_\varphi$$

(3.7.4)

Now, one has to solve the integral of (3.7.4) to get the simplified closed–form analytical expression:

$$-\frac{j}{2}\ {u_\varphi}^2\ \cot\varphi + j\ n\ u_\varphi\ \csc\varphi = -\frac{j}{2}\ \cot\varphi\left[\left(u_\varphi - n\ \sec\varphi\right)^2 - n^2\ \sec^2\varphi\right] \quad \textbf{(3.7.5)}$$

From (3.7.4) and (3.7.5), one gets the following expression:

$$h_d(n) = \sqrt{\frac{1+j\ \cot\varphi}{2\pi}} \exp\left[-\frac{j}{2}\ n^2\ \cot\varphi\right] \int_{-\pi\ \sin\varphi}^{\pi\ \sin\varphi} j \exp\left\{-\frac{j}{2}\ \cot\varphi\ \left[\left(u_\varphi - n\ \sec\varphi\right)^2 - n^2\ \sec^2\varphi\right]\right\} du_\varphi \quad \textbf{(3.7.6)}$$

$$h_d(n) = \sqrt{\frac{1+j\ \cot\varphi}{2\pi}} \exp\left[-\frac{j}{2}\ n^2\ \cot\varphi\right] \exp[\,j\ n^2\ \csc(2\varphi)] \int_{-\pi\ \sin\varphi}^{\pi\ \sin\varphi} j \exp\left[-\frac{j}{2}\ \cot\varphi\ \left(\left(u_\varphi - n\ \sec\varphi\right)^2\right)\right] du_\varphi \quad \textbf{(3.7.7)}$$

Now, solve the integral of (3.7.7):

By letting, $\left(u_\varphi - n\ \sec\varphi\right) = P$, one gets

$$du_\varphi = dP \quad \textbf{(3.7.8)}$$

Therefore, from (3.7.7) and (3.7.8),

$$h_d(n) = \sqrt{\frac{1+j\ \cot\varphi}{2\pi}} \exp[\,j\ n^2\ \cot(2\varphi)]\ \int_{-\pi\ \sin\varphi}^{\pi\ \sin\varphi} j \exp\left[-\frac{j}{2}\ \cot\varphi\ P^2\right]\ dP \quad \textbf{(3.7.9)}$$

Now, by letting $\left(\sqrt{\frac{j}{2}\ \cot\varphi}\right)\ P = Q$ **(3.7.10)**

$$\left(\sqrt{\frac{j}{2}\ \cot\varphi}\right)\ dP = dQ \quad \textbf{(3.7.11)}$$

or $dP = \sqrt{2} \exp\left(-\frac{j}{4}\pi\right)\ \sqrt{\tan\varphi}\ dQ$ **(3.7.12)**

From (3.7.9), (3.7.11) and (3.7.12), one gets

$$h_d(n) = \sqrt{\frac{1+j\ \cot\varphi}{2\pi}} \exp[\, j\, n^2\ \cot(2\varphi)]\ \int_{-\pi\ \sin\varphi}^{\pi\ \sin\varphi} j \exp(-\,Q^2)\, \sqrt{2} \exp\left(-\frac{j}{4}\pi\right)\ \sqrt{\tan\varphi}\ \ dQ \qquad \textbf{(3.7.13)}$$

Simplifying (3.7.13), one gets

$$h_d(n) = \sqrt{\frac{(-1+j\ \tan\varphi)}{\pi}} \exp[\, j\, n^2\ \cot(2\varphi)]\ \int_{-\pi\ \sin\varphi}^{\pi\ \sin\varphi} \exp(-Q^2)\, dQ \qquad \textbf{(3.7.14)}$$

Now since the integral $\int \exp\,(-Q^2) = \frac{\sqrt{\pi}}{2} \mathrm{erf}\ (Q)$ **(3.7.15)**

Using (3.7.14) and (3.7.15), one gets

$$h_d(n) = \sqrt{\frac{(-1+j\ \tan\varphi)}{\pi}} \exp[\, j\, n^2\ \cot(2\varphi)]\ \frac{\sqrt{\pi}}{2}\ [\mathrm{erf}\ (\pi \sin\varphi) -\ \mathrm{erf}\ (-\pi \sin\varphi)] \qquad \textbf{(3.7.16)}$$

Now using the property of error function, erf(·) of $\mathrm{erf}\ (-z) = -\mathrm{erf}\ (z)$, (3.7.16) reduces to,

$$h_d(n) = \sqrt{2\ (-1 + j\ \tan\varphi)} \exp[\, j\, n^2\ \cot(2\varphi)]\, \mathrm{erf}\ (\pi\ \sin\varphi) \qquad \textbf{(3.7.17)}$$

Thus, (3.7.17) represents the closed–form analytical expression of the impulse response for the IODD in the FrFT domain. It is clear from the above analytical expression that the coefficients of the desired impulse response of IODD in the FrFT domain is dependent on the parameter φ.

Now the coefficients $h_d(n)$ obtained are of infinite in duration, n ranging from $-\infty$ to ∞. So, to obtain the actual impulse response from the desired infinite impulse response $h_d(n)$ of (3.7.17), the ideal impulse response $h_d(n)$ must be truncated using the window function as:

$$h_{actual}(n) = h_d(n)\, w(n) \qquad \textbf{(3.7.18)}$$

$$h_{actual}(n) = \left\{\sqrt{2\ (-1 + j\ \tan\varphi)} \exp[\, j\, n^2\ \cot(2\varphi)]\, \mathrm{erf}\ (\pi\ \sin\varphi)\right\} w(n) \qquad \textbf{(3.7.19)}$$

Thus, the actual impulse response of IODD in the FrFT domain as represented by (3.7.19) is a function of φ and the window function $w(n)$, respectively.

For the analysis of the IODD in the FrFT domain, the window based design method is used, as is illustrated aboves. For the simulation purpose, the Hamming window function is used for the designing.

3.7.1 Simulation Results

Figure 3.5 below shows various plots of the impulse response coefficients of the IODD in the FrFT domain for Hamming window function and for the variation of the rotation angle φ.

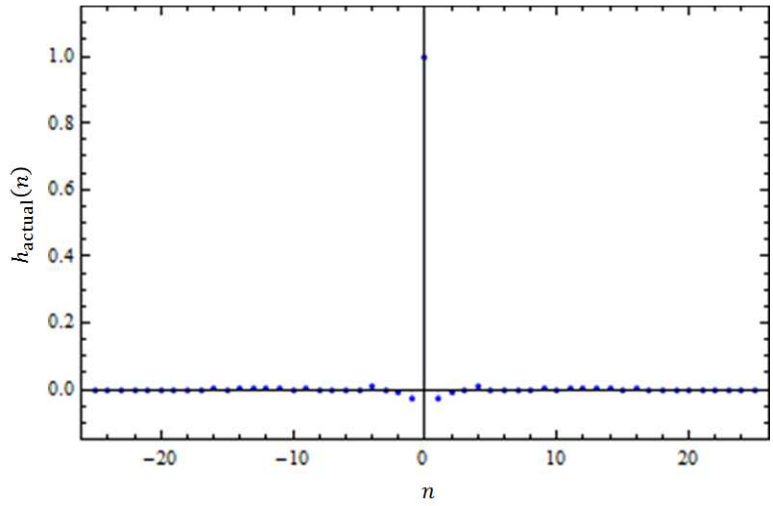

$a = 0$

(a)

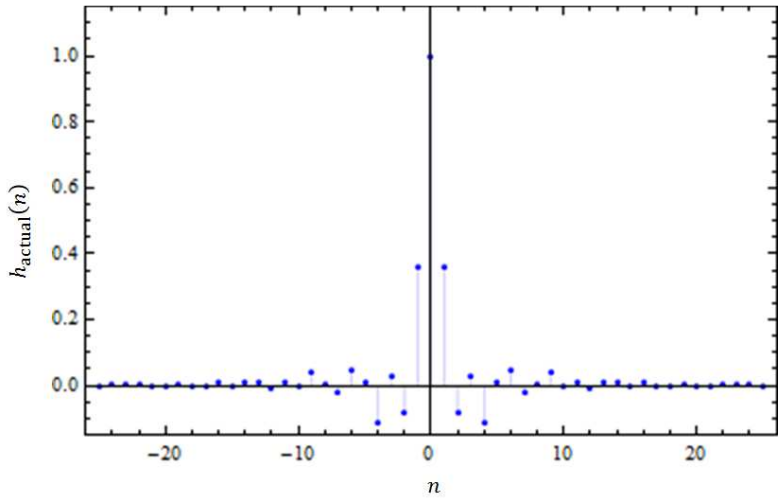

$a = 0.25$

(b)

Figure–3.5: Plots of the impulse response coefficients of the IODD in the FrFT domain for Hamming window function.

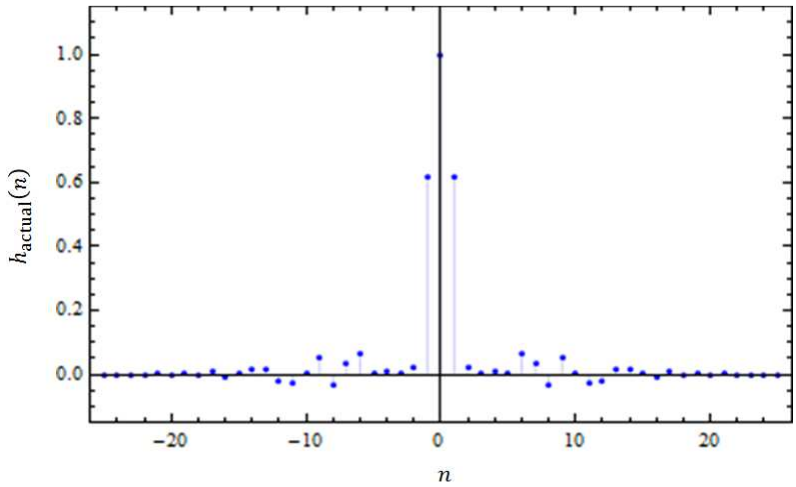

$a = 0.50$

(c)

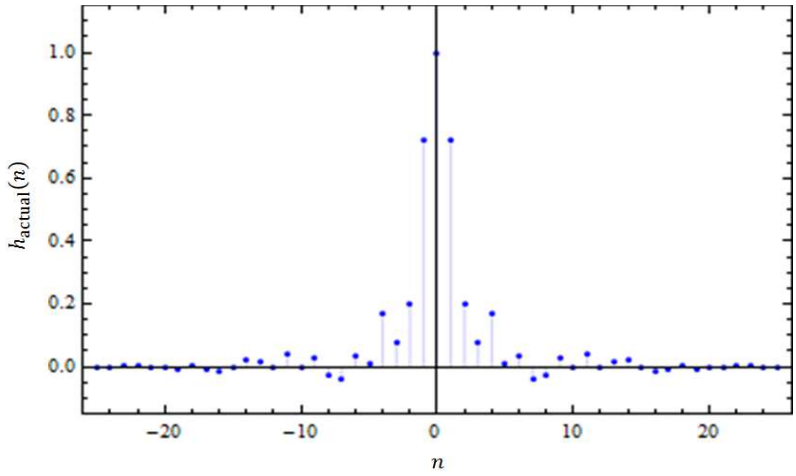

$a = 0.75$

(d)

Figure–3.5 (*Continued*)

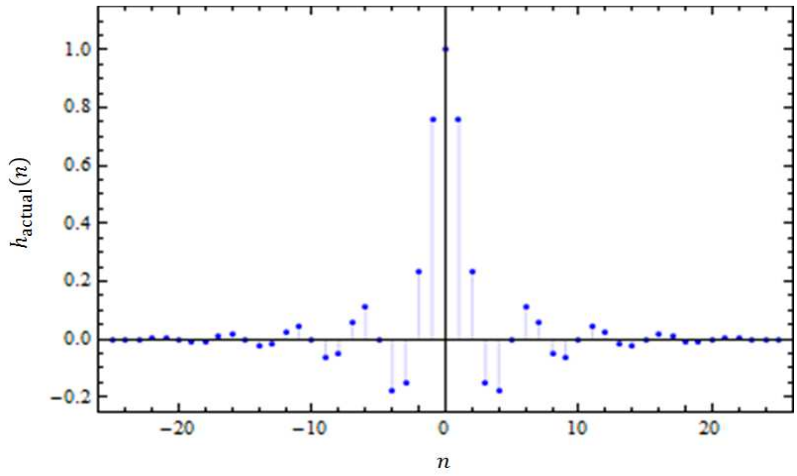

$a = 1$

(e)

Figure–3.5 (*Continued*)

3.8 DISCUSSION

In this chapter, the concept of digital differentiator is focused upon. Also, the fruitful insight into its configurations and classification are dealt with. The profound research of the signal processing community in the area of digital differentiators was very significant. It has many applications in the areas of signal processing, image processing and engineering sciences.

The analytical aspect of the behavior of various window functions in the fractional Fourier transform domain is considered and simulated accordingly. The variation of parameters like half main lobe width, maximum side lobe level and side–lobe fall–off rate of these window functions with the fractional Fourier transform parameter φ is also investigated.

Lastly, the closed–form analytical relation is established for the integer–order differentiator in the fractional Fourier transform domain and shows its results with the variation of the fractional Fourier transform parameter φ and the impulse response approaches to the Sinc pulse for $\varphi = \pi/2$.

CHAPTER 4

FRACTIONAL–ORDER DIGITAL DIFFERENTIATOR IN FrFT DOMAIN

FRACTIONAL ORDER CALCULUS (FOC) is a field of applied mathematics that deals with the derivatives and integrals of arbitrary orders (including complex orders), and has its applications in sciences, mathematics, economics and fields of geology and cosmology etc. It is an interdisciplinary collaboration of mathematicians, statisticians, physicists to develop the theory and practical applications of fractals, fractional derivatives, and heavy tailed stochastic processes.

The fractional order calculus is a generalization of the classical integer order calculus that leads to similar concepts and tools, but with a much wider applicability. At present, the number of applications of fractional order calculus grows very rapidly in the field of mathematics and physics, but is limited to the signal and image processing applications. This mathematical phenomenon allows us to describe and model the real objects more accurately than the classical integer methods.

In this chapter, the closed–form analytical expression of the fractional order differentiation in the signal processing framework of the fractional Fourier transform is investigated, taking into account the established preliminary definitions of the fractional order calculus.

4.1 FODD IN FrFTD

FOC is a field of mathematical study that grows out of the traditional definitions of Newtonian calculus integral and derivative operators in much the same way the fractional exponents is an outgrowth of exponents with the integer value. **[86, 89]**

FOC — an integration and differentiation of an arbitrary order or fractional/non–integer order, is a new and emerging tool that extends the descriptive power of the conventional calculus. The tools of FOC support mathematical models that in many cases more accurately describes the dynamic response of the actual physical systems in electrical, mechanical, and automatic control applications, and to name a few. **[140]**

The theoretical and practical interest of these fractional order operators is nowadays well established, and its applicability to science and engineering disciplines is considered as emerging new topics. In recent years, FOC has received great attentions in many engineering applications and science including automatic control systems, system modeling and identification, electrical networks, electromagnetic theory, speech signal modeling, biomedical and biosensor signal processing applications and signal–image processing applications.

In the research area of FOC, the integer order n of the derivative $D^n p(x) = d^n p(x)/dx^n$ of the function $p(x)$ is generalized to the fractional order $D^\mu p(x)$, where μ is a real number **[89]**. One of the important research issues in FOC is to implement the fractional order operator D^μ in continuous and discrete–time domains.

FOC has proved to be a successful candidate for signal processing, image processing and the related field's applications. Typical applications include:

(i) the fractional order derivative is used to detect the edges in images. **[26]**

(ii) noise reduction in images. **[87]**

(iii) to enhance the contrast of images **[40, 42, 159]**

(iv) the fractional derivative is applied to detect the R–wave of the electrocardiograph (ECG) signal in the biomedical signal processing. **[108, 160]**

(v) the speech processing in which the fractional differential operator is used to enhance the performance of linear prediction of the speech signal. **[88]**

(vi) in the adaptive filtering scheme, the fractional derivative is applied to update the coefficients of the adaptive filter, as per the adaptive learning algorithm. **[142]**

(vii) the signature verification, in which the fractional differential operator is applied to extract the dynamic features from the handwritten signature. **[32]**

(viii) the design of the fractional order differentiator can be used to compute the fractional order derivatives of the digital signals. **[33, 82]**

Thus, the main purpose of this chapter is to apply the mathematical aspects of FOC to analyze and design the fractional–order differentiating filter, also known as fractional–order digital differentiator (FODD) that behaves in the fractional Fourier transform domain.

Since, fractional order differentiation is the main theme of this chapter, it can be emphasized that on two occasions including **[6]** and **[38]**, the differentiation property was independently extended to the class of Fourier transform (FT) and fractional Fourier transform (FrFT) respectively, but not extended to the non–integer orders.

So, due to the success of the FOC concept in signal processing regime, it is interesting to apply the fractional derivative to design the differentiating filter in the signal processing framework of FrFT. Thus, an attempt is made to design the fractional–order differentiating filter both in the FrFT domain (FrFTD) for potential signal processing applications.

4.2 MATHEMATICAL FOUNDATIONS OF FODD IN FrFTD

The fractional order differentiation of a given signal in the fractional Fourier transform domain for different fractional derivative orders is proposed, by utilizing the inherent approach of fractional operators of the fractional order calculus. The concept behind the study is that it involves two different variable parameters — the fractional derivative order parameter μ and the fractional Fourier transform parameter φ. The involvement of these two parameters was

considered in finding the solutions of mathematics **[4, 43, 151]** and physics problems **[117, 154]**, but has not been dealt in the literature of the signal processing regime. In the context of **[89]**, the fractional order calculus generalizes the derivative operator D^{μ} by encompassing real and complex values for the parameter μ, which is ordinarily an integer–valued. The derivatives of non–integer order have been considered in physics, engineering and in the signal processing area **[13, 60]** following the work of Liouville and Riemann at the beginning of the 19th century.

The idea of this concept has been motivated by the work of Pei *et al*. **[38]** and McBride *et al*. **[6]**. The main differences between the proposed method and the work of Pei *et al*. **[38]** are: (i) Pei *et al*. used the Cauchy integral formula and generalized it to define the fractional derivative of the functions, whereas the Riemann–Liouville (RL) definition for the general fractional differintegral is used in the proposed method, (ii) The aim of Pei *et al*. **[38]** was to obtain the fractional derivative using Fourier transform approach, whereas in the proposed method the aim is to obtain the fractional derivative using the fractional Fourier transform approach. Similarly, McBride *et al*. **[6]** derives the differentiation property in the fractional Fourier transform to integer order only, whereas, the proposed method generalize it to obtain the differentiation property in the fractional Fourier transform to non–integer orders. Therefore, the outcome of this work, "establishing a closed form expression for the fractional differentiation in the fractional Fourier transform domain" is novel and unique.

4.3 UTILITY OF FRACTIONAL ORDER PARAMETER IN FODD

In recent years, the application of FOC is attracting more and more researchers in the research areas of science and engineering. For instance, the controllers that utilize the concept of fractional order derivatives and integrals could achieve better performance and robustness over the conventional integer order controllers **[67]**. The fractional order proportional integral derivative (PID) controller proposed in **[72]** is a generalization of PID controller. Here the fractional order derivatives and integrals can adjust the frequency response of the control system. Thus, this characteristic of great flexibility makes it possible to perform much better and more robust control is achieved as compared to the traditional PID controller.

In the signal processing framework of FrFT, there exist a varying parameter φ known as the fractional Fourier transform parameter, which makes use of the additional degree of freedom φ to achieve an optimum domain for which the performance is better. It is one of the most beneficial tools applicable in signal processing, image processing, optics applications, and so on.

By unifying the concepts of the fractional derivatives and the fractional Fourier transform, the fractional order differentiator is designed that has two degrees of freedom — first, is the fractional derivative order μ and second, the fractional Fourier transform parameter φ, respectively. Thus, one could get the advantage of two degrees of freedom for the designed fractional order differentiating filter, for different rotation angles in the time–frequency plane with varying fractional Fourier transform parameter φ, for potential engineering applications.

Thus, the proposed study possesses the benefit of having two degrees of freedom as compared to the conventional methods.

4.4 CLOSED–FORM ANALYTICAL EXPRESSION OF FODD IN FrFTD

This section deals with the mathematical derivation of the fractional order differentiation in the fractional Fourier transform domain, utilizing the mathematical principles of the fractional order calculus. The closed–form analytical expression is obtained in terms of the well–known higher transcendental function known as the confluent hypergeometric function.

The closed–form expression is obtained by incorporating the three most widely used fractional order calculus definitions viz., Riemann–Liouville (RL) definition, Grünwald–Letnikov (GL) definition, and the Caputo definition, respectively.

4.4.1 Riemann–Liouville (RL) Approach

To derive the closed–form analytical expression of the fractional derivative of the signal in the FrFT domain, the inherent approach of the FOC has been utilized. In this section, our FOC approach is confined to the RL definition **[73]** for the general fractional differintegral.

Let ${D_+}^{\mu}$ and ${D_-}^{\mu}$ be the left and right RL fractional derivatives of order μ on the real axis, defined by:

$${D_+}^{\mu}\, x(t) = \frac{d}{dt}\left\{{I_+}^{1-\mu}\, x(t)\right\} \tag{4.4.1}$$

where ${I_+}^{\mu}$ is the RL fractional integral operator,

$${I_+}^{\mu}\, x(t) = \frac{1}{\Gamma(\mu)}\int_{-\infty}^{t}(t-\tau)^{\mu-1}\, x(\tau)d\tau = \frac{t^{\mu-1}}{\Gamma(\mu)} * x(t) \tag{4.4.2}$$

Here, $\Gamma(\cdot)$ is the well known Euler's gamma function, and $\mu \in \mathbb{R}\,(0 < \mu < 1)$. The operator $'*'$ represents the convolution operation between the two signals of interest, here $\frac{t^{\mu-1}}{\Gamma(\mu)}$ and $x(t)$, respectively.

$${D_-}^{\mu}\, x(t) = \left(-\frac{d}{dt}\right)\left\{{I_-}^{1-\mu}\, x(t)\right\} \tag{4.4.3}$$

where ${I_-}^{\mu}$ is the RL fractional integral operator,

$${I_-}^{\mu}\, x(t) = \frac{1}{\Gamma(\mu)}\int_{t}^{+\infty}(t-\tau)^{\mu-1}\, x(\tau)d\tau \tag{4.4.4}$$

In this section, by considering ${D_+}^{\mu}$ RL fractional derivative operator and $0 < \mu < 1$, the following expression is obtained from (4.4.1) and (4.4.2):

$${D_+}^{\mu}\, x(t) = \frac{d}{dt}\left\{\frac{t^{-\mu}}{\Gamma(1-\mu)} * x(t)\right\} \tag{4.4.5}$$

Therefore, taking the FrFT of the fractional derivative of (4.4.5) results in the following expression:

$$\mathrm{T}_{\mathcal{F}}{}^{\varphi}\{{D_+}^{\mu}\, x(t)\} = \mathrm{T}_{\mathcal{F}}{}^{\varphi}\left[\frac{d}{dt}\left\{\frac{t^{-\mu}}{\Gamma(1-\mu)} * x(t)\right\}\right] \tag{4.4.6}$$

where the notation $\mathrm{T}_{\mathcal{F}}{}^{\varphi}(\cdot)$ represents the FrFT operator, with the rotation angle φ.

By letting, $b(t) = \frac{t^{-\mu}}{\Gamma(1-\mu)} * x(t)$, (4.4.6) becomes:

$$\mathrm{T}_{\mathcal{F}}{}^{\varphi}\{D_{+}{}^{\mu}\, x(t)\} = \mathrm{T}_{\mathcal{F}}{}^{\varphi}\left[\frac{db(t)}{dt}\right] \qquad \textbf{(4.4.7)}$$

Now, according to the differentiation property of the FrFT **[95]**, the right hand side of (4.4.7) reduces to:

$$\mathrm{T}_{\mathcal{F}}{}^{\varphi}\left[\frac{db(t)}{dt}\right] = \left[ju_{\varphi}\sin\varphi + \cos\varphi \cdot \frac{d}{du_{\varphi}}\right] B(u_{\varphi}) \qquad \textbf{(4.4.8)}$$

where $B(u_{\varphi}) = \mathrm{T}_{\mathcal{F}}{}^{\varphi}(b(t))$ is the FrFT of the signal $b(t)$.

Therefore,

$$B(u_{\varphi}) = \mathrm{T}_{\mathcal{F}}{}^{\varphi}[b(t)] = \mathrm{T}_{\mathcal{F}}{}^{\varphi}\left[\left\{\frac{t^{-\mu}}{\Gamma(1-\mu)} * x(t)\right\}\right] \qquad \textbf{(4.4.9)}$$

Now, from the convolution property of the FrFT **[9**, **12]**, the above expression reduces to:

$$B(u_{\varphi}) = \left(\sqrt{\frac{2\pi}{1-j\cot\varphi}} \cdot \exp\left[-\frac{j}{2}\, u_{\varphi}{}^{2}\cot\varphi\right]\right) \mathrm{T}_{\mathcal{F}}{}^{\varphi}[x(t)] \cdot \mathrm{T}_{\mathcal{F}}{}^{\varphi}\left[\frac{t^{-\mu}}{\Gamma(1-\mu)}\right]$$

Thus, $B(u_{\varphi}) = \left(\sqrt{\frac{2\pi}{1-j\cot\varphi}} \cdot \exp\left[-\frac{j}{2}\, u_{\varphi}{}^{2}\cot\varphi\right]\right) \cdot X(u_{\varphi}) \cdot \mathrm{T}_{\mathcal{F}}{}^{\varphi}\left[\frac{t^{-\mu}}{\Gamma(1-\mu)}\right]$ **(4.4.10)**

where $X(u_{\varphi})$ is the FrFT of the signal $x(t)$, i.e., $X(u_{\varphi}) = \mathrm{T}_{\mathcal{F}}{}^{\varphi}[x(t)]$.

$$\therefore\ B(u_{\varphi}) = X(u_{\varphi}) \int_{-\infty}^{\infty} \frac{t^{-\mu}}{\Gamma(1-\mu)} \exp\left[\frac{j}{2}\, t^{2}\cot\varphi - j\, u_{\varphi}\, t\, \csc\varphi\right] dt \qquad \textbf{(4.4.11)}$$

From **[51, (A.1.55)]**, the right hand side of (4.4.11) reduces to:

$$\int_{-\infty}^{\infty} t^{\gamma} \exp[\pm jbt - c^{2}t^{2}]dt = \frac{\pi j^{-\gamma}}{c^{\gamma+1}}\left[\frac{{}_1F_1\left(\frac{\gamma+1}{2};\frac{1}{2};\frac{-b^2}{4c^2}\right)}{\Gamma\left(\frac{1-\gamma}{2}\right)} \pm \frac{b}{c}\, j\, \frac{{}_1F_1\left(\frac{\gamma+2}{2};\frac{3}{2};\frac{-b^2}{4c^2}\right)}{\Gamma\left(\frac{-\gamma}{2}\right)}\right] \qquad \textbf{(4.4.12)}$$

The expression on the right hand side of (4.4.12) involves the function ${}_1F_1$, which is known as the Kummer confluent hyper–geometric function (CHF) of the first kind **[107]**, which

is an infinite power series. For computing the Kummer CHF using the computing machine, the series must be truncated to some finite number of terms. So, if the series truncation is used, there must exist the computation error. Abramowitz and Stegun **[107]** provide the methodology for determining the truncation error of an infinite power series. Figure-4.1 shows the variation of the relative error (in percentage) after truncating an infinite power series for different CHF functions (for different *a*'s and *b*'s) and it is clearly shown that the truncation error decreases to zero point wise, as the number of terms increases.

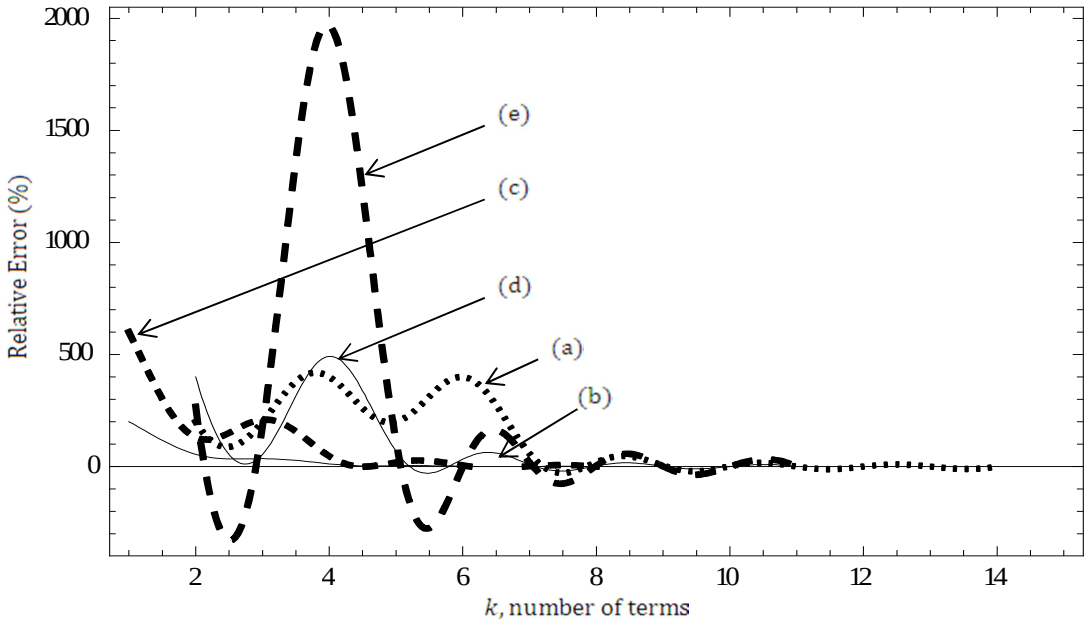

Figure–4.1: Variation of the Relative Error (in percentage) with the number of terms, *k* of the following CHF functions:

(a) ${}_1F_1(a;a;-x)=\exp(-x)$, **(b)** ${}_1F_1\left(\frac{1}{2};\frac{3}{2};-x\right)=\frac{1}{2}\sqrt{\frac{\pi}{x}}\operatorname{erf}\left(\sqrt{x}\right)$,

(c) ${}_1F_1\left(\frac{3}{2};\frac{5}{2};-x\right)=\frac{3}{2}\left[\frac{1}{2}\sqrt{\frac{\pi}{x}}\operatorname{erf}\left(\sqrt{x}\right)-e^{-x}\right]$,

(d) ${}_1F_1\left(1;\frac{3}{2};-x\right)=\frac{1}{2}\sqrt{\frac{\pi}{x}}\operatorname{erfi}\left(\sqrt{x}\right)e^{-x}$,

(e) ${}_1F_1\left(2;\frac{5}{2};-x\right)=\frac{3\sqrt{\pi}\cdot e^{-x}\cdot(1+2x)\cdot\operatorname{erfi}\left(\sqrt{x}\right)}{8x^{3/2}}-\frac{3}{4x}$, by letting $x=2$.

Solving (4.4.11) and (4.4.12) step by step, and by letting, $\gamma = -\mu$, $b = u_\varphi \csc\varphi$, $c^2 = \frac{-j}{2}\cot\varphi$ i.e., $c = \frac{(1-j)}{2}\sqrt{\cot\varphi}$ and $\frac{-b^2}{4c^2} = -ju_\varphi{}^2 \csc(2\varphi)$, (4.4.12) becomes:

$$\int_{-\infty}^{\infty} t^{-\mu} \exp\left[-j\,u_\varphi\,t\,\csc\varphi + \frac{j}{2}\,t^2\cot\varphi\right]dt = \frac{\pi j^\mu (1+j)^{1-\mu}}{(\cot\varphi)^{(1-\mu)/2}}\left[\frac{{}_1F_1\left(\frac{1-\mu}{2};\frac{1}{2};-ju_\varphi{}^2\csc(2\varphi)\right)}{\Gamma\left(\frac{1+\mu}{2}\right)} + ju_\varphi(1+j)\sqrt{2\csc(2\varphi)}\,\frac{{}_1F_1\left(\frac{2-\mu}{2};\frac{3}{2};-ju_\varphi{}^2\csc(2\varphi)\right)}{\Gamma\left(\frac{\mu}{2}\right)}\right] \quad \textbf{(4.4.13)}$$

Thus, it can be seen that the integral representation (4.4.13) is a generalized expression in terms of the fractional derivative order parameter μ and hence the closed form expression for the integral representation (4.4.13) can be obtained by considering different values of the parameter μ, respectively. The example is provided below, by considering the degenerate cases for $\mu = 0$ and $\mu = 1$, respectively.

For example, by letting $\mu = 0$, (4.4.13) becomes:

$$\int_{-\infty}^{\infty} \exp\left[-j\,u_\varphi\,t\,\csc\varphi + \frac{j}{2}\,t^2\cot\varphi\right]dt = \frac{\pi(1+j)}{\sqrt{\cot\varphi}}\quad {}_1F_1\left(\frac{1}{2};\frac{1}{2};-ju_\varphi{}^2\csc(2\varphi)\right) = \sqrt{\pi\tan\varphi}\,(1+j)e^{-ju_\varphi{}^2\csc(2\varphi)} \quad \textbf{(4.4.14)}$$

$\because\ {}_1F_1(a;a;-z) = e^{-z}$ **[107]**. This shows that (4.4.14) is a closed form expression for the integral representation (4.4.13) for the case $\mu = 0$.

Similarly, by letting $\mu = 1$, (4.4.13) becomes:

$$\int_{-\infty}^{\infty} t^{-1} \exp\left[-j\,u_\varphi\,t\,\csc\varphi + \frac{j}{2}\,t^2\cot\varphi\right]dt = j\pi\left[\frac{{}_1F_1\left(0;\frac{1}{2};-ju_\varphi{}^2\csc(2\varphi)\right)}{\Gamma(1)} + ju_\varphi(1+j)\sqrt{2\csc(2\varphi)}\,\frac{{}_1F_1\left(\frac{1}{2};\frac{3}{2};-ju_\varphi{}^2\csc(2\varphi)\right)}{\Gamma\left(\frac{1}{2}\right)}\right] \quad \textbf{(4.4.15)}$$

Simplifying further (4.4.15) becomes **[107]**:

$$\int_{-\infty}^{\infty} t^{-1} \exp\left[-j\,u_\varphi\,t\,\csc\varphi + \frac{j}{2}\,t^2\cot\varphi\right]dt = j\pi\left[1 + j\,\mathrm{erf}\left(\sqrt{ju_\varphi{}^2\csc(2\varphi)}\right)\right] \quad \textbf{(4.4.16)}$$

This shows that (4.4.16) is a closed form expression for the integral representation (4.4.15) for the case $\mu = 1$.

Now, from (4.4.11) and (4.4.13), the following expression results:

$$B(u_\varphi) = X(u_\varphi)\frac{\pi j^{\mu}(1+j)^{1-\mu}}{(\cot\varphi)^{(1-\mu)/2}}\left[\frac{{}_1F_1\left(\frac{1-\mu}{2};\frac{1}{2};-ju_\varphi{}^2\csc(2\varphi)\right)}{\Gamma\left(\frac{1+\mu}{2}\right)} + ju_\varphi(1+j)\sqrt{2\csc(2\varphi)}\,\frac{{}_1F_1\left(\frac{2-\mu}{2};\frac{3}{2};-ju_\varphi{}^2\csc(2\varphi)\right)}{\Gamma\left(\frac{\mu}{2}\right)}\right] \quad \textbf{(4.4.17)}$$

Now, by letting, $K(\mu,\varphi) = \frac{\pi(j^{\mu})(1+j)^{1-\mu}}{(\cot\varphi)^{(1-\mu)/2}}$ and, $M(\varphi) = j(1+j)\sqrt{2\csc(2\varphi)}$, (4.4.17) becomes:

$$B(u_\varphi) = X(u_\varphi)K(\mu,\varphi)\left[\frac{{}_1F_1\left(\frac{1-\mu}{2};\frac{1}{2};-ju_\varphi{}^2\csc(2\varphi)\right)}{\Gamma\left(\frac{1+\mu}{2}\right)} + u_\varphi\, M(\varphi)\,\frac{{}_1F_1\left(\frac{2-\mu}{2};\frac{3}{2};-ju_\varphi{}^2\csc(2\varphi)\right)}{\Gamma\left(\frac{\mu}{2}\right)}\right] \quad \textbf{(4.4.18)}$$

Now, from (4.4.7) and (4.4.8),

$$\mathrm{T}_{\mathcal{F}}{}^{\varphi}\{D_+{}^{\mu}\,x(t)\} = \left(ju_\varphi\sin\varphi + \cos\varphi\frac{d}{du_\varphi}\right)B(u_\varphi) = ju_\varphi\sin\varphi\,B(u_\varphi) + \cos\varphi\frac{dB(u_\varphi)}{du_\varphi} \quad \textbf{(4.4.19)}$$

Therefore, to solve (4.4.19), one has to determine $\frac{dB(u_\varphi)}{du_\varphi}$ and by knowing the fact that **[107]**:

$$\frac{d}{dz}\quad {}_1F_1(a;b;z) = \left(\frac{a}{b}\right)\quad {}_1F_1(a+1;b+1;z) \quad \textbf{(4.4.20)}$$

Solving for $\frac{dB(u_\varphi)}{du_\varphi}$, the following expression results:

$$\frac{dB(u_\varphi)}{du_\varphi} =$$
$$\frac{K(\mu,\varphi)}{\Gamma\left(\frac{1+\mu}{2}\right)}\Big[\quad {}_1F_1\left(\frac{1-\mu}{2};\frac{1}{2};-ju_\varphi{}^2\csc(2\varphi)\right)\frac{dX(u_\varphi)}{du_\varphi} +$$
$$(1-\mu)X(u_\varphi)\quad {}_1F_1\left(\frac{3-\mu}{2};\frac{3}{2};-ju_\varphi{}^2\csc(2\varphi)\right)\Big] +$$
$$\frac{K(\mu,\varphi)\cdot M(\varphi)}{\Gamma\left(\frac{\mu}{2}\right)}\Big[u_\varphi\,X(u_\varphi)\left(\frac{2-\mu}{3}\right)\quad {}_1F_1\left(\frac{4-\mu}{2};\frac{5}{2};-ju_\varphi{}^2\csc(2\varphi)\right) +$$
$$X(u_\varphi)\quad {}_1F_1\left(\frac{2-\mu}{2};\frac{3}{2};-ju_\varphi{}^2\csc(2\varphi)\right) + u_\varphi\quad {}_1F_1\left(\frac{2-\mu}{2};\frac{3}{2};-ju_\varphi{}^2\csc(2\varphi)\right)\frac{dX(u_\varphi)}{du_\varphi}\Big] \quad \textbf{(4.4.21)}$$

Now, by expressing the following confluent hyper–geometric functions by the corresponding functions as:

$${}_1F_1\left(\frac{1-\mu}{2};\frac{1}{2};-ju_\varphi{}^2\csc(2\varphi)\right)=H_1(\mu,\varphi,u_\varphi) \quad \textbf{(4.4.22a)}$$

$${}_1F_1\left(\frac{2-\mu}{2};\frac{3}{2};-ju_\varphi{}^2\csc(2\varphi)\right)=H_2(\mu,\varphi,u_\varphi) \quad \textbf{(4.4.22b)}$$

$${}_1F_1\left(\frac{3-\mu}{2};\frac{3}{2};-ju_\varphi{}^2\csc(2\varphi)\right)=H_3(\mu,\varphi,u_\varphi) \quad \textbf{(4.4.22c)}$$

$${}_1F_1\left(\frac{4-\mu}{2};\frac{5}{2};-ju_\varphi{}^2\csc(2\varphi)\right)=H_4(\mu,\varphi,u_\varphi) \quad \textbf{(4.4.22d)}$$

Therefore, from (4.4.19)–(4.4.22d):

$$\mathrm{T}_{\mathcal{F}}{}^{\varphi}\{D_+{}^{\mu}\,x(t)\}=K(\mu,\varphi)\,M(\varphi)\left\{\frac{1}{M(\varphi)}\,\frac{1}{\Gamma\left(\frac{(1+\mu)}{2}\right)}\,H_1(\mu,\varphi,u_\varphi)\left[ju_\varphi\sin\varphi+\cos\varphi\,\frac{d}{du_\varphi}\right]+\right.$$

$$u_\varphi\,\frac{1}{\Gamma\left(\frac{\mu}{2}\right)}\,H_2(\mu,\varphi,u_\varphi)\left[ju_\varphi\sin\varphi+\cos\varphi\,\frac{d}{du_\varphi}\right]+\frac{1}{\Gamma\left(\frac{\mu}{2}\right)}\cos\varphi\,H_2(\mu,\varphi,u_\varphi)+$$

$$\left.\frac{1}{M(\varphi)}\,\frac{(1-\mu)\cos\varphi}{\Gamma((1+\mu)/2)}\,H_3(\mu,\varphi,u_\varphi)+\left(\frac{2-\mu}{3}\right)\frac{1}{\Gamma\left(\frac{\mu}{2}\right)}\cos\varphi\,H_4(\mu,\varphi,u_\varphi)\,u_\varphi\right\}X(u_\varphi) \quad \textbf{(4.4.23)}$$

Thus, the above expression gives the fractional derivative of the input signal $x(t)$ for fractional orders varying from 0 to 1 and for different rotation angles (φ) in the time–frequency plane of the FrFT.

Now considering two degenerate cases of (4.4.23) for $\mu=0$ and $\mu=1$.

For $\mu=0$, (4.4.23) reduces to the following closed form expression:

$$\mathrm{T}_{\mathcal{F}}{}^{\varphi}\{D_+{}^{0}\,x(t)\}=\cot\varphi\,\sqrt{1+j\tan\varphi}\,\exp\left(-ju_\varphi{}^2\csc(2\varphi)\right)\left[-ju_\varphi\cos\varphi+\sin\varphi\,\frac{d}{du_\varphi}\right]X(u_\varphi) \quad \textbf{(4.4.24)}$$

For $\mu=1$, (4.4.23) reduces to the following closed form expression:

$$\mathrm{T}_{\mathcal{F}}{}^{\varphi}\{D_+{}^{1}\,x(t)\}=\sqrt{\frac{\pi}{2}(j\cot\varphi-1)}\left\{\left(ju_\varphi\sin\varphi+\cos\varphi\,\frac{d}{du_\varphi}\right)+j\,\mathrm{erf}\left(\sqrt{iu_\varphi{}^2\csc(2\varphi)}\right)\cdot\right.$$

$$\left.\left(ju_\varphi\sin\varphi+\cos\varphi\,\frac{d}{du_\varphi}\right)+\frac{2j\cos\varphi}{\sqrt{\pi}}\,\exp\left(-ju_\varphi{}^2\csc(2\varphi)\right)\right\}X(u_\varphi) \quad \textbf{(4.4.25)}$$

In a similar manner, for each value of μ, (4.4.23) reduces to a closed form analytical expression for obtaining the fractional derivative of the chosen input signal in the FrFT domain. Thus, achieving the flexibility of variations of two variables μ and φ, simultaneously.

4.4.2 Grünwald–Letnikov (GL) Approach

An efficient algorithm to compute a discrete counterpart of the proposed algorithm is derived in this section. There exists various fast discrete–time version of the continuous FrFT namely, direct form of discrete fractional Fourier transform (DFrFT), improved sampling–type DFrFT, linear combination–type DFrFT, eigenvectors decomposition–type DFrFT, group theory–type DFrFT and impulse train–type DFrFT. **[133]**

The discrete FrFT algorithm proposed in **[133]**, has an important advantage of efficient computation and implementation. As there are two chirp multiplications and one FFT, the total number of multiplication operations required is $2P + (P/2)\log_2 P$, where $P = 2M + 1$ is the length of the output. The DFrFT introduced in **[133]** have the lowest complexity among all the types of DFrFT that still work similarly to the continuous FrFT. Thus, utilizing the DFrFT algorithm of Type–I proposed in **[133]**, a discrete–time calculation of the fractional order derivative of a discrete–time signal can be realized. In this method, the fractional order derivative of a continuous–time input signal $x(t)$ is evaluated in discrete–time by the following steps.

First, uniformly sample the input function $x(t)$ and the output function $\mathrm{T}_{\mathcal{F}}{}^{\varphi}\big(x(t)\big) = X\big(u_{\varphi}\big)$ by the interval Δt, Δu_{φ} respectively as

$$g(n) = x(n \cdot \Delta t) \qquad G_{\varphi}(m) = X\big(m \cdot \Delta u_{\varphi}\big) \tag{4.4.26}$$

where $n = -N, -N+1, \cdots, N-1, N$, and $m = -M, -M+1, \cdots, M-1, M$.

Additionally, the constraints that

$M \geq N$ ($2N + 1, 2M + 1$ are the number of points in the time, frequency domain) and $\Delta u_{\varphi} \cdot \Delta t = S \cdot 2\pi \cdot \sin\varphi\,/(2M+1)$ must also be satisfied, where $|S|$ is some integer prime to $2M + 1$. **(4.4.27)**

For simplicity, choose $S = \mathrm{sgn}(\sin\varphi) = 1$ and obtain the transformation matrix as:

$$R_{\varphi}(m,n) = \sqrt{\frac{\mathrm{sgn}(\sin\varphi)\cdot(\sin\varphi - j\cos\varphi)}{2M+1}} \cdot e^{\frac{j}{2}\cdot\cot\varphi\cdot m^2\cdot(\Delta u_{\varphi})^2} \cdot e^{-j\cdot\frac{\mathrm{sgn}(\sin\varphi)\cdot 2\pi\cdot n\cdot m}{2M+1}} \cdot e^{\frac{j}{2}\cdot\cot\varphi\cdot n^2\cdot(\Delta t)^2} \tag{4.4.28}$$

Considering only the case for $\sin\varphi > 0$, the following formula of DFrFT is obtained:

$$G_{\varphi}(m) = \sqrt{\frac{\sin\varphi - j\ \cos\varphi}{2M+1}} \cdot e^{\frac{j}{2}\cdot\cot\varphi\cdot m^2\cdot(\Delta u_{\varphi})^2} \cdot \sum_{n=-N}^{N} e^{-j\cdot\frac{2\pi\cdot n\cdot m}{2M+1}} \cdot e^{\frac{j}{2}\cdot\cot\varphi\cdot n^2\cdot(\Delta t)^2} \cdot g(n) \qquad \textbf{(4.4.29)}$$

when $\varphi\ \in 2P\pi + (0,\pi)$, P is an integer.

Now the evaluation of the fractional derivative of the discrete–time signal in the DFrFT domain is described as follows:

Considering in this paper, the GL definition **[73, 89]** of computing the fractional derivative, based on the generalization of the backward difference as:

$$D^{\mu}x(t) = \frac{d^{\mu}x(t)}{dt^{\mu}} = \lim_{\Delta t\to 0}\sum_{k=0}^{\infty}\frac{(-1)^k \tilde{\mathrm{A}}_k{}^{\mu}}{(\Delta t)^{\mu}} x(t - k\cdot\Delta t) \qquad \textbf{(4.4.30)}$$

where coefficient $\tilde{\mathrm{A}}_k{}^{\mu}$ is given by:

$$\tilde{\mathrm{A}}_k{}^{\mu} = \frac{\Gamma(\mu+1)}{\Gamma(k+1)\Gamma(\mu-k+1)} = \begin{cases} 1 & k = 0 \\ \frac{\mu(\mu-1(\mu-2)\cdots(\mu-k+1))}{1\cdot 2\cdot 3\cdots k} & k \geq 1 \end{cases} \qquad \textbf{(4.4.31)}$$

The above notation $\Gamma(\cdot)$ is the gamma function. Based on this definition, it can be shown that the fractional derivatives of exponential, trigonometric and power functions (assuming sufficiently large) are given by:

$$D^{\mu}[\exp(\beta t)] = \beta^{\mu}\exp(\beta t) \qquad \textbf{(4.4.32a)}$$

$$D^{\mu}\left[\hat{\mathrm{A}}\sin(\omega t + \theta)\right] = \hat{\mathrm{A}}\omega^{\mu}\sin\left(\omega t + \theta + \frac{\pi}{2}\mu\right) \qquad \textbf{(4.4.32b)}$$

$$D^{\mu}\left[\hat{\mathrm{A}}\cos(\omega t + \theta)\right] = \hat{\mathrm{A}}\omega^{\mu}\cos\left(\omega t + \theta + \frac{\pi}{2}\mu\right) \qquad \textbf{(4.4.32c)}$$

$$D^{\mu}(t^{\gamma}) = \frac{\Gamma(\gamma+1)}{\Gamma(\gamma-\mu+1)}\cdot t^{\gamma-\mu} \qquad \textbf{(4.4.32d)}$$

Now, let us define the coefficient $\tilde{\mathrm{a}}(k)$ as:

$$\tilde{\mathrm{a}}(k) = (-1)^k \tilde{\mathrm{A}}_k{}^{\mu} \qquad \textbf{(4.4.33)}$$

then, the fractional derivative in (4.4.30) can be rewritten as:

$$D^{\mu}x(t) = \lim_{\Delta t\to 0}\sum_{k=0}^{\infty}\frac{\tilde{\mathrm{a}}(k)}{(\Delta t)^{\mu}}\, x(t - k\cdot\Delta t) \qquad \textbf{(4.4.34)}$$

The coefficient sequence $\tilde{a}(k)$ for various orders of fractional derivative order parameter μ can be plotted as in Figure-4.2. It can be seen from the Figure-4.2 that the sequence $\tilde{a}(k)$ is a rapidly decaying sequence for various orders of μ.

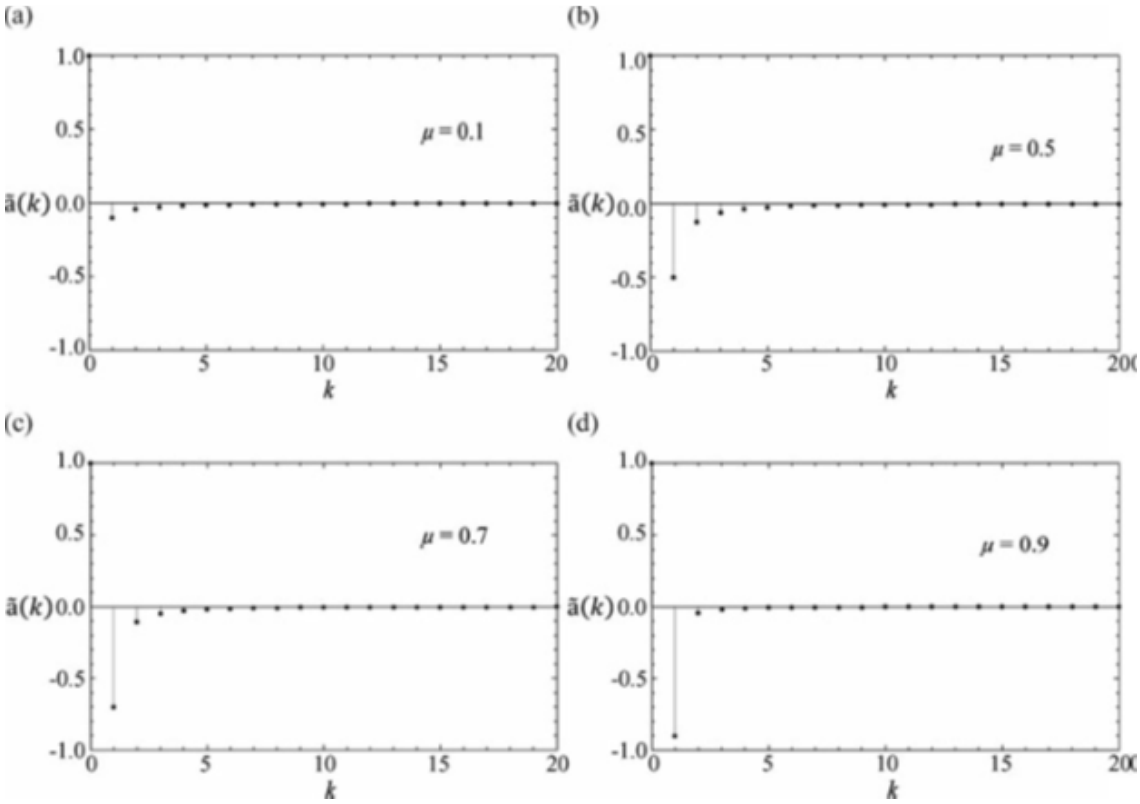

Figure–4.2: The coefficient sequence $\tilde{a}(k)$ for varying fractional derivative order parameter μ.

Thus, by truncation, (4.4.34) can be re–written as:

$$D^{\mu}x(t) \approx \lim_{\Delta t \to 0} \sum_{k=0}^{L} \frac{\tilde{a}(k)}{(\Delta t)^{\mu}} x(t - k \cdot \Delta t) \qquad \textbf{(4.4.35)}$$

where L is the truncation length.

Furthermore, by removing the limit, (4.4.35) can be further approximated by:

$$D^{\mu}x(t) \approx \sum_{k=0}^{L} \frac{\tilde{a}(k)}{(\Delta t)^{\mu}} x(t - k \cdot \Delta t) \qquad \textbf{(4.4.36)}$$

Obviously, the smaller Δt is, the better approximation in (4.4.36) has.

Now the operation $D^{\mu}x(t)$ at $t = n \cdot \Delta t$ is defined as:

$$D^{\mu}x(t)|_{t=n\cdot\Delta t} = D^{\mu}x(n\cdot\Delta t) \approx \sum_{k=0}^{L}\frac{\tilde{a}(k)}{(\Delta t)^{\mu}}x(n\cdot\Delta t - k\cdot\Delta t) \quad \textbf{(4.4.37)}$$

where the fractional order parameter is $\mu \in \mathbb{R}\ (0 < \mu < 1)$ and $\tilde{a}(k)$ is given by (4.4.33).

As the proposed algorithm attempts to determine the closed–form fractional order differentiation in the FrFT domain, thereby taking the DFrFT of (4.4.37), as illustrated by the DFrFT algorithm **[133]**, (4.4.37) becomes:

$$\mathfrak{Q}_{\mathcal{F}}{}^{\varphi}[D^{\mu}x(n\cdot\Delta t)] \approx \mathfrak{Q}_{\mathcal{F}}{}^{\varphi}\left[\sum_{k=0}^{L}\frac{\tilde{a}(k)}{(\Delta t)^{\mu}}x(n-k)\right] \quad \textbf{(4.4.38)}$$

$$\text{i.e., } \mathfrak{Q}_{\mathcal{F}}{}^{\varphi}[D^{\mu}g(n)] = \sum_{k=0}^{L}\frac{\tilde{a}(k)}{(\Delta t)^{\mu}}\cdot\left(\mathfrak{Q}_{\mathcal{F}}{}^{\varphi}\left(x(n-k)\right)\right) \quad \textbf{(4.4.39)}$$

where $g(n)$ is given by (4.4.26) and the notation $\mathfrak{Q}_{\mathcal{F}}{}^{\varphi}$ represents the DFrFT operator, respectively.

Thus,

$$\mathfrak{Q}_{\mathcal{F}}{}^{\varphi}[D^{\mu}g(n)] = \sum_{k=0}^{L}\frac{\tilde{a}(k)}{(\Delta t)^{\mu}}\exp\left[\frac{j}{2}(k\Delta t)^2\sin\varphi\cos\varphi - j\left(m\Delta u_{\varphi}\right)(k\Delta t)\sin\varphi\right]G_{\varphi}(m - k\cos\varphi) \quad \textbf{(4.4.40)}$$

where $G_{\varphi}(m)$ is given by (4.4.26), respectively.

Thus, (4.4.40) represents the DFrFT of the fractional order derivative of the discrete–time signal $g(n)$, respectively.

4.4.3 Caputo Approach

In this section, a novel closed–form analytical expression of the fractional derivative of the signal in the FrFT domain has been derived. This has been obtained by utilizing the inherent approach of the FOC. The FOC approach in this section is confined to the Caputo definition **[73]** for the general fractional differintegral.

Let, ${}_{l}^{C}D_{t}{}^{\mu}$ be the Caputo fractional derivative operator of order μ on the real axis, defined by:

$${}_{l}^{C}D_{t}{}^{\mu}\ x(t) = \frac{t^{-\mu}}{\Gamma(1-\mu)} * \frac{dx(t)}{dt} \quad \textbf{(4.4.41)}$$

Here, $\Gamma(\cdot)$ is the well–known Euler's gamma function, and $\mu \in \mathbb{R}\,(0 < \mu < 1)$. The operator $'*'$ represents the convolution operation between the two signals of interest, here $\frac{t^{\mu-1}}{\Gamma(\mu)}$ and $x(t)$, respectively.

Taking the Fourier transform (FT) of the fractional derivative of (4.4.41) results in the following expression:

$$\Im[{}_l^C D_t^{\mu}\, x(t)] = \Im\left[\frac{t^{-\mu}}{\Gamma(1-\mu)} * \frac{dx(t)}{dt}\right] \quad \textbf{(4.4.42)}$$

where $\Im$ denotes the FT operator.

Now, from the convolution property of the FT **[125]**, (4.4.42) reduces to:

$$\Im[{}_l^C D_t^{\mu}\, x(t)] = \Im\left[\frac{t^{-\mu}}{\Gamma(1-\mu)}\right] \Im\left[\frac{dx(t)}{dt}\right] \quad \textbf{(4.4.43)}$$

Therefore, the FT of the fractional derivative of (4.4.41) results in the following expression:

$$\Im[{}_l^C D_t^{\mu}\, x(t)] = (j\omega)^{\mu}\, X(\omega) \quad \textbf{(4.4.44)}$$

where $\Im[t^{-\mu}] = (j\omega)^{\mu-1}\,\Gamma(1-\mu)$.

Thus, the FT of the Caputo fractional derivative of order μ of a signal is $(j\omega)^{\mu}$ times the FT of the signal of interest, where $0 < \mu < 1$.

Now, we will consider the FrFT of the Caputo fractional derivative as follows:

Taking the FrFT of the Caputo fractional derivative of (4.4.41) results in the following expression:

$$\mathfrak{T}_{\mathcal{F}}{}^{\varphi}[{}_l^C D_t^{\mu}\, x(t)] = \mathfrak{T}_{\mathcal{F}}{}^{\varphi}\left[\frac{t^{-\mu}}{\Gamma(1-\mu)} * \frac{dx(t)}{dt}\right] \quad \textbf{(4.4.45)}$$

with the transform angle $\varphi = a\pi/2$, and $\mathfrak{T}_{\mathcal{F}}{}^{\varphi}$ denotes the CFrFT operator.

From the convolution property of the FrFT **[9]** and **[12]**, the above expression reduces to:

$$\mathfrak{T}_{\mathcal{F}}{}^{\varphi}[{}_l^C D_t^{\mu}\, x(t)] = \left(\sqrt{\frac{2\pi}{1-j\cot\varphi}}\,\exp\left[-\frac{j}{2}\,u_{\varphi}{}^2\cot\varphi\right]\right)\mathfrak{T}_{\mathcal{F}}{}^{\varphi}\left[\frac{t^{-\mu}}{\Gamma(1-\mu)}\right]\,\mathfrak{T}_{\mathcal{F}}{}^{\varphi}\left[\frac{dx(t)}{dt}\right] \quad \textbf{(4.4.46)}$$

According to the differentiation property of the FrFT **[95]**:

$$\mathrm{T}_{\mathcal{F}}{}^{\varphi}\left[\frac{dx(t)}{dt}\right] = \left[ju_{\varphi}\sin\varphi\, X(u_{\varphi}) + \cos\varphi\, \frac{dX(u_{\varphi})}{du_{\varphi}}\right] \quad \textbf{(4.4.47)}$$

where $X(u_{\varphi}) = \mathrm{T}_{\mathcal{F}}{}^{\varphi}[x(t)]$ is the FrFT of the signal $x(t)$.

Therefore, from (4.4.46) and (4.4.47), the following expression results:

$$\mathrm{T}_{\mathcal{F}}{}^{\varphi}[{}_{l}^{C}D_{t}{}^{\mu}\, x(t)] = \left\{\left[ju_{\varphi}\sin\varphi\, X(u_{\varphi}) + \cos\varphi\, \frac{dX(u_{\varphi})}{du_{\varphi}}\right]\right\}\left(\sqrt{\frac{2\pi}{1-j\cot\varphi}}\,\exp\left[-\frac{j}{2}\,u_{\varphi}{}^{2}\cot\varphi\right]\right)\mathrm{T}_{\mathcal{F}}{}^{\varphi}\left[\frac{t^{-\mu}}{\Gamma(1-\mu)}\right] \quad \textbf{(4.4.48)}$$

$$\mathrm{T}_{\mathcal{F}}{}^{\varphi}[{}_{l}^{C}D_{t}{}^{\mu}\, x(t)] = \left[ju_{\varphi}\sin\varphi\; X(u_{\varphi}) + \cos\varphi\, \frac{dX(u_{\varphi})}{du_{\varphi}}\right]\int_{-\infty}^{\infty}\frac{t^{-\mu}}{\Gamma(1-\mu)}\exp\left[\frac{j}{2}\,t^{2}\cot\varphi - j\,u_{\varphi}\,t\,\csc\varphi\right]dt \quad \textbf{(4.4.49)}$$

Now, for solving the integral in (4.4.49) results in **[51, (A.1.55)]**:

$$\int_{-\infty}^{\infty} t^{\gamma}\exp(\pm jbt - c^{2}t^{2})\,dt = \frac{\pi j^{-\gamma}}{c^{\gamma+1}}\left[\frac{{}_{1}F_{1}\left(\frac{\gamma+1}{2};\frac{1}{2};\frac{-b^{2}}{4c^{2}}\right)}{\Gamma\left(\frac{1-\gamma}{2}\right)} \pm \frac{b}{c}j\,\frac{{}_{1}F_{1}\left(\frac{\gamma+2}{2};\frac{3}{2};\frac{-b^{2}}{4c^{2}}\right)}{\Gamma\left(\frac{-\gamma}{2}\right)}\right] \quad \textbf{(4.4.50)}$$

The function ${}_{1}F_{1}$ on the right hand side of (4.4.50), which is known as the Kummer CHF of the first kind is an infinite power series. For computing the Kummer CHF using the computing machine, the series must be truncated to some finite number of terms. So, if the series truncation is used, there must exist a computation error. The methodology for determining the truncation error of an infinite power series is given in **[107]**.

The variation of the relative error (in percentages) after truncating an infinite power series for different CHF functions (for different *a*'s and *b*'s) is shown in Figure-4.1 and it is clearly shown that the truncation error decreases to zero pointwise, as the number of terms increases. The functions erf $(\cdot)$ and erfi $(\cdot)$ denotes the error function and the imaginary error function, respectively related by the relation erfi $(z) = -j\,\mathrm{erf}\,(jz)$. **[107]**

Now by letting, $\gamma = -\mu$, $b = u_{\varphi}\csc\varphi$, $c^{2} = \frac{-j}{2}\cot\varphi$, and $\frac{-b^{2}}{4c^{2}} = -ju_{\varphi}{}^{2}\csc(2\varphi)$, (4.4.48) becomes:

$$\int_{-\infty}^{\infty} t^{-\mu} \exp\left[-j\, u_\varphi\, t\, \csc\varphi + \frac{j}{2}\, t^2 \cot\varphi\right]\, dt = \frac{\pi j^{\mu}(1+j)^{1-\mu}}{(\cot\varphi)^{(1-\mu)/2}}\left[\frac{{}_1F_1\left(\frac{1-\mu}{2};\frac{1}{2};-ju_\varphi{}^2\csc(2\varphi)\right)}{\Gamma\left(\frac{1+\mu}{2}\right)} + ju_\varphi(1+j)\sqrt{2\csc(2\varphi)}\,\frac{{}_1F_1\left(\frac{2-\mu}{2};\frac{3}{2};-ju_\varphi{}^2\csc(2\varphi)\right)}{\Gamma\left(\frac{\mu}{2}\right)}\right] \quad \textbf{(4.4.51)}$$

Thus, it can be seen that the integral representation (4.4.51) is a generalized closed–form expression in terms of μ, and hence the closed–form expression for the integral representation (4.4.51) can be obtained by considering different values of the parameter μ, respectively. The example is provided below, by considering the degenerate cases for $\mu = 0$ and $\mu = 1$, respectively.

For example, by letting $\mu = 0$, (4.4.51) becomes:

$$\int_{-\infty}^{\infty} \exp\left(-j\, u_\varphi\, t\, \csc\varphi + \frac{j}{2}\, t^2 \cot\varphi\right) dt = \frac{\pi(1+j)}{\sqrt{\cot\varphi}}\quad {}_1F_1\left(\frac{1}{2};\frac{1}{2};-ju_\varphi{}^2\csc(2\varphi)\right) = \sqrt{\pi\tan\varphi}\,(1+j)\mathrm{e}^{-ju_\varphi{}^2\csc(2\varphi)} \quad \textbf{(4.4.52)}$$

$\because\quad {}_1F_1(a;a;-z) = e^{-z}$. Thus, (4.4.52) is a closed–form expression for the integral representation (4.4.49) for the case $\mu = 0$.

Similarly, by letting $\mu = 1$, (4.4.51) becomes:

$$\int_{-\infty}^{\infty} t^{-1} \exp\left(-j\, u_\varphi\, t\, \csc\varphi + \frac{j}{2}\, t^2 \cot\varphi\right)\, dt = j\pi\left[\frac{{}_1F_1\left(0;\frac{1}{2};-ju_\varphi{}^2\csc(2\varphi)\right)}{\Gamma(1)} + ju_\varphi(1+j)\sqrt{2\csc(2\varphi)}\,\frac{{}_1F_1\left(\frac{1}{2};\frac{3}{2};-ju_\varphi{}^2\csc(2\varphi)\right)}{\Gamma\left(\frac{1}{2}\right)}\right] \quad \textbf{(4.4.53)}$$

Simplifying further, (4.4.53) becomes:

$$\int_{-\infty}^{\infty} t^{-1} \exp\left(-j\, u_\varphi\, t\, \csc\varphi + \frac{j}{2}\, t^2 \cot\varphi\right) dt = j\pi\left[1 + j\,\mathrm{erf}\left(\sqrt{ju_\varphi{}^2\csc(2\varphi)}\right)\right] \quad \textbf{(4.4.54)}$$

Thus, (4.4.54) is a closed-form expression for the integral representation (4.4.49) for the case $\mu = 1$.

Now, from (4.4.49) and (4.4.51), the following expression results:

$$\mathrm{T}_{\mathcal{F}}{}^{\varphi}[{}_{l}^{C}D_{t}{}^{\mu}\, x(t)] = \left[ju_{\varphi}\sin\varphi\, X(u_{\varphi}) + \cos\varphi\,\frac{dX(u_{\varphi})}{du_{\varphi}}\right]\frac{\pi j^{\mu}(1+j)^{1-\mu}}{(\cot\varphi)^{(1-\mu)/2}}\left[\frac{{}_1F_1\left(\frac{1-\mu}{2};\frac{1}{2};-ju_{\varphi}{}^2\csc(2\varphi)\right)}{\Gamma(1-\mu)\cdot\Gamma\left(\frac{1+\mu}{2}\right)} + ju_{\varphi}(1+j)\sqrt{2\csc(2\varphi)}\,\frac{{}_1F_1\left(\frac{2-\mu}{2};\frac{3}{2};-ju_{\varphi}{}^2\csc(2\varphi)\right)}{\Gamma(1-\mu)\cdot\Gamma\left(\frac{\mu}{2}\right)}\right] \quad \textbf{(4.4.55)}$$

Thus, (4.4.55) gives the Caputo-based fractional derivative of the input signal $x(t)$ for varying fractional orders from 0 to 1 and for different rotation angles (φ) in the time–frequency plane of the FrFT.

Thus, (4.4.42) and (4.4.55) represents the FT and the FrFT representation of the Caputo fractional derivative of the input signal $x(t)$ with μ varying from 0 to 1 and for different φ's in the TF plane of the FrFT.

Further, the FrFT approaches the conventional FT for the rotation angle $\varphi = \pi/2$ and the integer-order derivative in the conventional FT can be obtained by substituting the parameters $\mu = 1$ and $\varphi = \pi/2$ in deriving the FrFT representation of the Caputo fractional derivative of the input signal $x(t)$ as follows:

Substituting $\varphi = \pi/2$ in (4.4.49) gives:

$$\mathrm{T}_{\mathcal{F}}{}^{\pi/2}\left[\frac{dx(t)}{dt}\right] = [j\omega\, X(\omega)]\frac{1}{\Gamma(1-\mu)}\int_{-\infty}^{\infty} t^{-1}\exp[-j\,\omega\,t]\,dt \quad \textbf{(4.4.56)}$$

where $\omega = u_{\pi/2}$

Solving (4.4.56):

$$\mathrm{T}_{\mathcal{F}}{}^{\pi/2}\left[\frac{dx(t)}{dt}\right] = [j\omega\, X(\omega)]\frac{1}{\Gamma(1-\mu)}(j\omega)^{\mu-1}\Gamma(1-\mu) \quad \textbf{(4.4.57)}$$

Now substituting $\mu = 1$ in (4.4.57) gives:

$$\mathrm{T}_{\mathcal{F}}{}^{\pi/2}\left[\frac{dx(t)}{dt}\right] = j\omega\, X(\omega) \quad \textbf{(4.4.58)}$$

Thus, (4.4.58) represents the conventional FT of the integer-order derivative of the input signal $x(t)$ using the FrFT representation of the Caputo fractional derivative of the input signal $x(t)$.

4.4.4 Uniqueness of FODD in FrFTD

The fractional order digital differentiator (FODD) designed by utilizing the inherent approach of fractional order calculus and amalgamating with the emerging signal processing tool of the fractional Fourier transform offers the generalization of the traditional differentiating filter from integer order to the fractional order.

A closed–form analytical expression for the fractional order differentiation in the Fourier transform and the fractional Fourier transform domains is derived by utilizing the basic principles of the fractional order calculus. The reported work is a generalization of the differentiation property to the fractional (non–integer or real) orders in the fractional Fourier transform domain.

The research is motivated towards investigating the behavior of the designed fractional order differentiator in the fractional Fourier transform domain. It is provided by the inherency of the fractional order calculus and the fractional Fourier transformation tool. Therefore, the research leads to the variation of two parameters: the fractional derivative order parameter (μ) and the fractional Fourier transform parameter (φ), which has not been taken into consideration earlier in the signal processing applications.

The analytical expression is established in terms of the well–known confluent hypergeometric function, which finds a great revival of interest in the last two decades. This function is ubiquitous in mathematical physics and in many areas of mathematics such as representation theory, algebraic geometry and Hodge theory, combinatorics, number theory, mirror symmetry, etc.

The confluent hypergeometric function also contains other functions as special cases, including many that are widely used in mathematical physics, digital communication applications, and the calculation of bit error rates for different fading channels. Special cases include the Bessel functions, the incomplete gamma (and hence further special cases including, error functions and Fresnel integrals), Laguerre polynomials, Hermite polynomials, Coulomb wave functions, and parabolic cylinder functions.

4.5 COMPARATIVE ANALYSIS BETWEEN RL AND CAPUTO BASED DEFINITIONS

A new closed–form analytical expression for the fractional order differentiation in the fractional Fourier transform domain is presented based on the popular definitions of Riemann–Liouville (RL) and Caputo. This work is the generalization of the differentiation property to the fractional orders in the fractional Fourier transform domain. Thus, it motivates for the variation of two parameters — fractional derivative order parameter (μ) and fractional Fourier transform parameter (φ). This closed form analytical expression derived is obtained with the help of the Kummer confluent hyper–geometric mathematical function.

The fractional order differentiation derived in the reported work proves to have a better definition, since it achieves the flexibility of different rotation angles $\boldsymbol{\varphi}$ in the time–frequency plane of the fractional Fourier transform with varying fractional derivative order parameter $\boldsymbol{\mu}$. Due to this variation of $\boldsymbol{\mu}$ with $\boldsymbol{\varphi}$ in the fractional Fourier transform domain, potential signal processing applications can be achieved as in one–dimensional signal processing of filtering operation and the two–dimensional signal processing of edge detection in image processing, etc.

The most known and popular fractional derivatives are almost surely the RL and Caputo derivatives as is well–established in **[30, 43, 68, 73, 110, 111]**. It has also been elaborated in rich literature that the definition based on Caputo fractional derivative sense is preferred because its initial conditions have a nice physical meaning as is elaborated by Podlubny **[71]**, and Monje *et al.* **[30]**. But still there has been a lot of debate about the usage and the practicality between the RL and Caputo based fractional derivative definitions in the research community.

Furthermore, the key difference that can be pointed between the two versions is the fact that these two approaches requires different types of initial conditions when they are used to formulate the differential equations and its necessary that these initial value problems be well–posed **[79]**. The Caputo fractional derivative is more suited than the usual RL derivative for the applications in several engineering problems due to the fact that it has better relations with the Laplace transform and because the differentiation appears inside instead outside the integral, so to alleviate the effects of noise and numerical differentiation **[71, 110]**.

Thus, based on the recommendations made by the renowned researchers, an attempt is made to validate the above viewpoint concerning the suitability of the two definitions from the signal processing application point of view. So, the one–dimensional signal processing application is concerned in the next chapter which attempts for the filtering operation in the fractional Fourier transform domain utilizing the approaches of the two aforementioned fractional derivative definitions.

Hence, the freedom of utilizing varying order of derivative (fractional derivative) in the entire time–frequency plane of the fractional Fourier transform domain can be enjoyed for different potential signal processing applications.

CHAPTER 5

FILTERING APPLICATION OF FODD IN FrFTD

AS THE RESEARCH MOTIVATION is focused on designing the fractional order differentiating filter that behaves in the fractional Fourier transform domain, so the foremost attempt is to establish its closed–form analytical expression. The closed–form expression has been established in the previous chapter, which shows that the proposed filter has two degrees of freedom namely; the fractional derivative order parameter μ and the fractional Fourier transform parameter φ, respectively. The involvement of these two parameters makes the design more effective and exhibits less error than the conventional methods.

In this chapter, the focus is on designing the fractional order differentiating filter in the fractional Fourier transform domain, so as to make the proposed study more effective in the design as compared to the conventional methods.

5.1 FILTERING: ONE–DIMENSIONAL SIGNAL PROCESSING

The theory of fractional order calculus was developed in the seventies of the last century. In 1695, Gottfried Wilhelm Leibniz was the first one who thought about non–integer derivatives. Other renowned mathematicians like L'Hôpital, Euler, Laplace and Lacroix contributed a lot to the development of calculus of fractional/non–integer orders. **[89]**

In the last decades, many scientific works and rich literature have been reported on the usage of the fractional order calculus in different regimes of engineering arenas such as, electrical circuits, chaotic circuits, fractional order filters and systems, fractional order control systems, and signal processing, to name a few.

Fractional order calculus concerns the generalization of differentiation and integration to non–integer (fractional) orders. This subject has a long mathematical history and over the centuries many mathematicians and physicists have built up a vast amount of mathematical knowledge on fractional integrals and derivatives. Although the fractional order calculus is a natural generalization of Newtonian calculus and has a long mathematical history, still plays a negligible role in the signal processing.

This chapter focuses on the one–dimensional signal processing filtering application of the fractional order differentiating filter in the fractional Fourier transform domain, by combining the elementary concepts of fractional order calculus and fractional Fourier transform. The filtering operation of the input signal is corrupted by the high–frequency chirp noise. The proposed filter is applied to filter out the noise, so that the output filtered signal is obtained. This filtering scheme utilizes the fundamental concepts of the fractional order calculus namely, the Riemann–Liouville and the Caputo based definitions. Also, an investigation is carried out to compare the performances of the two aforementioned fractional derivative definitions in designing the proposed filter.

5.2 FODD AS AN OPTIMAL FILTER IN FrFTD

Fractional order calculus has been attracting the attention of scientists and engineers from long time ago, resulting in the development of many applications. In recent years, the concepts of fractional order calculus have been applied in the design of fractional order digital differentiators, which received much attention in the signal processing research community. In general, the fractional order calculus with varying parameter μ known as the fractional derivative order parameter allows describing the systems more accurately. **[110]**

The research community has investigated the design of fractional order differentiator based on the mathematical principles of fractional order calculus. This fractional order differentiator so obtained proves its advantages in the signal processing framework of the Fourier transform and performs the signal filtering operation. But after following the introduction of the fractional Fourier transform (FrFT) **[154]**, there has been a surge of research in the application areas of signal processing and other research fields that encompasses the class of signals which

behaves in a time–variant phenomenon. That is to say, the FrFT is a time–frequency analysis tool that finds wide applications in the signal analysis of non–stationary signals. Specifically, the FrFT implements the so–called transform order parameter φ which acts on the classical Fourier transform operator. In other words, the φth order FrFT represents the φth power of the classical Fourier transform operator. Any intermediate value of φ $(0 < \varphi < \pi/2)$ produces a signal representation that can be considered as a rotated time–frequency representation of the signal **[54]**. The time–frequency analysis refers to the distribution of the energy of a signal simultaneously in time and frequency. The FrFT is a theory developed in recent years which processes signals in the time–frequency domain **[65]**. However the classical FT has the additional flexible parameter of the FrFT rotation angle φ. This gives an added advantage over the classical FT, which provides widespread potential applications for processing nonstationary signals.

From the best of our knowledge, most of research was based on applying the concepts of FOC and FrFT separately to investigate the differentiation operation in signal processing that leads to have the flexibility of only one individual varying parameter for each of them. So far the research community has not combined these two concepts of FOC and FrFT in unison. By having two varying parameters of interest (fractional order differentiation and transformation), a more generalized definition could be obtained which could prove to be beneficial in the signal processing applications. So, by combining these two revolutionary ideas, the fractional order differentiator could be designed based on the principles of fractional order differentiation in the signal processing framework of FrFT, thereby obtaining the potential applications in signal and image processing areas.

Thus, the designed fractional order differentiator in the fractional Fourier transform domain possesses the benefit of having two degrees of freedom as compared to the conventional methods. The proposed fractional order differentiator is based on the added flexibility of the fractional–order operators in the optimum fractional Fourier transform domain.

5.3 DESIGN OF LOW–PASS FINITE IMPULSE RESPONSE (LP–FIR) FODD IN FrFTD

In this section, the design of the fractional order differentiating filter based on the definitions of the Riemann–Liouville (RL) and Caputo fractional derivatives is illustrated. The proposed filter is a generalized form of the traditional integer order filter.

The proposed filter is designed using the fractional Fourier transformation tool **[65]** and the established convolution theorem **[12]**. Subsequently, the simulation results are exposited that shows the effectiveness of the proposed method over the conventional methods. Thereby, the performance of the RL and Caputo based fractional derivatives definitions are compared with each other in the context of the proposed design.

5.3.1 Design based on the Riemann–Liouville (RL) Fractional Derivative Definition

The proposed fractional order differentiating filtering scheme based on the Riemann–Liouville (RL) based fractional derivative definition in the φth fractional Fourier transform domain is shown in Figure–5.1.

In this configuration, first the φth domain of FrFT **[133]** of the input signal $s(n)$ corrupted with the high–frequency chirp noise $\Omega(n)$ is obtained and then the fractional order impulse response filter $H^{\mu}(u_{\varphi})$ is applied. The weighted convolution theorem for FrFT of **[12]** is used in the proposed filtering scheme. Here, the notation $\mathrm{T}_{\mathcal{F}}{}^{\varphi}(\cdot)$ represents the FrFT operator, with the rotation angle φ.

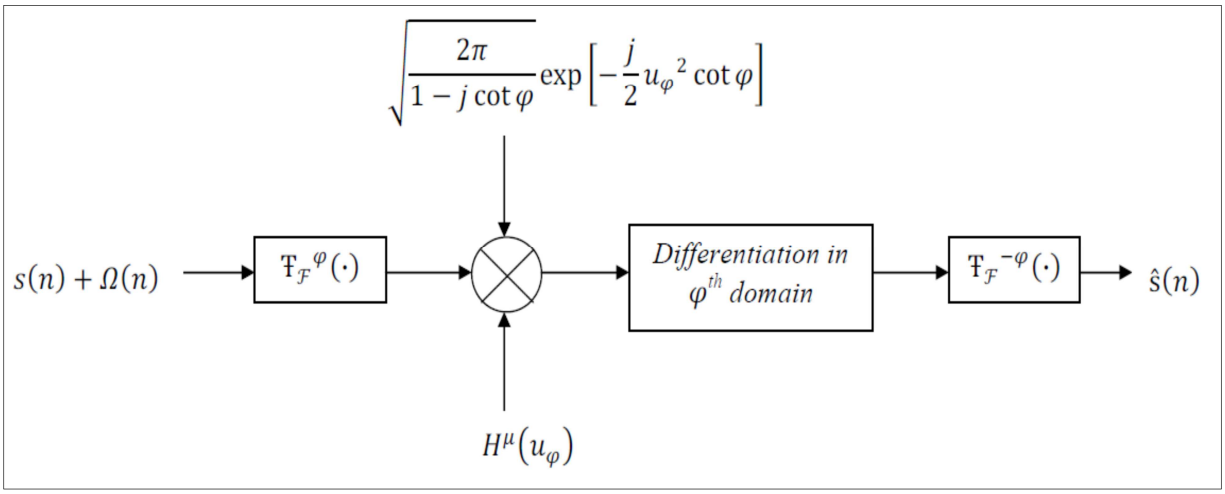

Figure–5.1: Fractional order differentiating filter in fractional Fourier transform domain based on RL fractional derivative definition.

Finally, the resulting output filtered signal is transformed with order $'-\varphi'$ to obtain the output signal $\hat{s}(n)$ in the time domain. The optimum fractional Fourier transform domain (or optimum FrFT rotation angle φ) is chosen, which minimizes the root mean square error $(RMSE)$. The $RMSE$ is used as the metric parameter to judge its performance.

5.3.2 Design based on the Caputo Fractional Derivative Definition

Another approach is elaborated to design the proposed design utilizing the definition of the Caputo based fractional derivative. The proposed fractional order differentiating filtering scheme in the φth fractional Fourier transform domain is shown in Figure-5.2.

In this configuration, the φth domain of FrFT **[133]** of the input signal $s(n)$ corrupted with the high–frequency chirp noise $\Omega(n)$ is obtained. The fractional order impulse response filter $H^{\mu}(u_\varphi)$ is applied in this domain and then the convolution theorem based on **[12]** for FrFT is used to get the filtered output signal, $\hat{s}(n)$.

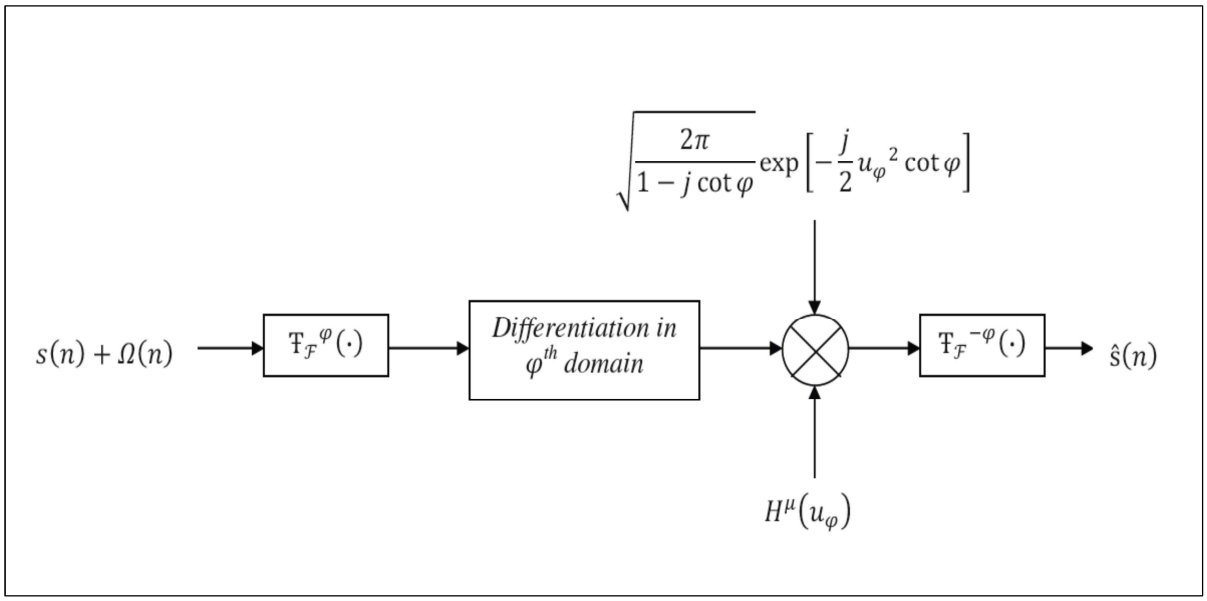

Figure–5.2: Fractional order differentiating filter in fractional Fourier transform domain based on Caputo fractional derivative definition.

To retrieve the output filtered signal in the time domain, the resulting waveform is transformed with order $'-\varphi'$. The optimum fractional Fourier transform domain (or optimum FrFT rotation angle φ) is obtained which minimizes the metric parameter of root mean square error $(RMSE)$.s

5.4 PERFORMANCE METRIC

The root mean square error $(RMSE)$ is a frequently used measure of the difference between the values predicted by a model and the values actually observed from the system being modeled.

The $RMSE$ of a model prediction with respect to the estimated variable X_{model} is defined as the square root of the mean squared error as:

$$RMSE = \sqrt{\frac{\sum_{i=1}^{n}\left(X_{obs,i}-X_{model,i}\right)^2}{n}} \qquad \textbf{(5.4.1)}$$

where X_{obs} is observed values and X_{model} is modeled values at time i.

In the proposed filtering scheme, the $RMSE$ is used as the performance metric parameter for judging the performance of the designed fractional order differentiating filter in the fractional Fourier transform domain, for both cases of Riemann–Liouville and Caputo based fractional derivative definitions.

5.5 SIMULATION RESULTS

The proposed model which describes the fractional order differentiation in the fractional Fourier transform domain is simulated and the description of the simulation platform is provided in Section 2.7 of Chapter 2.

The proposed model of Figure-5.1 and Figure-5.2 is used to simulate the fractional order differentiating filter in the fractional Fourier transform domain.

5.5.1 Simulation Results based on Riemann–Liouville (RL) Definition

For the design of the proposed filter based on Riemann–Liouville (RL) fractional derivative definition, the input signal is taken as $s(n) = 2e^{18jn\pi/32} + e^{-8jn\pi/32}$. Then, $s(n)$ is corrupted by the high frequency chirp noise $\Omega(n) = 0.3e^{0.06j(n-1)^3-7jn}$, as shown in Figure-5.3 (a) to (d) (both real and imaginary parts). The obtained noise–corrupted signal $s(n) + \Omega(n)$, in Figure-5.3 (e) and (f) (both real and imaginary parts), is input to the proposed filter model shown in Figure-5.1.

The filtering is performed to compare the performance of time–domain $(\varphi = 0)$, frequency–domain $(\varphi = 1)$ and fractional Fourier domain filtering (φ), as shown in Figure-5.3 (g) to (l). Various iterations have been carried out by varying both parameters μ and φ to get minimum error between the original signal and the filtered signal.

It is shown through simulations that the fractional Fourier domain filtering exhibits better filtering operation for the fractional derivative order parameter of $\mu = 0.35$ and the optimum fractional Fourier transform parameter of $\varphi = 0.05\pi$, as compared to the time–domain and

frequency–domain filtering. The root mean square error ($RMSE$) is used for judging the optimal filtering between the original signal and the filtered signal.

The $RMSE$ between the original and the filtered signals is observed for different values of fractional order parameter μ, which varies from 0 to 1. This confirms that the FrFT domain filtering produces minimum $RMSE$ for optimum φ and μ as compared with the time–domain and frequency–domain filtering, as is illustrated in Figure-5.4.

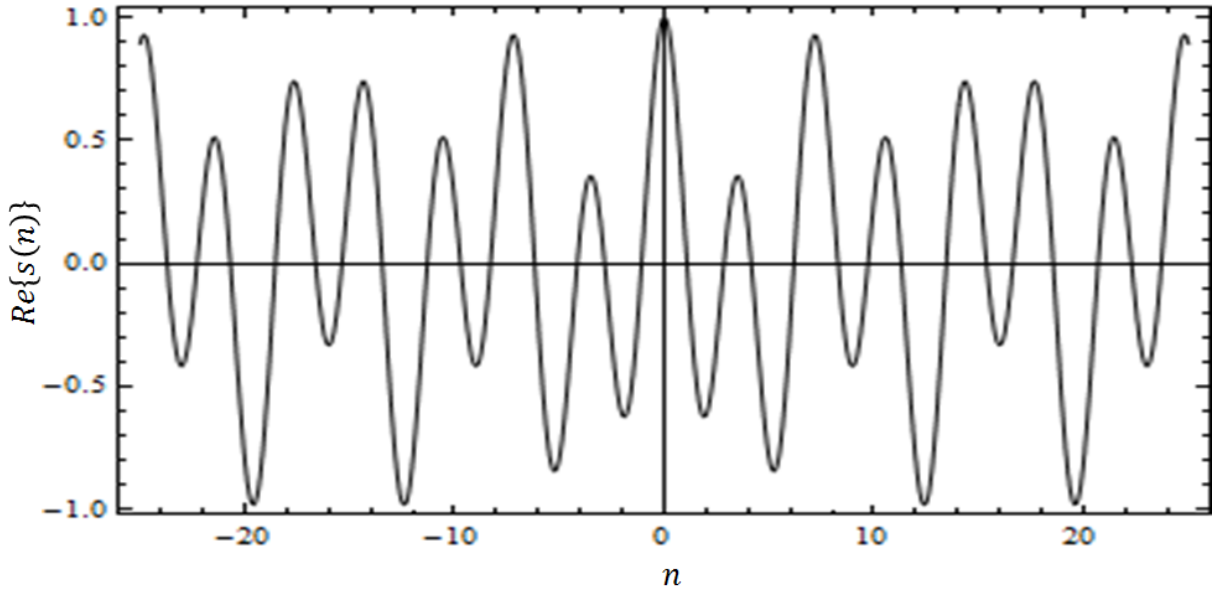

(a)

Figure–5.3: **Fractional order filtering results based on Riemann–Liouville (RL) fractional derivative definition: (a), (b)** original signal $s(n)$ (real (*Re*) and imaginary (*Im*) parts respectively) in time domain; **(c), (d)** high–frequency chirp noise (real (*Re*) and imaginary (*Im*) parts respectively) in time domain; **(e), (f)** corrupted signal, $s(n) + \Omega(n)$ (real (*Re*) and imaginary (*Im*) parts respectively) in time domain; **(g), (h)** time–domain filtered signal, $\hat{s}(n)$ (real (*Re*) and imaginary (*Im*) parts respectively); **(i), (j)** frequency–domain filtered signal, $\hat{s}(n)$ (real (*Re*) and imaginary (*Im*) parts respectively); **(k), (l)** fractional order FrFT–domain filtered signal $\hat{s}(n)$ (real (*Re*) and imaginary (*Im*) parts respectively).

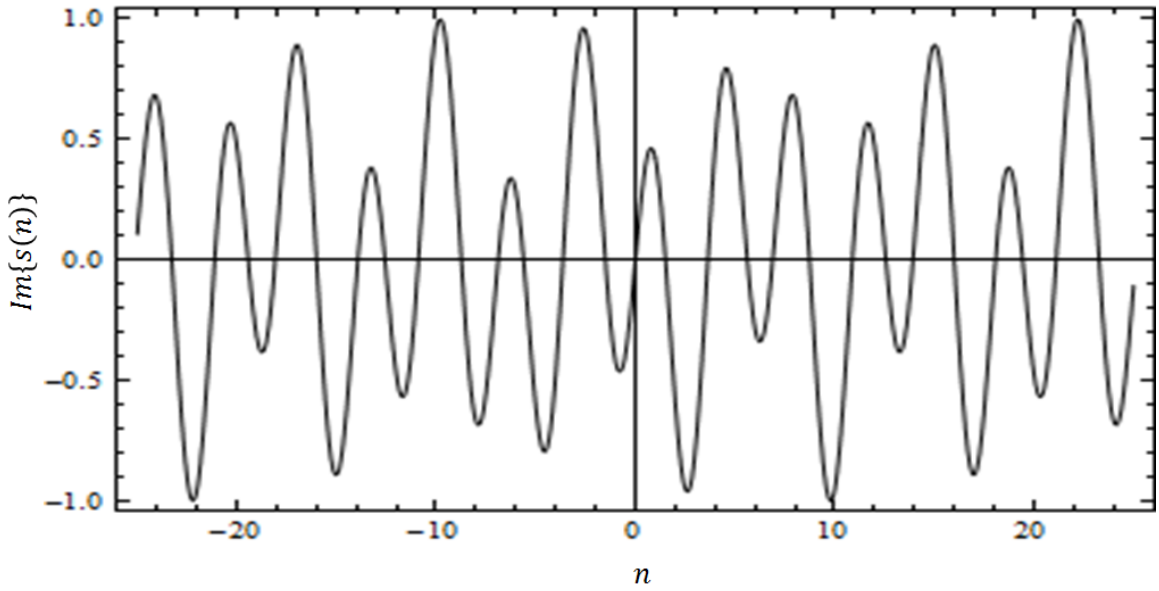

(b)

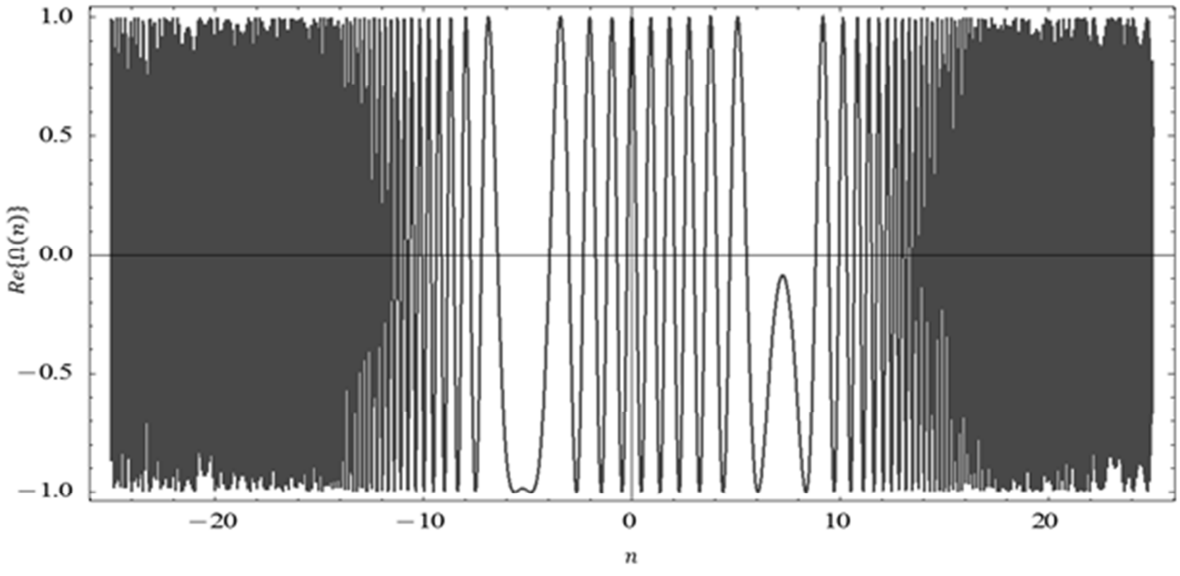

(c)

Figure–5.3 (*Continued*)

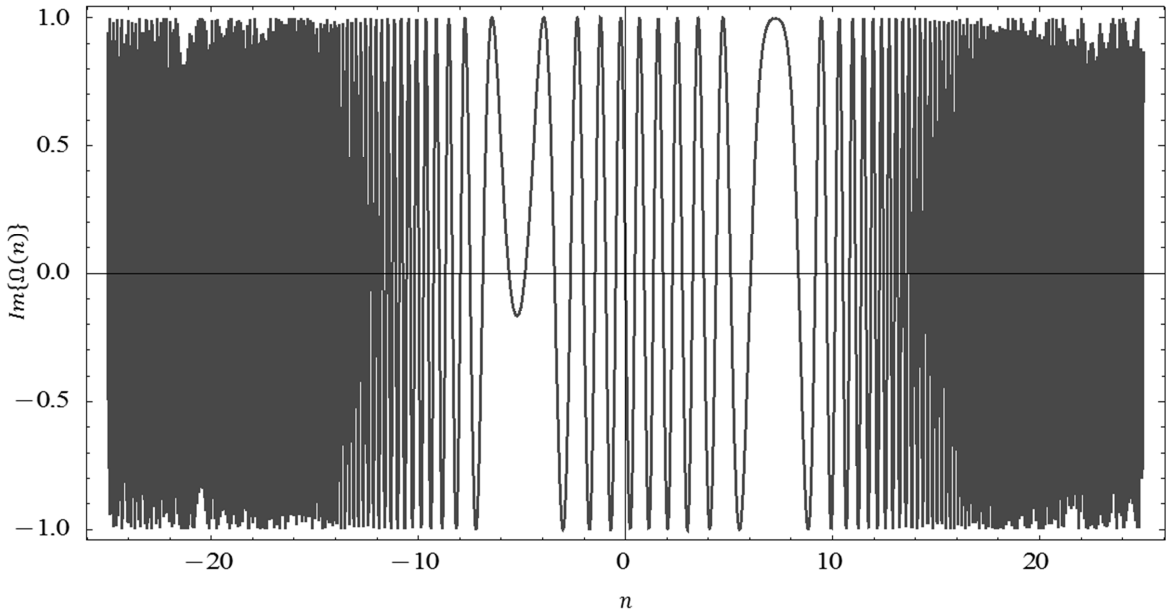

(d)

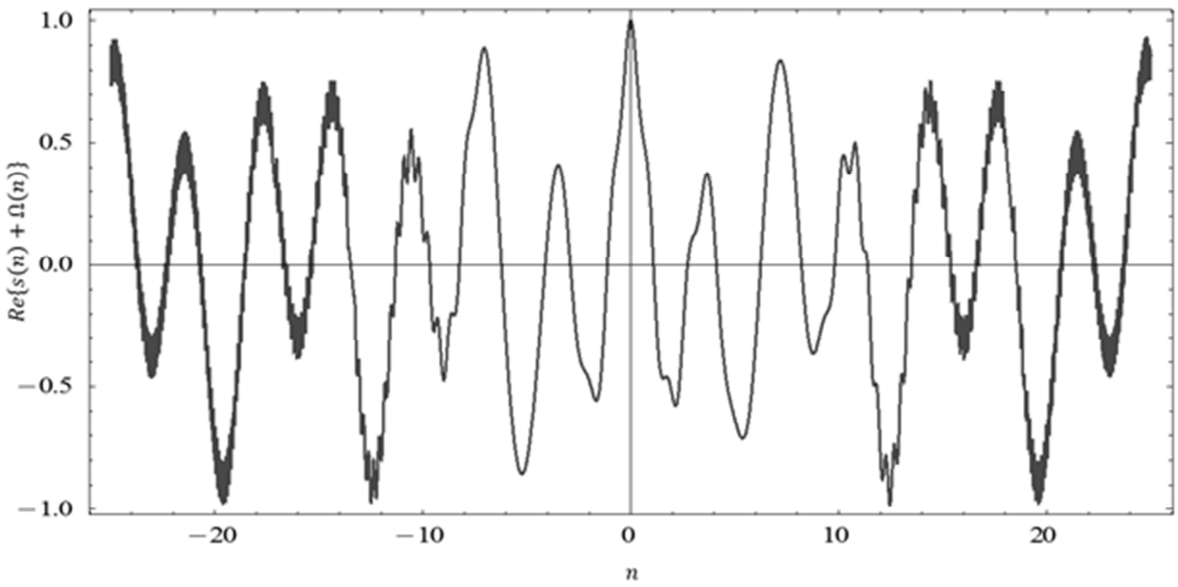

(e)

Figure–5.3 (*Continued*)

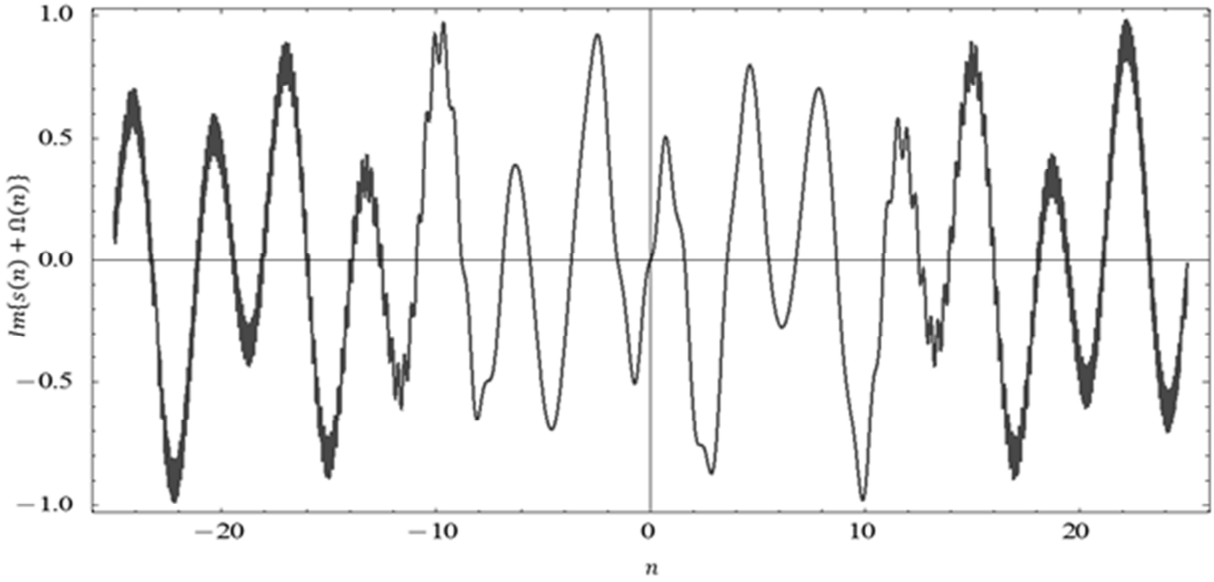

(f)

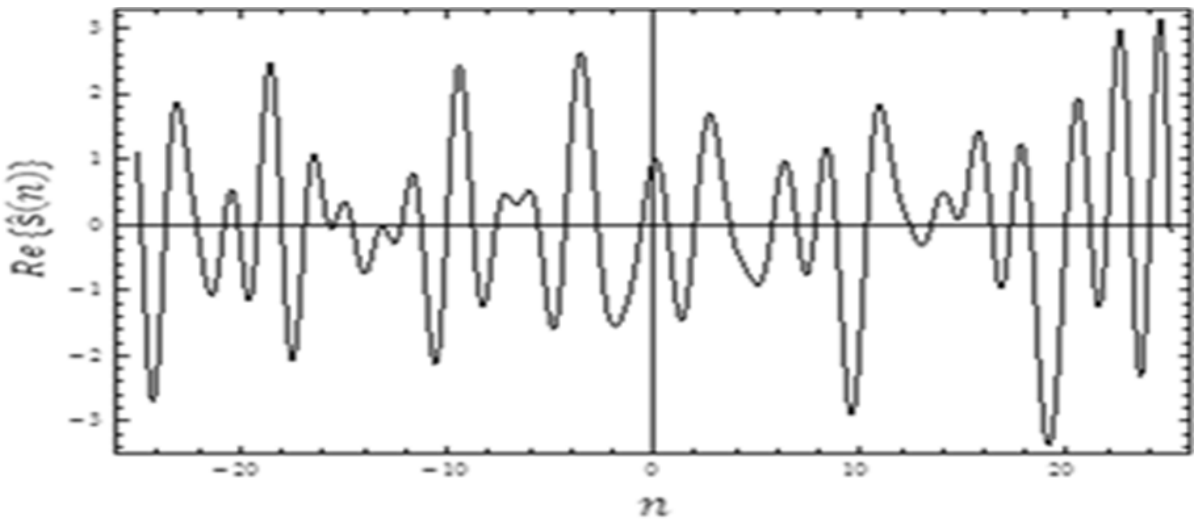

(g)

Figure–5.3 (*Continued*)

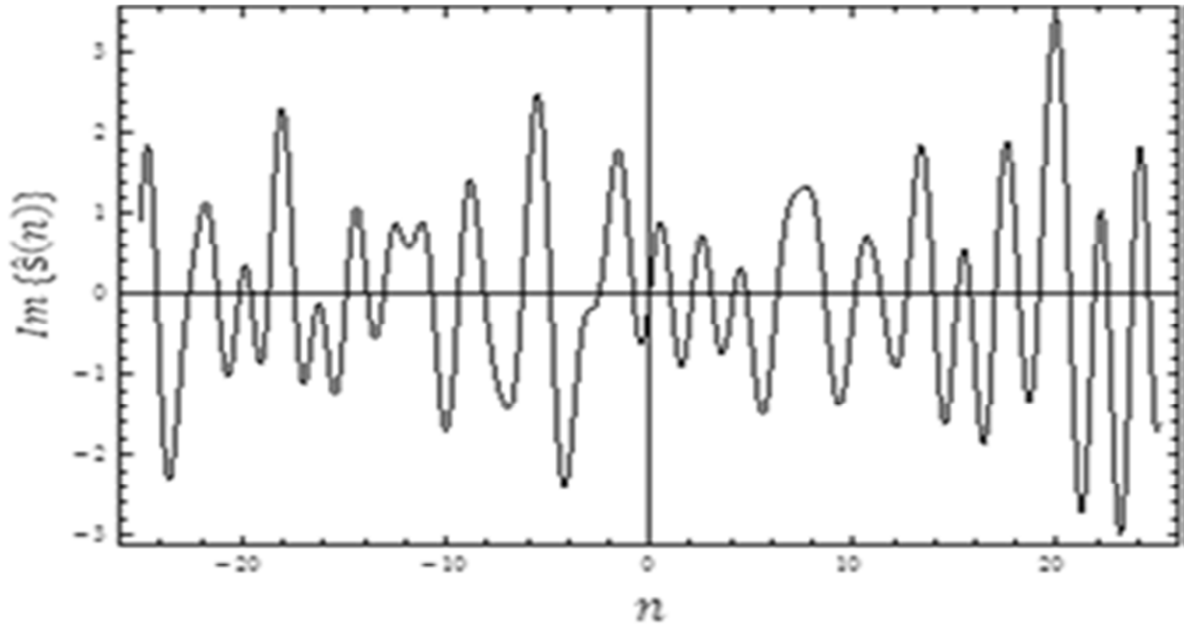

(h)

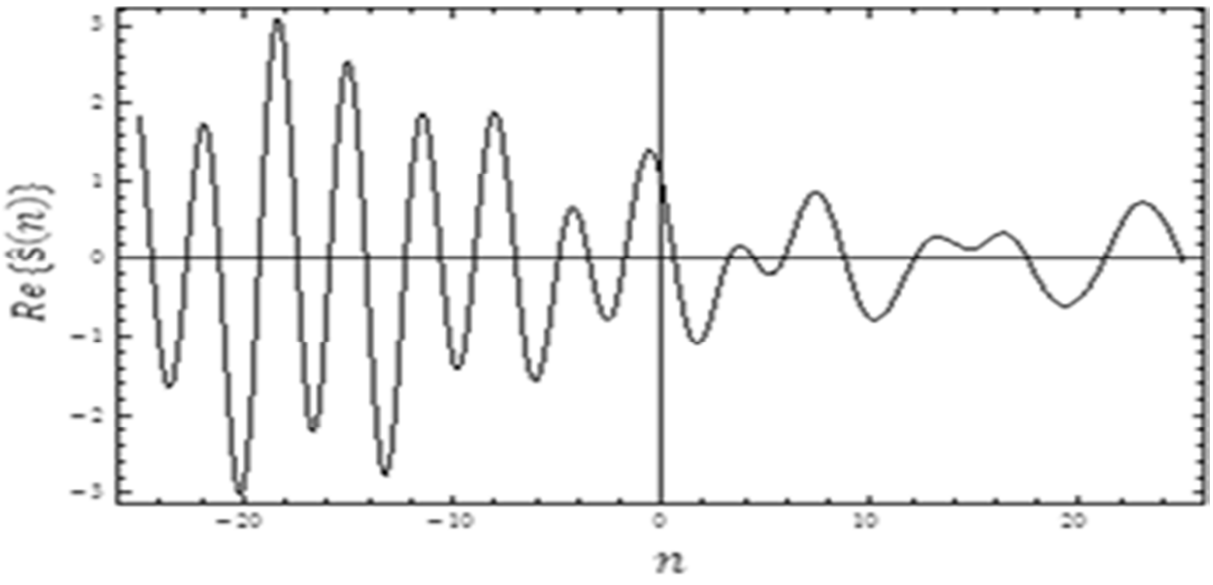

(i)

Figure–5.3 (*Continued*)

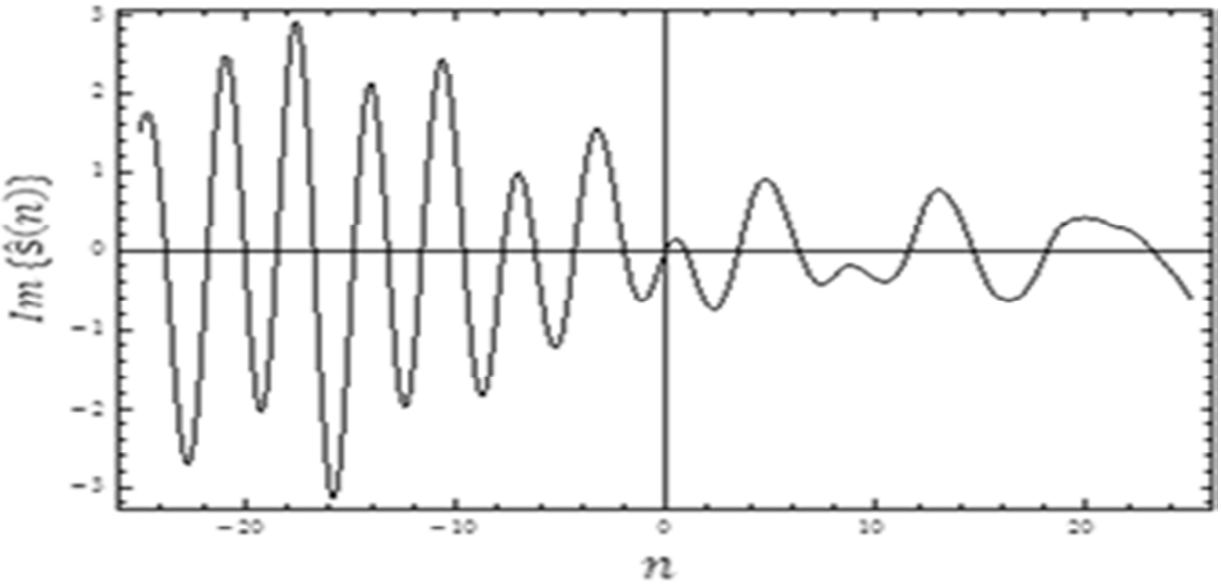

(j)

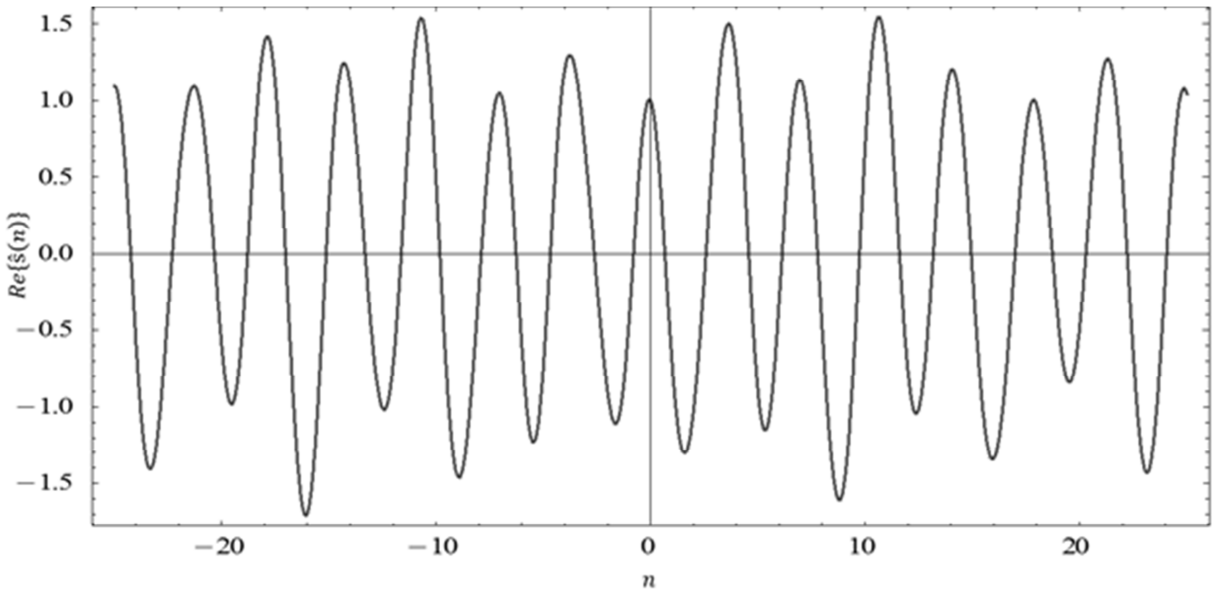

(k)

Figure–5.3 (*Continued*)

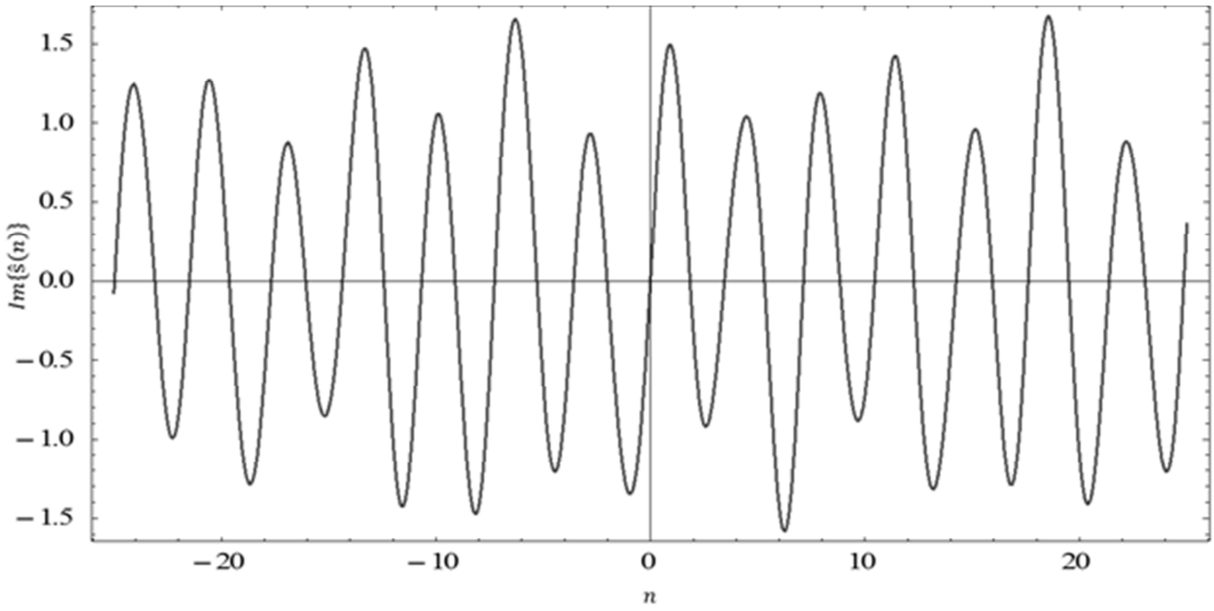

(l)

Figure–5.3 (*Continued*)

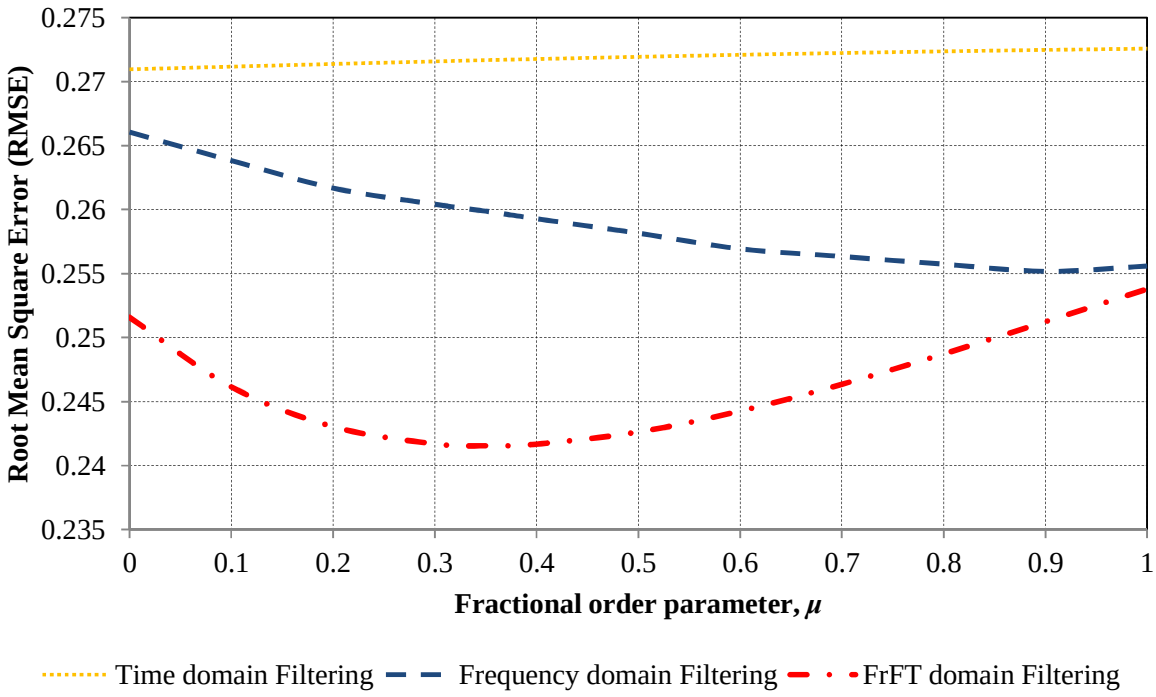

Figure–5.4: *RMSE* vs. fractional derivative order parameter, μ for the RL based definition.

Therefore, it can be seen from Figure-5.3 (g) to (l) that the fractional Fourier domain filtered signal matches maximally with the original signal as compared with the time–domain and frequency–domain filtered signals for the case of Riemann–Liouville based fractional derivative definition.

5.5.2 Simulation Results based on Caputo Definition

For the design of the proposed filter based on Caputo fractional derivative definition, the input signal is taken as $s(n) = 2e^{18jn\pi/32} + e^{-8jn\pi/32}$. Then, $s(n)$ is corrupted by the high frequency chirp noise $\Omega(n) = 0.3e^{0.06j(n-1)^3-7jn}$, as shown in Figure-5.5 (a) to (d) (both real and imaginary parts). The obtained noise–corrupted signal $s(n) + \Omega(n)$, in Figure-5.5 (e) and (f) (both real and imaginary parts), is input to the proposed filter model shown in Figure-5.2.

The filtering is performed to compare the performance of time–domain $(\varphi = 0)$, frequency–domain $(\varphi = 1)$ and fractional Fourier domain filtering (φ), as shown in Figure-5.5 (g) to (l). It is shown through simulations that the fractional Fourier domain filtering exhibits better filtering operation for the fractional derivative order parameter of $\mu = 0.5$ and the optimum fractional Fourier transform parameter of $\varphi = 0.05\pi$, as compared to the time–domain and frequency–domain filtering. The criterion used for judging the performance of the filtering operation is the root mean square error $(RMSE)$ between the original signal and the filtered signal.

The $RMSE$ between the original and the filtered signals is observed for different values of fractional order parameter μ, which varies from 0 to 1. This confirms that the FrFT domain filtering produces minimum $RMSE$ for optimum φ and μ as compared with the time–domain and frequency–domain filtering, as is illustrated in Figure-5.6.

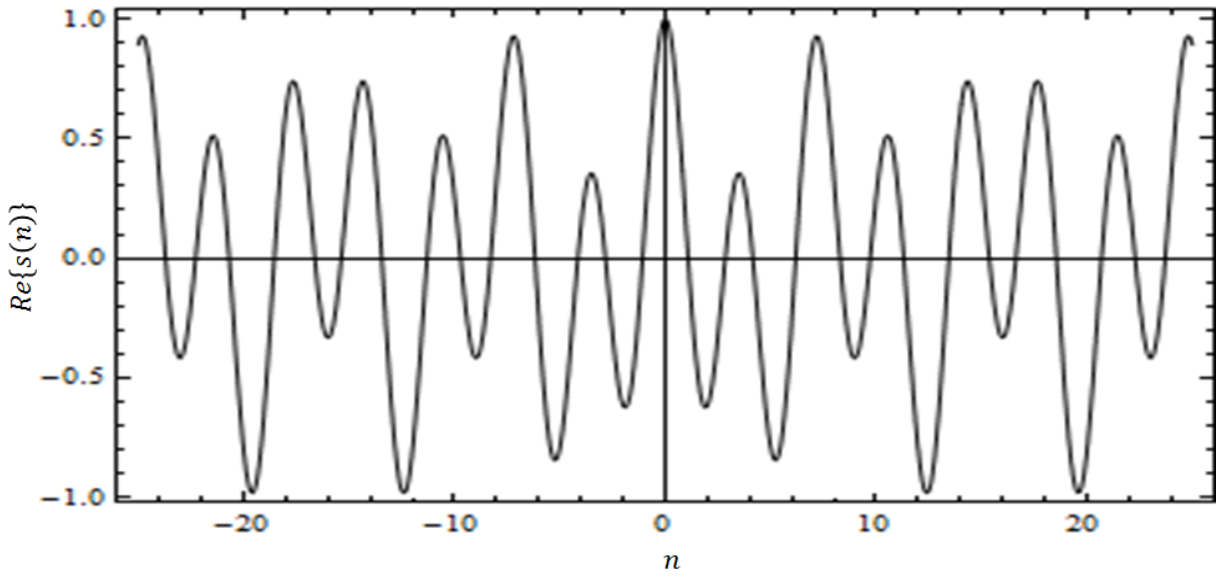

(a)

Figure–5.5: **Fractional order filtering results based on Caputo fractional derivative definition:** **(a), (b)** original signal $s(n)$ (real (*Re*) and imaginary (*Im*) parts respectively) in time domain; **(c), (d)** high–frequency chirp noise (real (*Re*) and imaginary (*Im*) parts respectively) in time domain; **(e), (f)** corrupted signal, $s(n) + \Omega(n)$ (real (*Re*) and imaginary (*Im*) parts respectively) in time domain; **(g), (h)** time–domain filtered signal, $\hat{s}(n)$ (real (*Re*) and imaginary (*Im*) parts respectively); **(i), (j)** frequency–domain filtered signal, $\hat{s}(n)$ (real (*Re*) and imaginary (*Im*) parts respectively); **(k), (l)** fractional order FrFT–domain filtered signal $\hat{s}(n)$ (real (*Re*) and imaginary (*Im*) parts respectively).

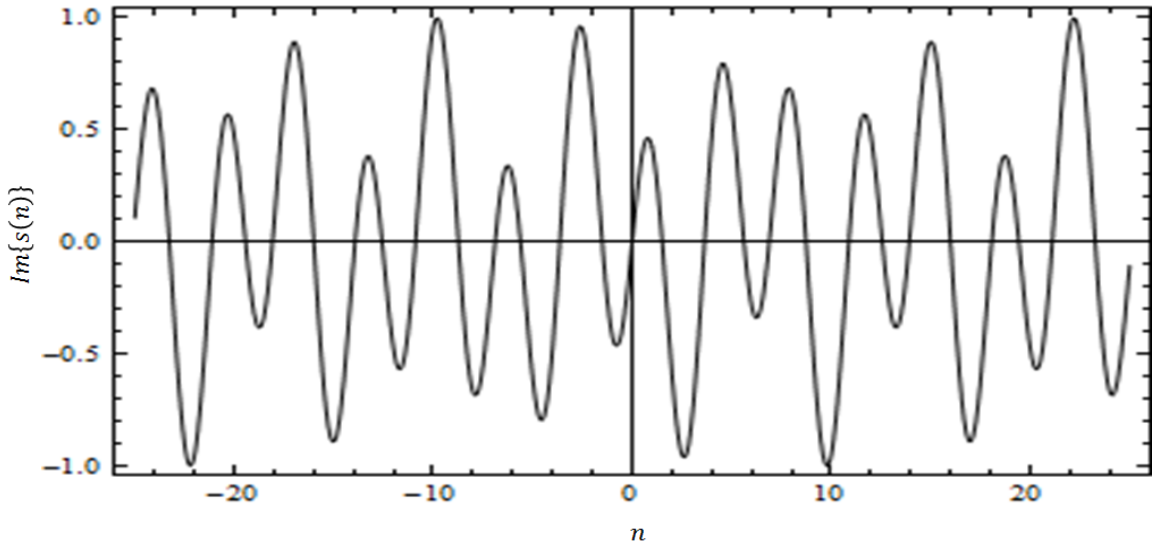

(b)

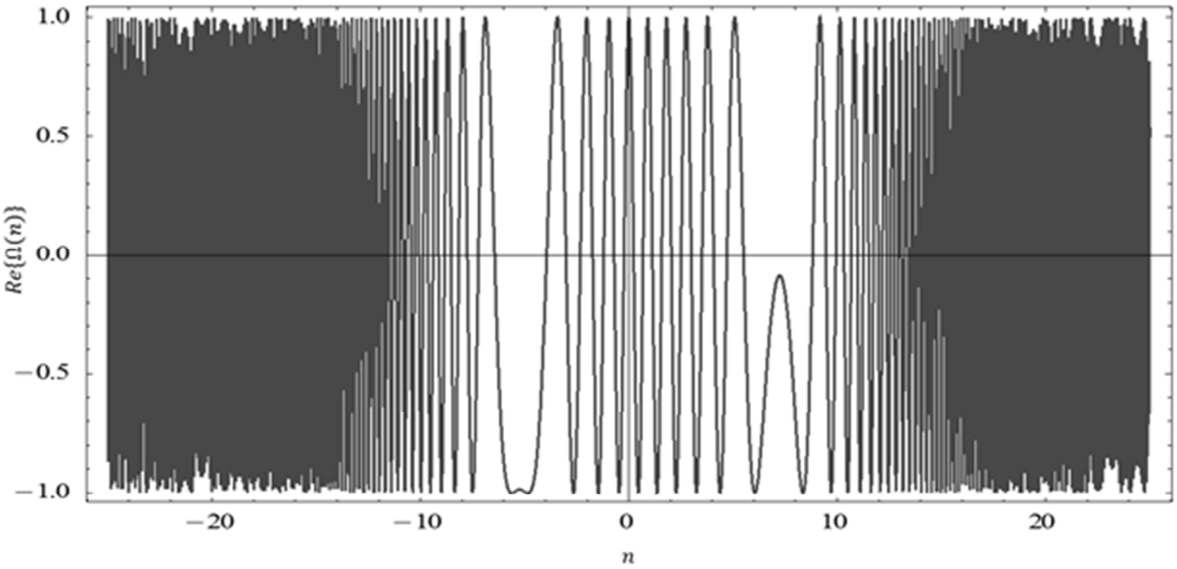

(c)

Figure–5.5 (*Continued*)

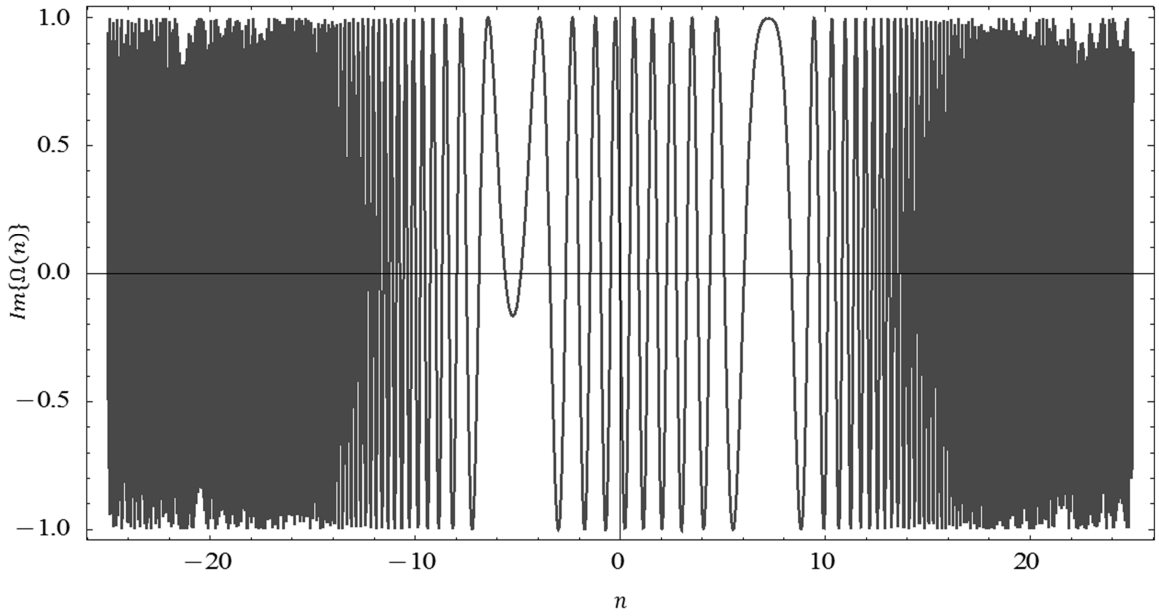

(d)

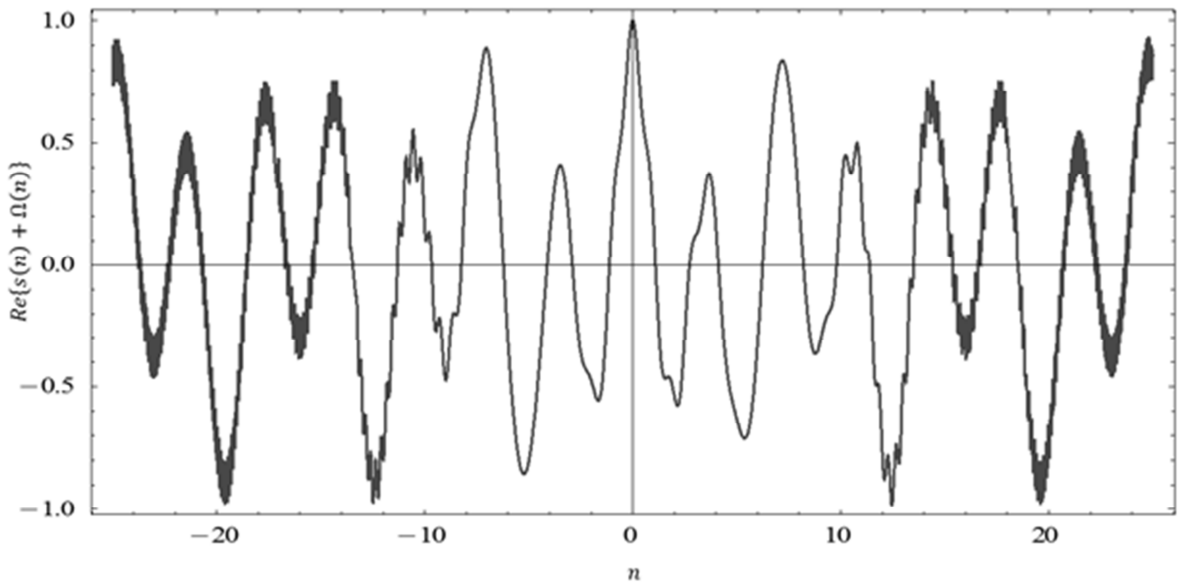

(e)

Figure–5.5 (*Continued*)

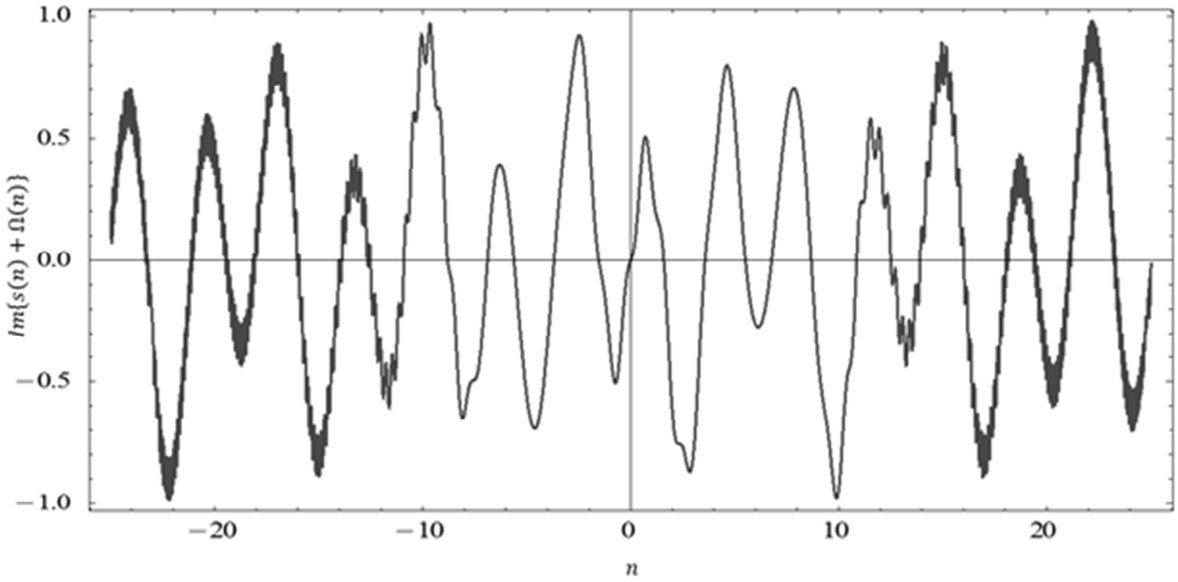

(f)

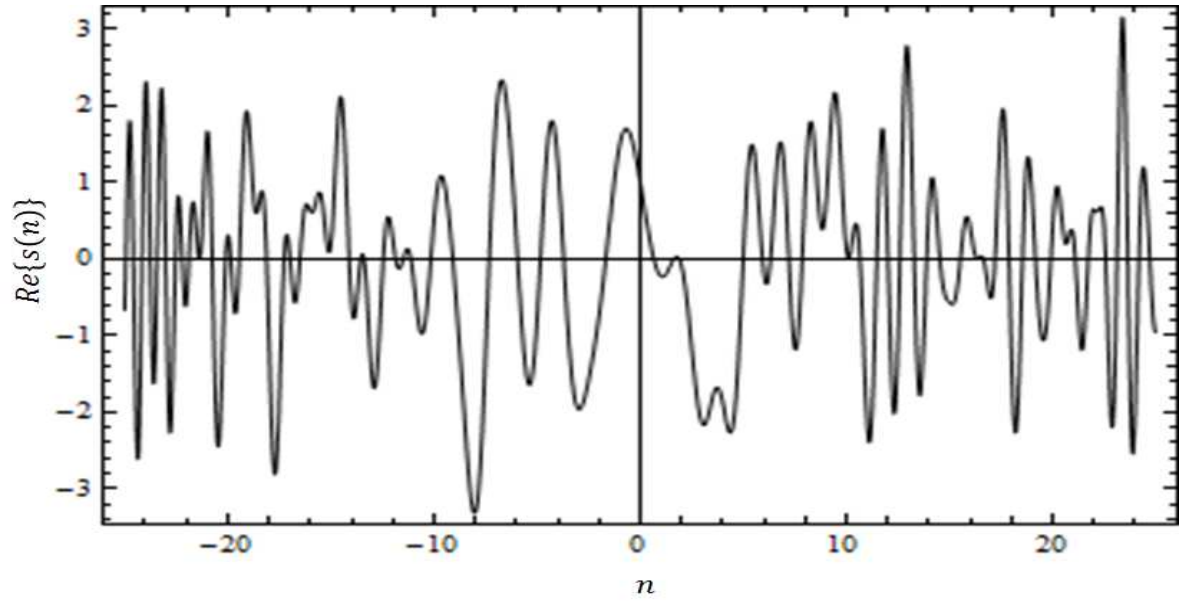

(g)

Figure–5.5 (*Continued*)

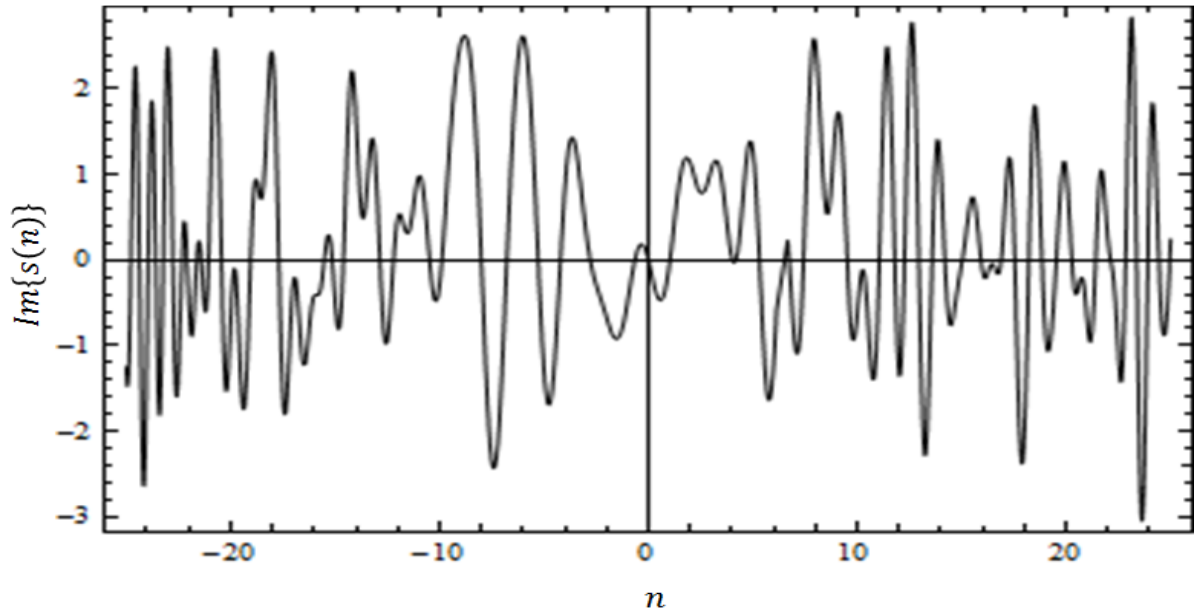

(h)

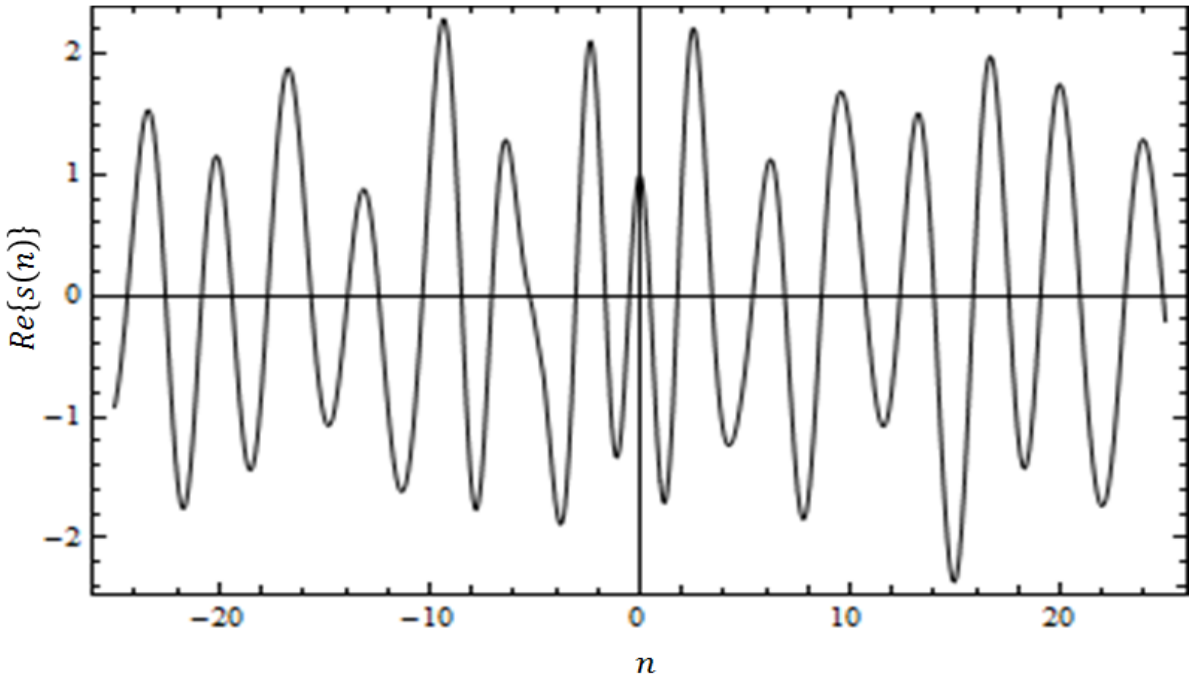

(i)

Figure–5.5 (*Continued*)

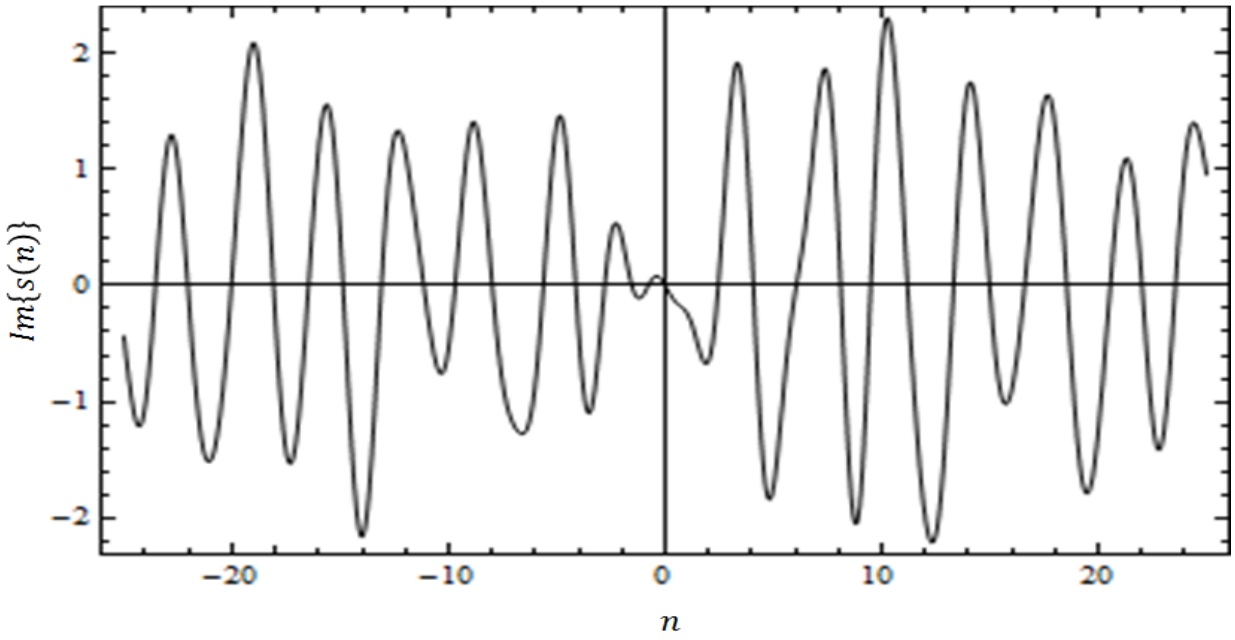

(j)

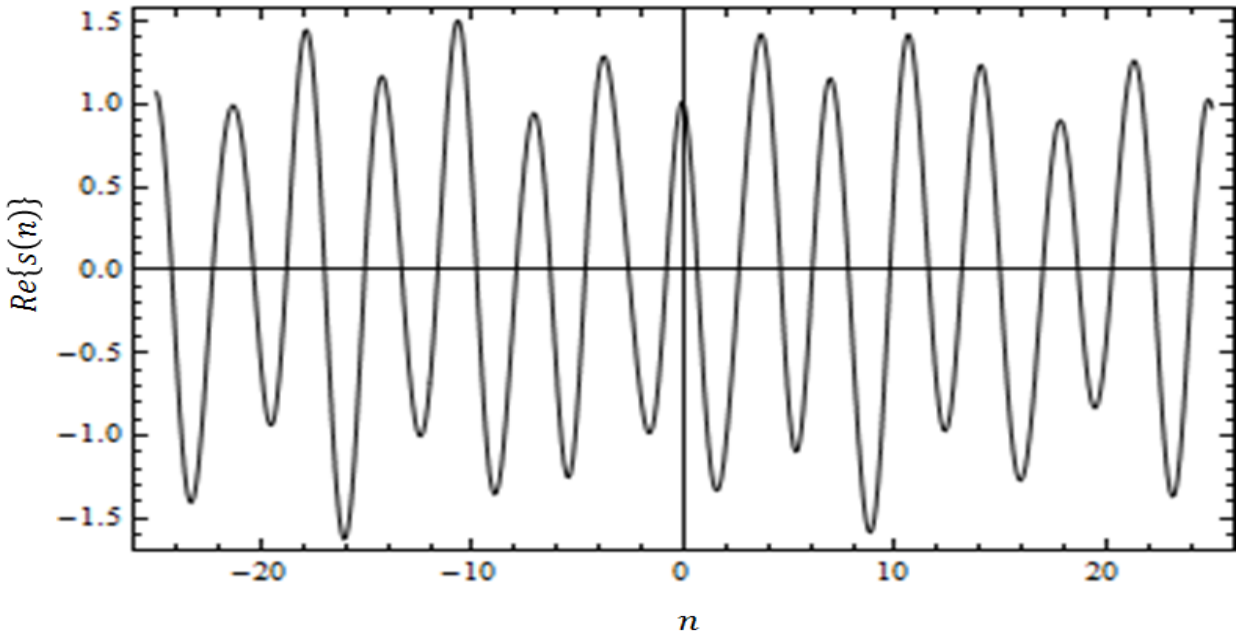

(k)

Figure–5.5 (*Continued*)

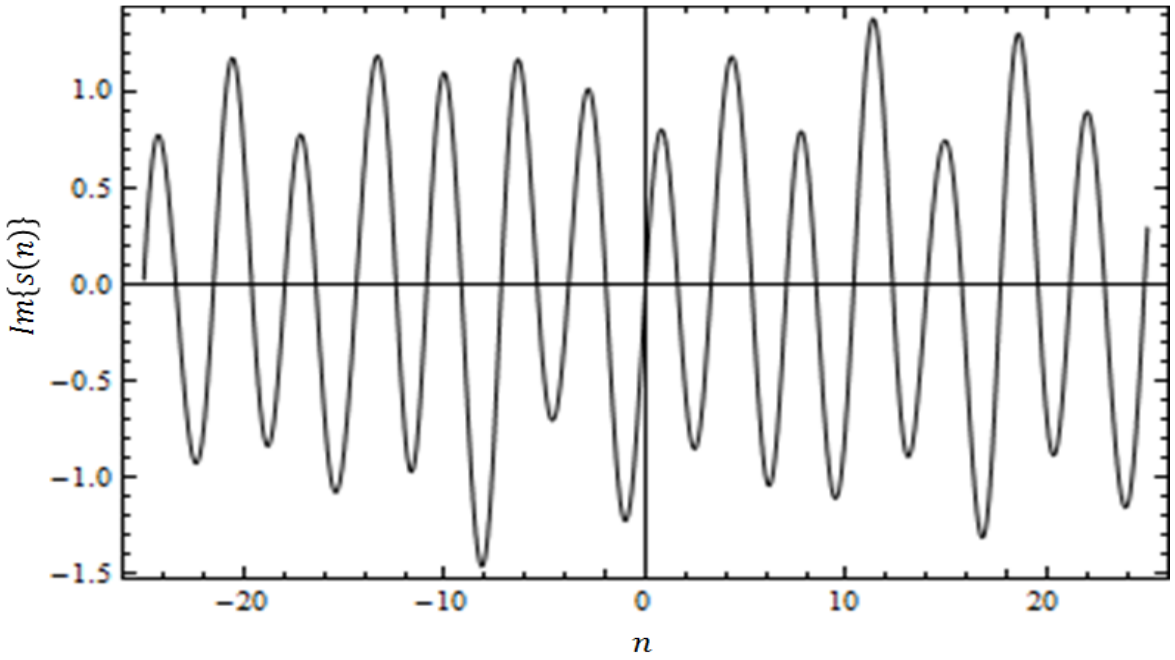

(l)

Figure–5.5 (*Continued*)

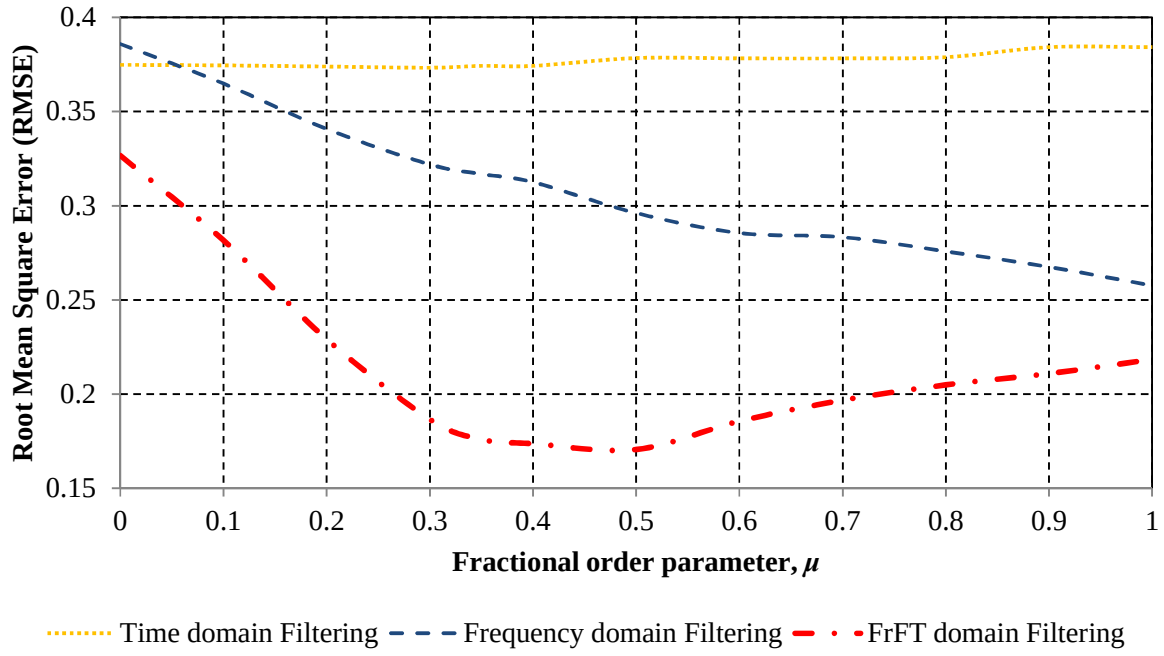

Figure–5.6: *RMSE* vs. fractional derivative order parameter, μ for the Caputo based definition.

5.6 PERFORMANCE ANALYSIS BETWEEN RL AND CAPUTO BASED ALGORITHMS

In this section, the comparative analysis between the two aforementioned fractional derivative definitions is carried out to examine the performance of the proposed design. As is been discussed in Section 4.5 of Chapter 4, the proposed fractional–order differentiating filter in the FrFT domain is designed using Riemann–Liouville (RL) and Caputo based fractional derivative definitions so it's necessary to have an insightful view between these two definitions.

The focus here is on the usage of the Caputo based definition in the one–dimensional signal processing filtering application and compares its performance with the RL based definition as is illustrated below. But still there has been a lot of conflict on the usage of these two definitions for the modeling of physical signals; which have shown to possess inherent fractional order dynamics and that are characterized by heavy–tailed distributions (α −stable distributions) **[140]**, and it remains an open research domain for the modeling of stable distributions; that provides a useful theoretical tool for non–Gaussian signals and noises **[68]**.

Figure-5.7 plots the comparison results of the two definitions used in the design. It plots the variation of the $RMSE$ between the original signal and the filtered signal. The design example of Section 5.5.1 is used for the performance analysis between the two definitions. The two parameters of interest μ and φ are varied for different numerical values and the different values of $RMSE$ are noted. It is found that in the case of RL based definition, the lowest value of $RMSE$ obtained is 0.241609 for the values of the parameters $\mu = 0.35$ and optimal $\varphi = 0.05\pi$. So, for this particular value of the parameters μ and φ, comparison is seen between these two definitions as is shown in Figure-5.7.

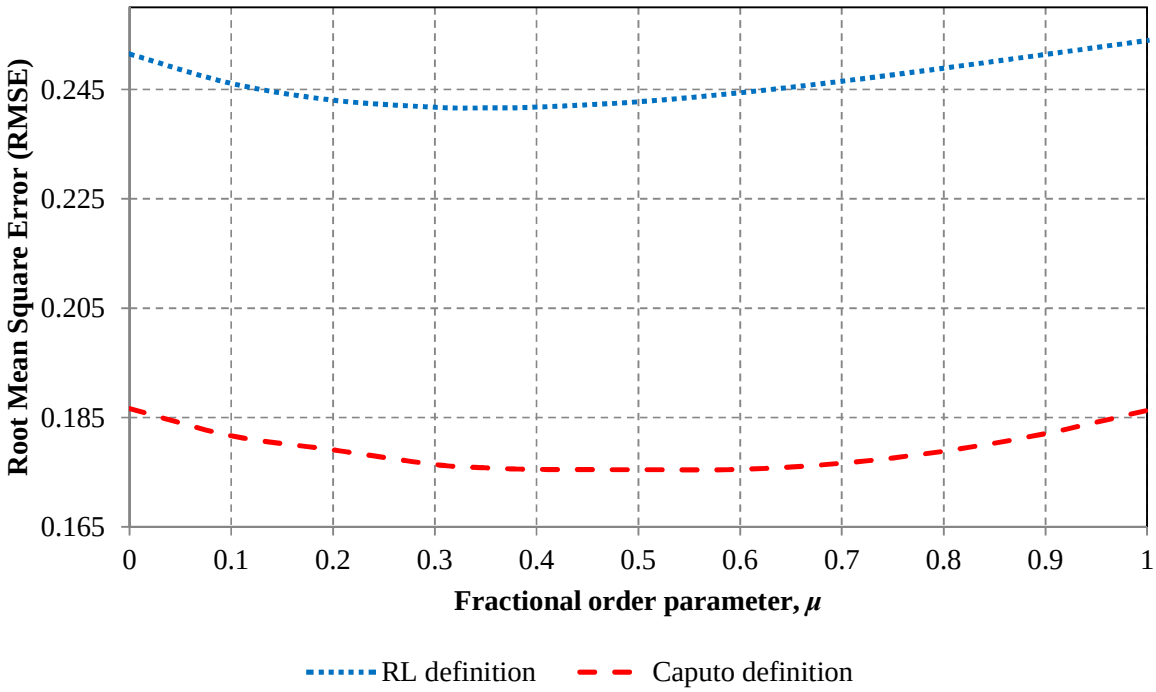

Figure–5.7: Comparison of the fractional Fourier domain filtering between the RL based fractional derivative definition method and the Caputo based fractional derivative definition.

Therefore, it is found that for the values of the parameters $\mu = 0.35$ and optimal $\varphi = 0.05\pi$, the fractional order differentiating filter designed by the Caputo based fractional derivative definition method exhibits a smaller error, computed as 0.175813 than that of RL based fractional derivative definition, whose corresponding error is computed as 0.241609 as is shown in Figure-5.7. Hence, the smaller the error is, the better the fractional order differentiating filtering operation.

Thus, it can be inferred from the above example that the Caputo based fractional derivative definition performs well as compared to the RL based definition. This is in conformity with the available literature **[30, 68, 73, 86, 90, 110]** which also quote the same statement of superiority of Caputo definition over RL definition. So it can be suggested that the Caputo based definition is well–suited for the one–dimensional signal processing filtering application.

CHAPTER 6

EDGE DETECTION ON IMAGES

THE ONE DIMENSIONAL APPLICATION of the fractional order differentiation in the fractional Fourier transform have been discussed previously in an expatiate manner. Now research motivation is focused on the two dimensional application utilizing the concepts of fractional order calculus and the fractional Fourier transform. Edge detection is considered here for the two dimensional application in image processing. Edge detection is a fundamental issue in image processing, computer vision and pattern recognition. The investigation of the Fourier frequency domain filtering and the fractional Fourier frequency domain filtering are considered for this application investigating both the qualitative as well as the quantitative analysis.

6.1 CONCEPT OF EDGE DETECTION: TWO–DIMENSIONAL SIGNAL PROCESSING

Edge detection is the most ubiquitous step in low–level image processing. An edge is described as "the outside limit of an object, area or surface; a place or part farthest away from the center of something: (Oxford American Dictionary)". Traditionally, edges have been defined as locations of sharp changes in image intensities, and edge detection formulated as a problem of differentiation of the image. The edges are often the vital clues toward the analysis and interpretation of the image information, both in biological vision and in computer image analysis. **[5]**

The image edge is defined as the abrupt intensity changes of an image. The intensity changes usually correspond to the physical changes in some property of the images 3D objects'

surfaces. Thus, the edge detection is the process of finding meaningful transitions in an image. It is very important for the subsequent higher level vision tasks and can lead to some inference about the physical properties of the 3D world. **[5]**

Thus, edge detection is the process of determining which pixels are the edge pixels. The result of the edge detection process is typically an edge map that is, a new image that describes each original pixel's edge classification and perhaps additional edge attributes, such as magnitude and orientation. **[5]**

An edge in a gray scale image occurs when there is a transition in gray level over an amount of pixels. A perfect edge would be a transition from black to white over one pixel as shown in Figure-6.1. In many images, edges like these won't occur (unless it's a binary image). The transition will be blurred spreading the transition over more pixels, resulting in a slope–like profile of the gray level transition as seen in Figure-6.2.

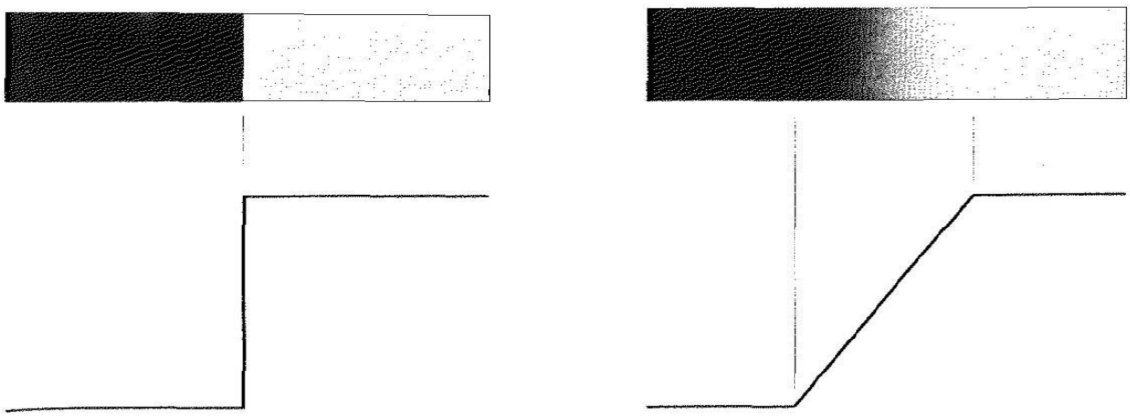

Figure–6.1: Edge profile of a gray scale image. [5]

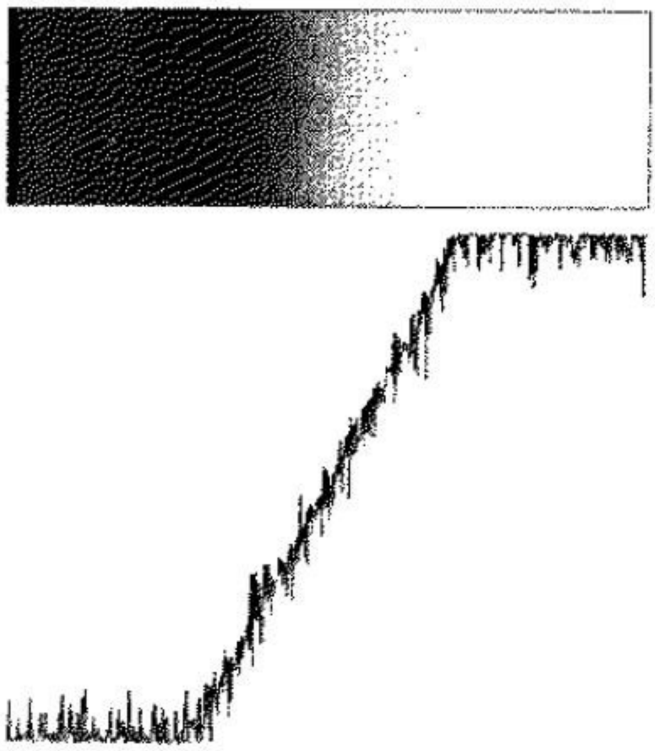

Figure–6.2: Illustration that a transition is almost never perfect. [5]

An image can be interpreted as a two–dimensional function, $f(x, y)$ where, x and y are the spatial coordinates, and the amplitude of f at any pair of coordinates (x, y) is called the intensity or gray level of the image at that point. Thus, an image can be represented by a matrix of bounded positive integer values. **[10]**

In image processing, edge detection often makes use of the integer–order differentiation operators, especially order 'one' used by the gradient and order 'two' by the Laplacian of the grey levels **[80]**. The estimation of the gradient vector is based on the usage of masks, which are the low–dimensional convolution matrices. The convolution with the grey level is performed by sliding the kernel (mask) over the image. The kernel is moved through all the positions where the kernel fits entirely within the boundaries of the image.

6.1.1 Edge Detection using First–Order Derivatives

The derivative of a digital pixel can be defined in terms of differences. The first derivative of an image containing gray value pixel must fulfill the following conditions **[10]**:

(a) it must be zero in flat segments i.e., in areas of constant gray–level values;

(b) it must be non–zero at the beginning of a gray–level step or ramp; and

(c) it must be non- zero along the ramp (constant change in gray values).

The first–order derivative of a one–dimensional (1D) function $f(x)$ can be obtained using:

$$\frac{df}{dx} = f(x+1) - f(x) \quad \textbf{(6.1.1)}$$

where (6.1.1) only refers to the partial derivative along the x–axis.

Since an image is a function of two variables (x, y), therefore to estimate the derivative of an image represented by a discrete set of pixels, we need to resort to an approximation. The derivatives are approximated by finite differences. So, the method to calculate the first–order derivative is given by estimating the finite difference as:

$$\frac{\partial f}{\partial x} = \lim_{h\to 0} \frac{f(x+h,y)-f(x,y)}{h} \quad \textbf{(6.1.2)}$$

$$\frac{\partial f}{\partial y} = \lim_{h\to 0} \frac{f(x,y+h)-f(x,y)}{h} \quad \textbf{(6.1.3)}$$

Thus, the finite difference can be approximated as:

$$\frac{\partial f}{\partial x} = \lim_{h\to 0} \frac{f(x+h,y)-f(x,y)}{h_x} = f(x+1,y) - f(x,y);\ (h_x = 1) \quad \textbf{(6.1.4)}$$

$$\frac{\partial f}{\partial y} = \lim_{h\to 0} \frac{f(x,y+h)-f(x,y)}{h_y} = f(x,y+1) - f(x,y);\ \left(h_y = 1\right) \quad \textbf{(6.1.5)}$$

Thus, based on the above finite difference approach, one obtains various edge detection operators or masks, which find wide usage in image processing applications.

6.1.2 Edge Detection Operators

Edge detection plays a pivotal role in image processing. It is known that the edges in digital images are areas with strong intensity contrasts and a jump in intensity from one pixel to the next can create variation in the picture quality **[123]**. The identification of accurate edges helps to analyze and measure the basic properties related with the objects. So it is essential to detect accurately the discontinuities in the intensity levels in an image. Such discontinuities are detected using edge detection operators, which are illustrated below.

6.1.2.1 Gradient Operator

The integer–order derivative operator is an important tool to detect the meaningful discontinuities in the intensity values.

The first–order derivative in image processing is the *gradient*. The gradient of a two–dimensional image, $f(x,y)$ at location (x,y) is defined as the vector:

$$\nabla \boldsymbol{f} = \begin{bmatrix} G_x \\ G_y \end{bmatrix} = \begin{bmatrix} \frac{\partial f}{\partial x} \\ \frac{\partial f}{\partial y} \end{bmatrix} \quad \textbf{(6.1.6)}$$

The gradient vector points in the direction of maximum rate of change of f at coordinates (x,y).

The magnitude of the gradient is calculated by:

$$\nabla f = \text{mag}\,(\nabla \boldsymbol{f}) = \sqrt{{G_x}^2 + {G_y}^2} = \sqrt{\left(\frac{\partial f}{\partial x}\right)^2 + \left(\frac{\partial f}{\partial y}\right)^2} \quad \textbf{(6.1.7)}$$

The above quantity ∇f gives the maximum rate of increase of $f(x,y)$ per unit distance in the direction of $\nabla \boldsymbol{f}$ **[123]**. The computation of the gradient of an image is based on obtaining the partial derivatives $\partial f/\partial x$ and $\partial f/\partial y$ at every pixel location.

Another important quantity in edge detection in addition to the gradient is the direction of the gradient vector. If $\theta(x,y)$ represents the direction angle of the vector $\nabla \boldsymbol{f}$ at (x,y), then

$$\theta(x,y) = \tan^{-1}\left(\frac{G_y}{G_x}\right) \quad \textbf{(6.1.8)}$$

where the angle is measured with respect to the x–axis. The direction of an edge at (x, y) is perpendicular to the direction of the gradient vector at that point.

Figure-6.3 indicates the gradient of the edge pixel. The circle indicates the location of the pixel. An edge pixel is described using two important features:

(a) *Edge strength*, which is equal to the magnitude of the gradient.

(b) *Edge direction*, which is equal to the angle of the gradient.

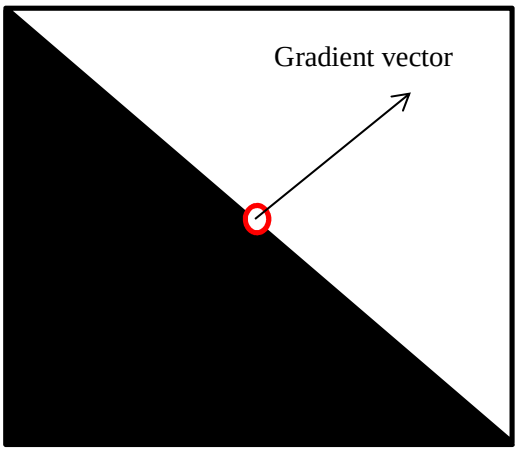

Figure–6.3: Gradient of edge pixel. [5]

Thus since the edges are the positions in the image where the image function changes, so to find these positions one has to calculate the gradient of the 2D function $f(x, y)$. The gradient of a 2D function is a 2D vector with components, the partial derivatives of the function along the two orthogonal directions. In the discrete case, these partial derivatives are the partial differences computed along the two orthogonal directions by using masks like for example, the Sobel masks. **[115]**

6.1.2.2 Roberts operator

It is one of the simplest and oldest edge detection operator that is of historical interest today. It employs two extremely small filters of size 2×2 for estimating the directional gradient along the image diagonals, as illustrated below:

$$G_x{}^R = \begin{bmatrix} 0 & 1 \\ -1 & 0 \end{bmatrix} \text{ and } G_y{}^R = \begin{bmatrix} -1 & 0 \\ 0 & 1 \end{bmatrix} \quad \textbf{(6.1.9)}$$

These filters naturally respond to the diagonal edges but are not highly selective to orientation; i.e., both filters show strong results over a relatively wide range of angles. **[155]**

6.1.2.3 Prewitt and Sobel operators

The edge detection operators by Prewitt and Sobel are the two classic methods that differ only marginally in the filters they use.

The Prewitt and Sobel operators use linear filters that extend over three adjacent lines and columns, respectively, to counteract the noise sensitivity of the simple (single line/column) gradient operators. **[155]**

The Prewitt operator uses the filters

$$G_x{}^P = \begin{bmatrix} -1 & 0 & 1 \\ -1 & 0 & 1 \\ -1 & 0 & 1 \end{bmatrix} \text{ and } G_y{}^P = \begin{bmatrix} -1 & -1 & -1 \\ 0 & 0 & 0 \\ 1 & 1 & 1 \end{bmatrix} \quad \textbf{(6.1.10)}$$

which compute the average gradient components across the three neighboring lines or columns, respectively.

The filters for the Sobel operator are almost identical; however, the smoothing part assigns higher weight to the current center line and column **[155]**, respectively as:

$$G_x{}^S = \begin{bmatrix} -1 & 0 & 1 \\ -2 & 0 & 2 \\ -1 & 0 & 1 \end{bmatrix} \text{ and } G_y{}^S = \begin{bmatrix} -1 & -2 & -1 \\ 0 & 0 & 0 \\ 1 & 2 & 1 \end{bmatrix} \quad \textbf{(6.1.11)}$$

6.1.3 Second Derivative Method–The Laplacian

The common interpretation of finding an ideal edge is equivalent to finding a point where the derivative is maximum or minimum. The maximum and the minimum value of a function can be computed by differentiating the given function and finding the places where the derivative is zero. The differentiation of the first derivative gives the second derivative. The second–order derivative in image processing is generally computed by using the Laplacian operation **[123]**.

The Laplacian of a 2D function or an image $f(x, y)$ is defined by:

$$\nabla^2 f(x, y) = \frac{\partial^2 f(x,y)}{\partial x^2} + \frac{\partial^2 f(x,y)}{\partial y^2} \quad \textbf{(6.1.12)}$$

Because the derivatives of any order are linear operations, the Laplacian is a linear operator. The Laplacian method for edge detection searches for zero crossings in the second derivative of the image to find edges.

For digital image processing, (6.1.12) needs to be discretized. The partial second–order derivative in the x–direction is given as:

$$\frac{\partial^2 f(x,y)}{\partial x^2} = f(x+1, y) + f(x-1, y) - 2\, f(x, y) \quad \textbf{(6.1.13)}$$

Similarly, in the y–direction, the partial second–order derivative is given as:

$$\frac{\partial^2 f(x,y)}{\partial y^2} = f(x, y+1) + f(x, y-1) - 2\, f(x, y) \quad \textbf{(6.1.14)}$$

Thus, the digital implementation of the two–dimensional Laplacian of (6.1.14) is obtained by summing these two components as:

$$\nabla^2 f = [f(x+1, y) + f(x-1, y) + f(x, y+1) + f(x, y-1)] - 4\, f(x, y) \quad \textbf{(6.1.15)}$$

Therefore, (6.1.15) can be implemented using the mask as shown in Figure-6.4.

0	1	0
1	−4	1
0	1	0

Figure–6.4: Filter mask used to implement the digital Laplacian.

1	1	1
1	−8	1
1	1	1

Figure–6.5: Filter mask used to implement the digital Laplacian that includes the diagonal neighbors.

The Laplacian generally is not used in its original form for edge detection for following reasons **[123]**:

(a) As a second–order derivative, the Laplacian is unacceptably sensitive to noise. The magnitude of the Laplacian produces double edges, an undesirable effect because it complicates segmentation.

(b) Useful directional information is not available by the use of a Laplacian operator.

6.2 ANALYTICAL ASPECTS OF EDGE DETECTION BASED ON FRACTIONAL ORDER DIFFERENTIATION IN FrFTD

As it has been stated earlier that the fractional order differentiation of a given signal in the fractional Fourier transform domain can be obtained by utilizing the analytical approach of fractional order operators of the fractional order calculus. To say, this concept involves two degrees of freedom to achieve the fractional derivative order operation in the fractional Fourier transform domain that is, the fractional derivative order parameter μ and the fractional Fourier transform parameter φ.

In this chapter, an attempt is made to amalgamate these two concepts of μ and φ parameters in the image processing application. The application of edge detection is taken for consideration in this work that utilizes these two above mentioned parameters and outputs the results for an image and evaluates the metric parameters with the established edge operators or masks.

Before considering the edge detection operation in the proposed work, let's go through the analytical aspects of the two–dimensional fractional order calculus and how it can be applied to design the fractional differential mask for the edge detection application.

6.2.1 Mathematical Foundation of Finite Difference for Fractional Derivative

The fractional derivative or differential **[89]** is the result of the extension of the integral order derivative or differential. In classical theory, given a derivative of certain order $g^{(n)}$, there is a finite difference approximation of the form **[63, 90]**:

$$g^{(n)}(x) = \lim_{h\to 0} \frac{1}{h^n} \sum_{k=0}^{n} (-1)^k \binom{n}{k} g(x - kh), \qquad \textbf{(6.2.1)}$$

where, $\binom{n}{k} = \frac{n(n-1)(n-2)\cdots(n-k+1)}{k!}$.

This is generalized to derivatives of arbitrary order and gives rise to the Grünwald–Letnikov (GL) fractional order derivative definition as illustrated below.

6.2.2 Grünwald–Letnikov Fractional Order Derivative Definition

GL fractional order derivative definition was introduced in the original papers of Grünwald and Letnikov in 1867 and 1868, respectively. The analytical aspect of GL based fractional derivative definition is used in the edge detection operation to devise the fractional differential mask. The details regarding the mathematical definition of GL based definition can be found in Section (2.2.2) of Chapter 2.

6.2.3 Fractional Differential Mask

For the edge detection operation in the fractional domain, the motive is to perform the edge detection on images utilizing the fractional order differentiation in the fractional Fourier

transform domain, so as to get inherent advantages as compared to the traditional edge detection operators.

As it is obvious that the edges are significant local changes of intensity in an image that typically occur on the boundary between two different regions in an image. For fulfilling the task of edge detection, the mask is required. The mask is slid over an area of the input image, changes that pixel's value and then shifts one pixel to the right and continues to the right until it reaches the end of a row. It then starts at the beginning of the next row and the process continues and finally the edge detected image is obtained.

For the purpose of edge detection in the fractional domain, the fractional differential mask is devised. The utility of the fractional differential mask for the edge detection in the fractional domain is to show how effective is the detection of edges in the noisy environment.

So, for the purpose of edge detection in the fractional domain, the input image is made to corrupt with the noise and the traditional as well as the fractional mask edge detectors are then applied to detect the high intensity edges of the images. It is also important to see how different edge detectors (both traditional and the proposed) are capable to reduce the noise from the images and highlight the edges at the output. [**46, 62, 158**]

Pu *et al*. **[159]** devised the fractional differential mask based on both RL and GL fractional derivative definitions for dealing with digital image processing applications. Most of the typical edge detection operators such as Roberts, Prewitt, Sobel, second–order Laplace etc. are based on the classical Newtonian calculus. To deal with many natural phenomena, it has been proven in scientific findings that fractional order mathematical approaches are proven to be the best tools. Now in the modern scenario of signal analysis and processing, many of the signals that are encountered features nonlinearity, noncausality, non–Gaussian characteristics, nonadditive white noise etc. So for analyzing and processing these kinds of nonproblems in signal processing, the fractional differential–based algorithms prove to be an important mathematical tool. It is also proved that the fractional differential is an effective analytical tool for dealing with fractal problems, where the integral based tool does not suffice.

In addition, the fractional differential masks can be used for nonlinearly enhancing complex fractal–like texture details. **[41, 159, 163]**

In **[159]**, Pu *et al*. have theoretically analyzed the six fractional differential masks and algorithms based on both GL and RL definitions. The performance of the six fractional differential masks is investigated and the relative error analysis have been carried out and it is proved that the performance of $YiFeiPU-2$ is the best amongst all.

Thus, for the edge detection operation in the fractional domain, the fractional differential mask of **[159]** is used for further analysis and compared with the traditional approaches. So the coefficients of the fractional differential mask $YiFeiPU-2$ given by (18) of **[159]** are taken for the study.

6.2.4 Two–Dimensional Fractional Fourier Transform (2D–FrFT)

It is well–known that the fractional Fourier transform (FrFT) performs the rotation of signals in the time–frequency plane and exhibits many theories and applications in time–varying signal analysis **[65]**. Many definitions pertaining to establish the discrete version of the FrFT has been established by the research communities and their easy classification is provided in **[133]** for the interested readers.

For the two–dimensional signal analysis or for processing images in the frequency domain, the two–dimensional signal transform is required to process the images. In the initial stages of image processing research, the two–dimensional Fourier transform (2D–FT) was the first transform in great use and it is in continuous usage for many applications of filtering and image processing. The detailed theoretical and analytical aspects of 2D–FT for image processing can be found in many books and scientific papers. **[10, 123]**

For the proposed work, the FrFT is utilized in two–dimensions so as to have 2D–FrFT. A good number of research papers have come up with the establishment of 2D–DFrFT algorithms — a discretized version of the 2D–FrFT. **[15, 66, 129]**

For one–dimensional FrFT (1D–FrFT), the mathematical representation of the FrFT of the signal $f(t)$ **[95]** is as follows:

$$\mathrm{T}_{\mathcal{F}}{}^{\varphi}[f(t)] = \mathcal{F}^{\varphi}(u_{\varphi}) = \int_{-\infty}^{\infty} f(t)\ \mathrm{K}_{\varphi}(t, u_{\varphi})dt, \qquad \textbf{(6.2.2)}$$

where $\mathrm{K}_{\varphi}(t, u_{\varphi}) = \frac{1}{2\pi}\sqrt{1 - j\cot\varphi}\exp\left[\frac{j}{2}\left(t^2 + {u_{\varphi}}^2\right)\cot\varphi - j\,t\,u_{\varphi}\csc\varphi\right]$ **(6.2.3)**

is the transform kernel, the notation $\mathrm{T}_{\mathcal{F}}{}^{\varphi}(\cdot)$ represents the FrFT operator and φ represents the fractional Fourier transform rotation angle.

The signal $f(t)$ can be recovered back by the FrFT operation with the backward rotation angle $'\varphi'$ as follows:

$f(t) = \int_{-\infty}^{\infty} \mathrm{K}_{-\varphi}(t, u_{\varphi})\,\mathcal{F}^{\varphi}(u_{\varphi})du_{\varphi}$ **(6.2.4)**

The FrFT definition can easily be extended to two dimensions of one assumes a separable kernel. The separable 2D–FrFT is nothing but a repetition of the transform in the x and the y directions independently and is not the most general definition possible in the two dimensions **[16]**. These definitions have separable kernels and possess properties similar to 1D– FrFT. The separable 2D–FrFT of orders φ for the x axis and γ for the y axis for $0 < \varphi < \pi/2$ and $0 < \gamma < \pi/2$, respectively, is defined as:

$\mathrm{T}_{\mathcal{F}}{}^{\varphi,\gamma}[f(x,y)] = \mathcal{F}^{\varphi,\gamma}(u_{\varphi}, v_{\gamma}) = \int_{-\infty}^{\infty}\int_{-\infty}^{\infty} f(x,y)\,\mathrm{K}_{\varphi,\gamma}(x, y, u_{\varphi}, v_{\gamma})\,dx\,dy,$ **(6.2.5)**

where $\mathrm{K}_{\varphi,\gamma}(x, y, u_{\varphi}, v_{\gamma}) = \mathrm{K}_{\varphi}(x, u_{\varphi})\,\mathrm{K}_{\gamma}(y, v_{\gamma})$ **(6.2.6)**

$= \frac{1}{2\pi}\sqrt{1 - j\cot\varphi}\sqrt{1 - j\cot\gamma}\exp\left[\frac{j}{2}\left(x^2 + {u_{\varphi}}^2\right)\cot\varphi - j\,x\,u_{\varphi}\csc\varphi\right]\exp\left[\frac{j}{2}\left(y^2 + {v_{\gamma}}^2\right)\cot\gamma - j\,y\,v_{\gamma}\csc\gamma\right]$ **(6.2.7)**

Here φ and γ indicates the rotation angles of the transformed signal for 2D–FrFT, respectively. The properties of the 2D–FrFT have been well–established in **[15]**.

The signal$f(x,y)$ can be recovered by a 2D–FrFT operation with the backward angles $(-\varphi, -\gamma)$ as:

$f(x,y) = \int_{-\infty}^{\infty}\int_{-\infty}^{\infty} \mathcal{F}^{\varphi,\gamma}(u_{\varphi}, v_{\gamma})\,\mathrm{K}_{-\varphi,-\gamma}(u_{\varphi}, v_{\gamma}, x, y)\,du_{\varphi}\,dv_{\gamma}$ **(6.2.8)**

Now the (M, N)–point 2D discrete transform is computed as:

$$\mathcal{F}^{\varphi,\gamma}(u_\varphi, v_\gamma) = \sum_{x=0}^{M-1}\sum_{y=0}^{N-1} f(x,y)\exp\left[\frac{j}{2}\left(x^2 + {u_\varphi}^2\right)\cot\varphi - j\,x\,u_\varphi\csc\varphi\right]\exp\left[\frac{j}{2}\left(y^2 + {v_\gamma}^2\right)\cot\gamma - j\,y\,v_\gamma\csc\gamma\right] \quad \textbf{(6.2.9)}$$

For 2D–separable kernel, its 2D transform can be implemented by row–column computation as:

$$\mathcal{F}^{\varphi,\gamma}(u_\varphi, v_\gamma) = \sum_{y=0}^{N-1}\left[\sum_{x=0}^{M-1} f(x,y)\exp\left[\frac{j}{2}\left(x^2 + {u_\varphi}^2\right)\cot\varphi - j\,x\,u_\varphi\csc\varphi\right]\right]\exp\left[\frac{j}{2}\left(y^2 + {v_\gamma}^2\right)\cot\gamma - j\,y\,v_\gamma\csc\gamma\right] \quad \textbf{(6.2.10)}$$

Thus, for an $M \times N$ matrix, the 2D–DFrFT is computed in a simple way: The 1D–DFrFT is applied to each row of the matrix and then to each column of the result. Thus, the generalization of the DFrFT to two–dimension is given by taking the DFrFT of the rows of the matrix and then taking the DFrFT of the resultant matrix columnwise.

6.2.5 Block Diagram Representation of the Proposed Edge Detection in the FrFTD

The proposed work focuses on achieving the edge detection on images in the fractional Fourier transform domain utilizing the fractional differential mask, obtained from the analytical aspects of the fractional order calculus. Figure-6.6 shows the general block diagram of the proposed filtering in the FrFTD.

There are two popular methods of filtering operation in image processing applications. First method encompasses the convolution operation between the input image and the filter mask to get the processed image. This method of filtering is known as the ‘spatial domain filtering’. The second method employs the ‘frequency domain filtering’. It involves taking the transforms of the input image and the filter mask respectively, and thereby using the convolution theorem in that transformed domain, so as to multiply the two quantities of interest in the transformed domain. Then, the output processed image can be obtained by the inverse transform of the resulting convolved image in the frequency domain, as is illustrated in Figure-6.6 below.

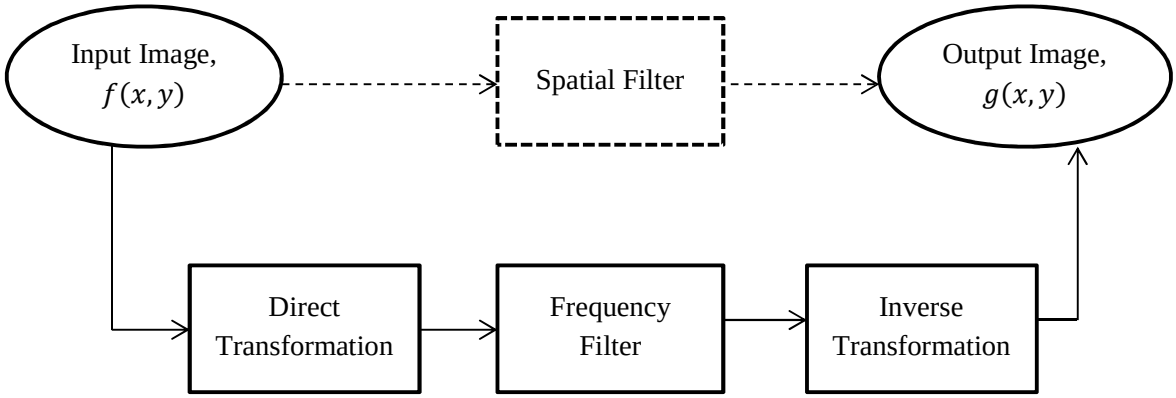

Figure–6.6: General block diagram of the filtering operation in image processing.

In the proposed work, the block diagram of Figure-6.7 is used for the edge detection operation in the 'frequency domain'. The fractional Fourier transform of the input image $f(x,y)$ and the fractional differential mask, μ are obtained. According to the convolution theorem of the fractional Fourier transform **[9, 12]**, the two transformed quantities are then multiplied. The output from this convolution operation is then inverse transformed in the fractional Fourier transformed domain to get the output image, $g(x,y)$ as shown in Figure-6.7, respectively. On the similar ground of Figure-6.7, the comparative analysis is performed between various edge detector masks such as, Roberts, Sobel, Prewitt and Laplacian and the fractional differential mask (μ), which is dealt in the section that follow.

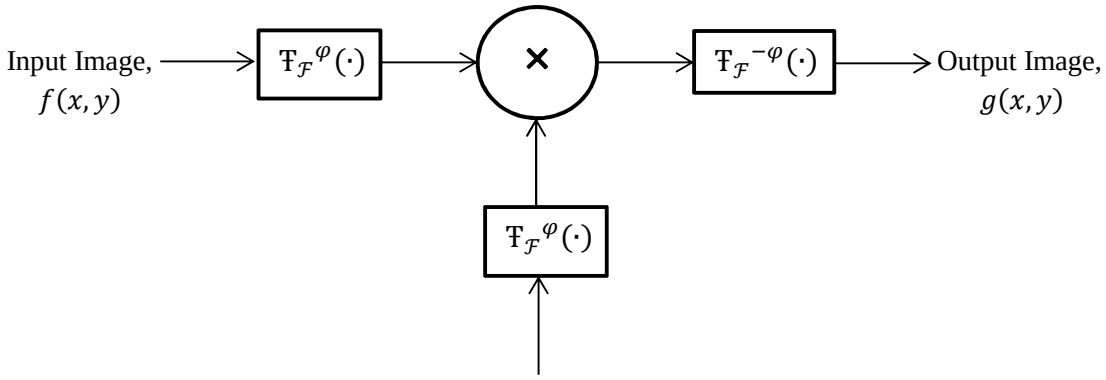

Figure–6.7: Block diagram representation of the proposed edge detection system in the FrFT domain utilizing fractional differential mask. The notation $\mathrm{T}_{\mathcal{F}}{}^{\varphi}(\cdot)$ represents the fractional Fourier transform operator.

6.3 PERFORMANCE METRIC PARAMETERS

To illustrate the performance of the edge detection operation, the two performance metric parameters — mean square error (MSE) and peak signal to noise ratio $(PSNR)$ are chosen. That is, MSE and $PSNR$ parameters assess the quality of the restored output images, in addition to the visual examination. The two performance metric parameters obtained are both dependent upon the fractional differential mask parameter, μ and the fractional Fourier transform parameter, φ or fractional Fourier order parameter, a; related by $\varphi = a(\pi/2)$.

The output edge detected images obtained are compared with the traditional and the proposed edge detection operators and the tabular values of MSE and $PSNR$ are obtained for varying μ and φ parameters and examined accordingly for their variations.

The performance metric parameters are defined as follows:

$$MSE = \frac{1}{MN}\sum_{x=0}^{M-1}\sum_{y=0}^{N-1}\big(f(x,y) - g(x,y)\big)^2 \qquad \textbf{(6.2.11)}$$

$$PSNR = 10 \log \left(\frac{(MAX_I)^2}{MSE} \right) \quad \textbf{(6.2.12)}$$

where $f(x, y)$ and $g(x, y)$ represents the input and the output images, respectively, and MAX_I is the maximum possible pixel value of the image. When the pixels are represented using the 8 bits per sample, this value is 255. **[10, 123]**

Thus, the quantity MSE is an estimator to quantify the amount by which the output image differs from the input image and the quantity $PSNR$ (in dB) is commonly used as a measure of the quality reconstruction of an image. Higher the value of $PSNR$, higher the quality of an image.

Therefore, both the above metric parameters depend on the fractional Fourier transform rotation angle parameter, φ and the fractional differential mask operator (or fractional order differentiation operator), μ.

For the traditional edge detection operators, the output image visualization (qualitative analysis) and the metric parameters (quantitative analysis), both depends on only one varying parameter i.e., φ only, and for the fractional differential mask edge detection operator, they depends on the two flexible varying parameters μ and φ, respectively.

Figure-6.15 and 6.16 shows various plots of MSE and $PSNR$ with respect to the parameter a of the FrFT operation for various traditional and proposed edge detection operators. It is observed through simulations that by utilizing the fractional differential mask (μ) for the edge detection, the optimum performance is achieved for values of a varying between 0.90 to 0.98. The values of MSE and $PSNR$ are also tabulated in Tables 6.1 and 6.2, respectively to show the variation of MSE and $PSNR$ with the parameter a of FrFT for different edge detection operators.

6.4 SIMULATION RESULTS AND DISCUSSION

Numerical simulations are performed for the proposed edge detection operation utilizing the fractional differential mask along with the various traditional edge detection operators like Roberts, Sobel, Prewitt and Laplacian in the fractional Fourier transform domain.

The proposed model describing the edge detection operation using the fractional order differentiation in the fractional Fourier transform domain is simulated in the platform illustrated in the Section 2.7 of Chapter 2.

The experiment is performed on the image of Lena with 256×256 pixels. The various traditional edge detection operators such as Roberts, Sobel, Prewitt and Laplacian that are used in rich literature, show good results on the noise free images, but their performance degrades in the presence of noise.

Thus, the study is performed between the various traditional edge detection operators and the fractional differential mask edge detection operator in the 'noisy environment' and the comparison is made between the two, both through qualitative and quantitative analysis. An attempt is also made to show that the fractional differential mask edge detection operator performs better in the noisy environment.

The input image is corrupted with Gaussian noise of zero mean and variance of 0.1, and then input to the proposed model. The fractional Fourier transform of various traditional edge detection operators (masks) are taken and the edge detection operation is performed. In this study, the edge detection operation is dependent on only one varying parameter φ of the fractional Fourier transform and the processed output image is obtained after inverse transform with $'-\varphi'$, as illustrated in the proposed model.

For the fractional differential edge detection mask operator in the fractional Fourier transform domain, there are two varying parameters namely, μ for the fractional differential mask employing the fractional order differentiation in the two dimensions and φ for the fractional Fourier transform domain.

Thus, the edge detection operation performed with these two varying parameters, μ and φ eliminates the noise corrupted in the input image and shows the detected edges much more clearly (visually) as is shown in Figure-6.13 $(a = 0.95, \mu = 0.5)$ and Figure-6.14 $(a = 0.95, \mu = 0.6)$, as compared to the traditional case of edge detection operators where only one varying parameter φ is employed, as is shown in Figure-6.9 to 6.12, respectively.

Thus, it can be seen from the Figure-6.13 and Figure-6.14 that the proposed fractional differential mask (named as 'FOC–FrFT approach' in the respective figures) performs better for eliminating the noise for optimum $a = 0.95$ and for two different values of the parameter μ, as can be visualized from the qualitative analysis and yield better quantitative metric parameters of MSE and $PSNR$ as compared to the traditional edge detection operators, as indicated in the tabular form in Tables 6.1 and 6.2 and in the plots of Figures-6.15 and 6.16, respectively.

Figure-6.8 (a) and (b) shows the input Lena image and the noise corrupted Lena image. It is input to the proposed model and the edge detection operation is performed. The output edge detected images are obtained as shown in Figures-6.9 to 6.14, both for traditional edge detection operators and the fractional differential mask edge detection operator for spatial–domain, fractional Fourier frequency domain and frequency–domain, respectively.

Figure–6.8 (a): Original Lena Image.

Figure–6.8 (b): Original Lena Image corrupted with Gaussian Noise.

$a = 0$

$a = 0.8$

$a = 1$

Figure–6.9: Roberts mask–FrFT based edge detection.

$a = 0$

$a = 0.4$

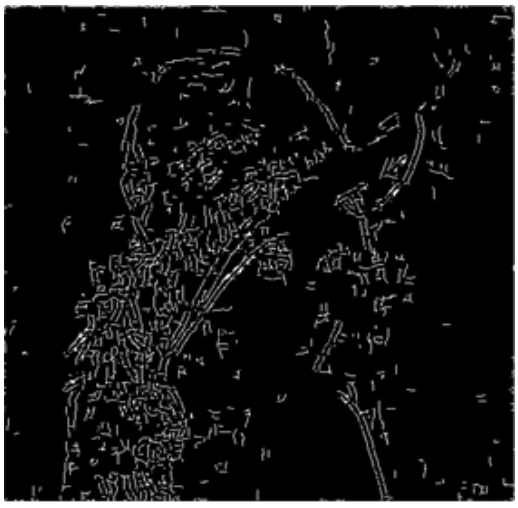

$a = 1$

Figure–6.10: Sobel mask–FrFT based edge detection.

$a = 0$

$a = 0.2$

$a = 1$

Figure–6.11: Prewitt mask–FrFT based edge detection.

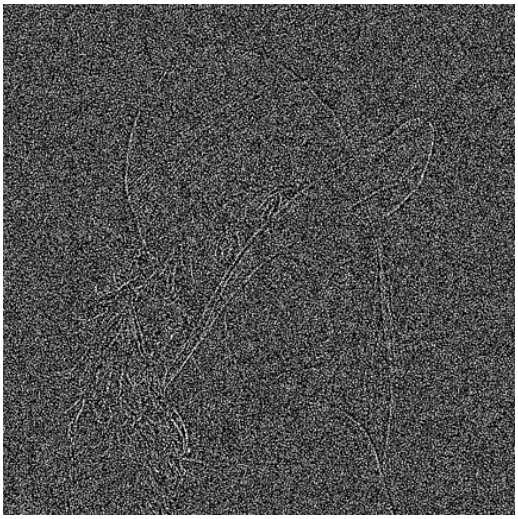

$a = 0$

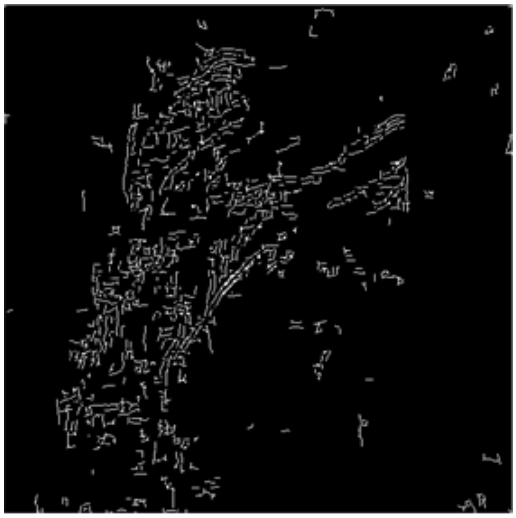

$a = 0.3$

$a = 1$

Figure–6.12: Laplacian mask–FrFT based edge detection.

$a = 0, \mu = 0.5$ FOC–FrFT approach

$a = 0.95, \mu = 0.5$ FOC–FrFT approach

$a = 1, \mu = 0.5$ FOC–FrFT approach

Figure–6.13: Fractional differential mask based edge detection for $\mu = 0.5$ and for varying FrFT order a.

$a = 0, \mu = 0.6$ FOC–FrFT approach

$a = 0.95, \mu = 0.6$ FOC–FrFT approach

$a = 1, \mu = 0.6$ FOC–FrFT approach

Figure–6.14: Fractional differential mask based edge detection for $\mu = 0.6$ and varying FrFT order a.

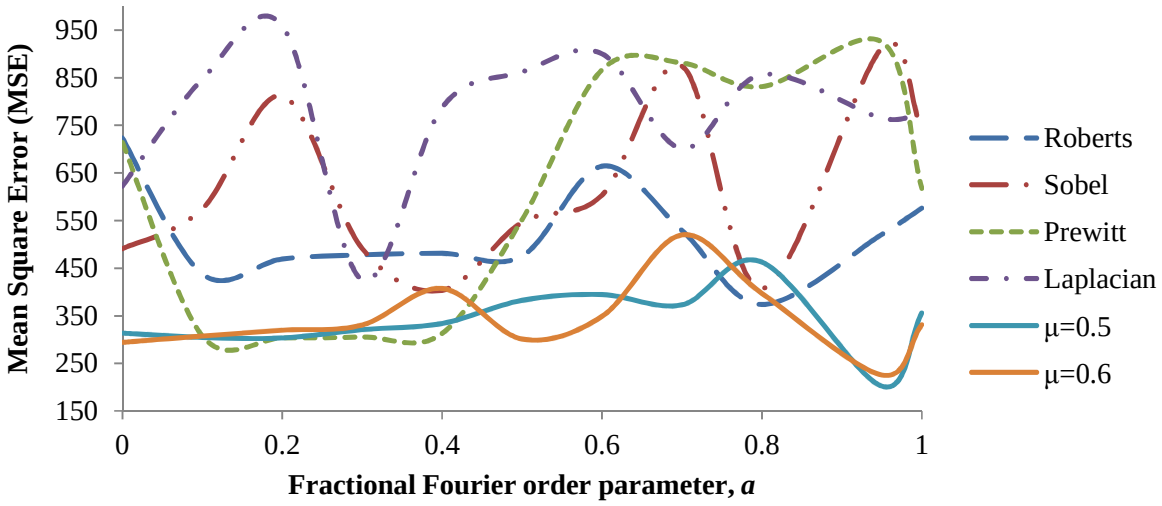

Figure–6.15: **Variation of Mean Square Error (MSE) versus fractional Fourier order parameter, a for different mask operators and the fractional differential mask μ using FrFT.**

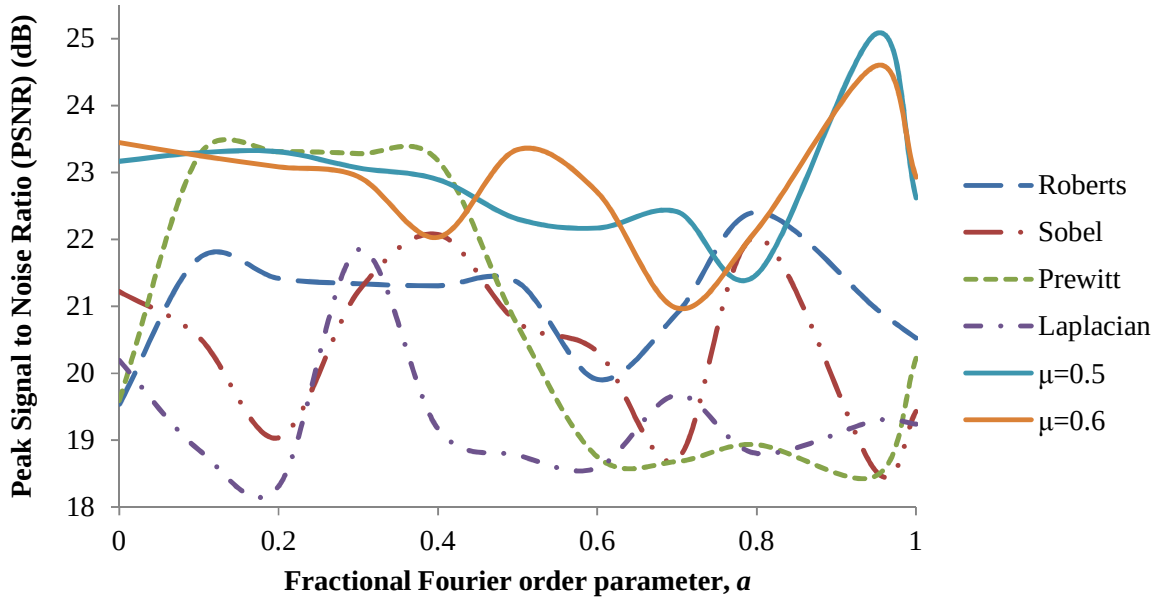

Figure–6.16: **Variation of Peak Signal to Noise Ratio ($PSNR$) (in dB) versus fractional Fourier order parameter, a for different mask operators and the fractional differential mask μ using FrFT.**

TABLE 6.1

VARIATION OF MSE OF LENA IMAGE FOR VARYING a OF DIFFERENT EDGE DETECTION OPERATORS

a	Roberts	Sobel	Prewitt	Laplacian	$\mu = 0.5$	$\mu = 0.6$
0	723.400	490.854	714.300	622.190	313.600	294.034
0.1	437.606	574.540	307.357	846.940	304.477	307.476
0.2	469.256	811.787	**303.472**	958.880	303.445	319.623
0.3	477.913	491.017	305.375	**425.034**	320.821	330.620
0.4	481.166	**403.467**	312.863	787.460	333.922	407.394
0.5	475.528	546.277	552.098	862.160	382.433	301.150
0.6	664.233	603.510	866.780	900.290	394.570	348.862
0.7	529.158	874.270	880.920	700.770	372.970	519.747
0.8	**373.647**	407.147	831.360	856.770	462.766	397.078
0.95	520.844	911.890	925.250	764.990	**202.117**	**225.692**
1	576.122	741.449	617.498	774.730	355.691	331.146

TABLE 6.2

VARIATION OF $PSNR$ (IN dB) OF LENA IMAGE FOR VARYING a OF DIFFERENT EDGE DETECTION OPERATORS

a	Roberts	Sobel	Prewitt	Laplacian	$\mu = 0.5$	$\mu = 0.6$
0	19.53702	21.22128	19.59200	20.19160	23.16704	23.44683
0.1	21.71997	20.53760	23.25437	18.85228	23.29526	23.25269
0.2	21.41671	19.03638	**23.30960**	18.31316	23.31000	23.08442
0.3	21.33732	21.21984	23.28247	**21.84660**	23.06818	22.93751
0.4	21.30785	**22.07270**	23.17726	19.16852	22.89435	22.03066
0.5	21.35904	20.75667	20.71064	18.77492	22.30525	23.34297
0.6	19.90760	20.32396	18.75171	18.58698	22.16956	22.70427
0.7	20.89495	18.71435	18.68144	19.67505	22.41406	20.97288
0.8	**22.40620**	22.03329	18.93291	18.80216	21.47719	22.14205
0.95	20.96373	18.53138	18.46821	19.29425	**25.07480**	**24.59560**
1	20.52566	19.42999	20.22445	19.23930	22.62007	22.93061

Thus, the edge detection operation is performed utilizing the traditional edge detection operator masks like Roberts, Sobel, Prewitt and Laplacian and the fractional differential mask (μ) in the fractional Fourier transform domain. The qualitative (visual perception) and the quantitative analysis (performance metric parameters) are shown for an input image corrupted with the Gaussian noise in three domains— spatial–domain, fractional Fourier frequency domain and frequency–domain, respectively.

The edge detection results are obtained for spatial–domain $(a = 0)$, fractional Fourier frequency domain (varying a) and frequency–domain $(a = 1)$. The values of the fractional Fourier order parameter a is varied between 0 and 1. For the traditional edge detection mask operators of Roberts, Sobel, Prewitt and Laplacian, it is seen from Figures-6.9 to 6.12 that the output edge detected images obtained are *not* much clearer visually as seen by the qualitative analysis. That is, for the input noise–corrupted image, the output edge detected image also exhibits noise. It implies that the traditional edge detection mask operators are incapable to eliminate the noise from the output edge detected image, which is in conformity with the literature **[123]**.

On the other hand, in the case of the fractional differential mask operator (μ) in the fractional Fourier transform domain, the performance is much better as compared to the traditional mask operators. In the rigorous simulations, the values of μ and a are varied between 0 to 1. The quantitative results of MSE and $PSNR$ are also shown in Figures-6.15 and 6.16 and Tables 6.1 and 6.2 for the traditional edge detection mask operators and for the two values of μ = 0.5 and 0.6, respectively.

Also, it can be seen from Table 6.1 that for the traditional edge detection mask operators; Roberts, Sobel, Prewitt and Laplacian, the metric parameter MSE shows the variation with the parameter a. For example, typical values of MSE for Roberts, Sobel, Prewitt and Laplacian mask operators are 373.647, 403.467, 303.472 and 425.034 for different values of a = 0.8, 0.4, 0.2, and 0.3, respectively. Also, these values correspond to the minimum value of MSE and maximum value of $PSNR$ as compared to spatial–domain $(a = 0)$ and frequency–domain $(a = 1)$ as is exhibited by Tables 6.1 and 6.2, respectively.

The MSE and $PSNR$ are used as the metric parameters to evaluate the performance of different edge detection operators with varying parameters, μ and a. The edge detection operation is performed for different values of the parameter a. The value of optimum a is recorded with varying a, where the metric parameters show sudden change (MSE and $PSNR$ shows dip and peak in their respective curves with varying a). In the other case of fractional differential mask in the FrFT domain, the parameter a is varied and the values of the metric parameters, MSE and $PSNR$ are noted. With varying fractional differential parameter μ between 0 and 1, different values of MSE and $PSNR$ are obtained and the best results are obtained where the MSE shows minimum and the $PSNR$ shows maximum values.

Thus, the performance of the fractional order differentiation (μ) in the FrFT domain (φ) is observed to perform better than the traditional edge detection operators in the FrFT domain (φ). Furthermore, the fractional differential mask based edge detection operator is capable of eliminating the noise in the image. The output edge detected images utilizing the fractional differential mask performs well in the noisy environment as compared to the traditional edge detection operators, which under performs in the presence of noise. Thus, it has been ascertained that the fractional order differentiation in the fractional Fourier transform domain outperforms in comparison to the traditional edge detection operators.

CHAPTER 7

CONCLUSIONS AND FUTURE SCOPE OF WORK

Taking mathematics from the beginning of the world to
the time when Newton lived, what he had done was much the between half.

— Gottfried Wilhelm Leibniz (1646–1716).

7.1 CONCLUSIONS

THIS STUDY EXAMINES THE ANALYSIS OF fractional order differentiation in the fractional Fourier transform domain. The concept of fractional order differentiation is based on the mathematical tool of 'Fractional Order Calculus', which is a calculus of derivatives and integrals of arbitrary (real) order, fractional differential equations and methods of their solution, approximations and implementation techniques.

The advantages of fractional order calculus (FOC) that are described and pointed out by many researchers and authors are that the fractional order models of the real systems are regularly more adequate than the usual integer order models.

This study has established the new signal processing approach of investigating the fractional order differentiation that behaves in the fractional Fourier transform (FrFT) domain. The dual concepts of fractional order calculus and fractional Fourier transform are amalgamated

to examine the proposed differentiation operation in the time–frequency plane of the fractional Fourier transform.

Based on the proposed differentiation operation in the FrFT domain, the study has explored to design the differentiating filter; namely both integer–order and fractional–order differentiators.

The work was set out to explore the concept of integer–order and fractional–order differentiators and has identified the analytical aspects of their behavior in the fractional Fourier transform domain.

For designing the integer–order differentiator, an examination is done (both analytically and through simulations) for the behavior of different signal processing window functions in the time–frequency plane of the FrFT domain. The closed–form analytical expression of the behavior of Dirichlet and Generalized ‘‘Hamming’’ window functions is established, utilizing various special mathematical functions in the fractional Fourier transform domain. It is shown that the fractional Fourier transform of Dirichlet and Generalized ‘‘Hamming’’ window functions are directly dependent on the fractional Fourier transform parameter φ, thus exhibiting the flexibility of various applications in signal and image processing.

It is also shown that the increasing value of the fractional Fourier order parameter a reduces the side lobe levels, which in turn broadens the main lobe width, thus reducing resolution. It can further be concluded that for Dirichlet window function, as the parameter a is increased, maximum side lobe level (MSLL), half main lobe width (HMLW) and side–lobe fall–off rate (SLFOR) starts increasing. Similarly, for Hanning window function (for $\beta = 0.5$), MSLL, HMLW and SLFOR starts increasing with increasing value of the parameter a. Also, it is seen that below the value of the parameter $a = 0.2$, it is impossible to detect the variations in the window parameters. This is because of oscillations that occur at around $a = 0.2$ and also it can be seen that all the lobes are merging to the main lobe.

Thus, it is revealed that there is a variation in the window function parameters with the variation in the fractional Fourier order parameter a and a best optimal solution can be obtained for the variety of practical applications such as, in image compressions. Efforts have also been made to choose the most convenient parameter adjustment to reduce the side lobe effect and to

increase the intensity of the main lobe. Also, the results discussed in the above techniques can be beneficial to reduce the undesirable effects of the spectral leakage.

Following the work of designing integer–order differentiator in the FrFT framework, an attempt is made to design fractional–order differentiator in the FrFT framework. To start with, the concept of FOC is used as an assistance tool. The analytical approach of deriving the new closed–form analytical expression of the fractional order differentiation in the FrFT domain is investigated. This expression is the generalization of the differentiation property to fractional (non–integer) orders in the FrFT domain. The proposed fractional order differentiation expression is derived based on the three well–known definitions of FOC namely, Riemann–Liouville (RL), Grünwald–Letnikov (GL) and Caputo approach. It motivates for the variation of two parameters: the fractional derivative order parameter (μ) and the fractional Fourier transform parameter (φ), which was not communicated earlier by the research community, to the best of our knowledge. This closed–form analytical expression is obtained with the help of special mathematical function of Kummer confluent hypergeometric function.

The fractional order differentiation thus derived is a more generalized definition, since it achieves the flexibility of different rotation angles φ in the time–frequency plane of the FrFT with varying μ. Due to this variation of μ with φ in the FrFT domain, potential signal processing applications can be achieved, for example in filter design and edge detection in image processing, and so on.

Next, the established fractional order differentiation property in the FrFT domain is examined for potential applications in the signal and image processing research areas. The application example of designing an FrFT–based low–pass finite impulse response fractional order differentiator is demonstrated. The proposed differentiator is designed based on the underlying principles of fractional order calculus and the fractional Fourier transform. The design results are presented by utilizing the familiar FOC definitions and demonstrate its validity.

Thus, the proposed fractional order differentiator includes the following advantages. First it is the first and new attempt of combining the FOC concept with the FrFT and it provides a new way of designing the digital fractional order differentiator. Second, it provides the flexibility of

two different varying parameters, which could be beneficial in different signal and image processing applications. Thus, the freedom of utilizing varying order of the derivative (fractional derivative) in the entire time–frequency plane of the FrFT domain can be utilized for different potential signal processing applications. Also the comparative analysis between the two proposed definitions used in designing the proposed differentiator is examined. As it is evident from the mathematics literature that the Caputo based definition outperforms the RL definition, so the superiority of the Caputo based definition over RL based definition is also established through the use of metric parameter, which is in conformity with the available mathematics literatures.

Thus, the design example of one–dimensional fractional order differentiating filter in the FrFT domain is demonstrated and shows the effectiveness of the proposed method.

Following the work introduced above, the curiosity leads to extend the proposed method to design the two–dimensional fractional order differentiating filter in the FrFT domain. For this, the edge detection operation in image processing is examined through the analytical approach of combining the FOC concept with the two–dimensional fractional Fourier transform concept. The fractional differential mask based on the Grünwald–Letnikov fractional differentiation definition is utilized for the edge detection operation based on its utility. Thus, the comparative study of the traditional edge detection operators with the fractional differential mask edge detection operator in the fractional Fourier transform domain is examined in the noisy environment. For judging the performance, the metric parameters of peak signal–to–noise ratio and mean square error are used and it is shown that with two varying parameters of μ and φ, the edge information is extracted more specifically as compared to the traditional approaches.

Thus, the image edge detection results utilizing the fractional order operator show that the proposed method is not only effective but also exhibits good noise immunity. Furthermore, the fractional differential approach in the field of image processing will have broad application prospects in the near future.

7.2 FUTURE SCOPE OF WORK

The design of fractional order differentiator is a topic without boundaries. Further, studies can be extended in areas like:

(i) The closed–form analytical expression of the fractional order differentiation in the FrFT domain is established for the fractional order parameter of the differentiation operation restricted in the range $0 < \mu < 1$. So further studies could be established for the general class of fractional order parameter, μ.

Further, this task can be extended for other signal processing transforms which exhibits more than one extra degree of freedom and thus more potential applications in signal and image processing could be examined.

(ii) In image processing application, the operation of edge detection is performed utilizing the fractional differential mask based on Grünwald–Letnikov definition in the FrFT domain. The comparative analysis of different fractional differential masks based on Riemann–Liouville and Caputo definitions in the FrFT domain was not made. This stimulates to analyze the different fractional differential masks for the edge detection operation. So the conclusion can be made for a better approach. Also, different transform techniques can be applied for the edge detection operation in addition to the FrFT techniques and analyze the results.

(iii) There exist many definitions of fractional order differentiation in the available research literatures. We have restricted our proposed work in only three of the well–known definitions, and presented their results in the pursuit of signal and image processing applications. Further studies could be examined by incorporating other known definitions of FOC and analyze their results in the engineering fields.

(iv) Practical solutions for the implementation of the fractional order differentiation in the FrFT domain could be established.

REFERENCES

[1] A. Antoniou, *Digital Signal Processing: Signals, Systems, and Filters*. McGraw Hill, 2005.

[2] A. Antoniou, "New improved method for the design of weighted–Chebyshev, nonrecursive, digital filters," *IEEE Transactions on Circuits and Systems*, vol. 30, no. 10, pp. 740–750, 1983.

[3] A. Antoniou, and C. Charalambous, "Improved design method for Kaiser differentiators and comparison with equiripple method," *IEEE Proceedings on Computers and Digital Techniques*, vol. 128, no.5, pp. 190–196, 1981.

[4] A. Ashyralyev, "A note on fractional derivatives and fractional powers of operators," *Journal of Mathematical Analysis and Applications*, vol. 357, no. 1, pp. 232–236, 2009.

[5] A. Bovik, *The Essential Guide to Image Processing*. Academic Press, 2009.

[6] A. C. McBride, and F. H. Kerr, "On Namias's fractional Fourier transforms," *IMA Journal of Applied Mathematics*, vol. 39, no. 2, pp. 159–175, 1987.

[7] A. Carpinteri, P. Cornetti, and A. Sapora, "A fractional calculus approach to nonlocal elasticity," *The European Physical Journal–Special Topics*, vol. 193, no. 1, pp. 193–204, 2011.

[8] A. Charef, H. H. Sun, Y. Y. Tsao, and B. Onaral, "Fractal system as represented by singularity function," *IEEE Transactions on Automatic Control*, vol. 37, no. 9, pp. 1465–1470, 1992.

[9] A. I. Zayed, "A convolution and product theorem for the fractional Fourier transform," *IEEE Signal Processing Letters*, vol. 5, no. 4, pp. 101–103, 1998.

[10] A. K. Jain, *Fundamental of Digital Image Processing*. NJ: Prentice–Hall, 1989.

[11] A. K. Singh, and R. Saxena, "Correlation theorem for fractional Fourier transform," *International Journal of Signal Processing, Image Processing and Pattern Recognition*, vol. 4, no. 2, pp. 31–40, 2011.

[12] A. K. Singh, and R. Saxena, "On convolution and product theorems for FrFT," *Wireless Personal Communications*, vol. 65, no. 1, pp. 189–201, 2012.

[13] A. Oustaloup, F. Levron, B. Mathieu, and F. M. Nanot, "Frequency–band complex noninteger differentiator: characterization and synthesis," *IEEE Transactions on Circuits and Systems–I: Fundamental Theory and Applications*, vol. 47, no. 1, pp. 25–39, 2000.

[14] A. Qadir, "The generalization of special functions," *Applied Mathematics and Computation*, vol. 187, no. 1, pp. 395–402, 2007.

[15] A. Sahin, H. M. Ozaktas, and D. Mendlovic, "Optical implementations of two–dimensional fractional Fourier transforms and linear canonical transforms with arbitrary parameters," *Applied Optics*, vol. 37, no. 11, pp. 2130–2141, 1998.

[16] A. Sahin, M. A. Kutay, and H. M. Ozaktas, "Nonseparable two–dimensional fractional Fourier transform," *Applied Optics*, vol. 37, no. 23, pp. 5444–5453, 1998.

[17] A. Sandryhaila, S. Saba, M. Püschel, and J. Kovacevic, "Efficient compression of QRS complexes using Hermite expansion," *IEEE Transactions on Signal Processing*, vol. 60, no. 2, pp. 947–955, 2012.

[18] A. Tepljakov, E. Petlenkov, and J. Belikov, "Applications of Newton's method to analog and digital realization of fractional–order controllers," *International Journal of Microelectronics and Computer Science*, vol. 2, no. 2, pp. 45–52, 2012.

[19] Ashutosh, and P. K. Jain, "Study of metallic photonic band gap cavity for high power microwave devices," *Applied Electromagnetics Conference*, Kolkata, India, 14–16 December 2009, pp. 1–3.

[20] B. Kumar, and S. C. Dutta Roy, "Design of digital differentiators for low frequencies," *Proceedings of the IEEE*, vol. 76, no. 3, pp. 287–289, 1988.

[21] B. Kumar, and S. C. Dutta Roy, "Maximally linear FIR digital differentiators for midband frequencies," *International Journal of Circuit Theory and Applications*, vol. 17, no. 1, pp. 21–27, 1989.

[22] B. Kumar, and S. C. Dutta Roy, "Design of efficient FIR digital differentiators and Hilbert transformers for midband frequency ranges," *International Journal of Circuit Theory and Applications*, vol. 17, no. 4, pp. 483–488, 1989.

[23] B. Kumar, and S. C. Dutta Roy, "Maximally linear FIR digital differentiators for high frequencies," *IEEE Transactions on Circuits and Systems*, vol. 36, no. 6, pp. 890–893, 1989.

[24] B. Kumar, S. C. Dutta Roy, and H. Shah, "On the design of FIR digital differentiators

which are maximally linear at the frequency (π/p), $p \in$ {positive integers}," *IEEE Transactions on Signal Processing*, vol. 40, no. 9, pp. 2334–2338, 1992.

[25] B. M. Vinagre, Y. Q. Chen, and I. Petráš, "Two direct Tustin discretization methods for fractional–order differentiator/integrator," *Journal of the Franklin Institute*, vol. 340, no. 5, pp. 349–362, 2003.

[26] B. Mathieu, P. Melchior, A. Oustaloup, and Ch. Ceyral, "Fractional differentiation for edge detection," *Signal Processing*, vol. 83, no. 11, pp. 2421–2432, 2003.

[27] B. Ross, "A brief history and exposition of the fundamental theory of fractional calculus," *Fractional Calculus and Its Applications*, Lecture Notes in Mathematics, NY: Springer–Verlag, vol. 457, pp. 1–36, 1975.

[28] B. Santhanam, and J. H. McClellan, "The discrete rotational Fourier transform," *IEEE Transactions on Signal Processing*, vol. 44, no. 4, pp. 994–998, 1996.

[29] B. V. K. Vijaya Kumar and C. A. Rahenkamp, "Calculation of geometric moments using Fourier plane intensities," *Applied Optics*, vol. 25, no. 6, pp. 997–1007, 1986.

[30] C. A. Monje, Y. Q. Chen, B. M. Vinagre, D. Xue, and V. Feliu, *Fractional–Order Systems and Controls*. NY: Springer, 2010.

[31] C. C. Shih, "Fractionalization of Fourier transform," *Optics Communications*, vol. 118, no. 5–6, pp. 495–498, 1995.

[32] C. C. Tseng, "Design of variable and adaptive fractional order FIR differentiators," *Signal Processing*, vol. 86, no. 10, pp. 2554–2566, 2006.

[33] C. C. Tseng, "Design of fractional order digital FIR differentiators," *IEEE Signal Processing Letters*, vol. 8, no. 3, pp. 77–79, 2001.

[34] C. C. Tseng, and S. L. Lee, "Design of fractional order digital differentiator using radial basis function," *IEEE Transactions on Circuits and Systems–I: Regular Papers*, vol. 57, no. 7, pp. 1708–1718, 2010.

[35] C. C. Tseng, and S. L. Lee, "Design of linear phase FIR filters using fractional derivative constraints," *Signal Processing*, vol. 92, no. 5, pp. 1317–1327, 2012.

[36] C. C. Tseng, and S. L. Lee, "Design of fractional order differentiator using discrete Fourier transform interpolation," *International Symposium on Communication and Information Technologies*, Tokyo, Japan, 26–29 October 2010, pp. 306–311.

[37] C. C. Tseng, and S. L. Lee, "Closed–form design of fractional order differentiator using

discrete cosine transform," *IEEE International Symposium on Circuits and Systems*, Beijing, China, 19–23 May 2013, pp. 2609–2612.

[38] C. C. Tseng, S. C. Pei, and S. C. Hsia, "Computation of fractional derivatives using Fourier transform and digital FIR differentiator," *Signal Processing*, vol. 80, no. 1, pp. 151–159, 2000.

[39] C. Candan, M. A. Kutay, and H. M. Ozaktas, "The discrete fractional Fourier transform, *IEEE Transactions on Signal Processing*," vol. 48, no. 5, pp. 1329–1337, 2000.

[40] C. Gao, J. Zhou, and W. Zhang, "Fractional directional differentiation and its application for multiscale texture enhancement," *Mathematical Problems in Engineering*, vol. 2012, Article ID 325785, 2012.

[41] C. Gao, J. Zhou, and W. Zhang, "Edge detection based on the Newton interpolation's fractional differentiation," *The International Arab Journal of Information Technology*, 2011.

[42] C. Gao, J. Zhou, X. Zheng, and F. Lang, "Image enhancement based on improved fractional differentiation," *Journal of Computational Information Systems*, vol. 7, no. 1, pp. 257–264, 2011.

[43] C. Li, and W. Deng, "Remarks on fractional derivatives," *Applied Mathematics and Computation*, vol. 187, no. 2, pp. 777–784, 2007.

[44] C. M. Leung, and W. S. Lu, "Detection of edges of noisy images by 1–D and 2–D linear FIR digital filters," *IEEE Pacific Rim Conference on Communications, Computers and Signal Processing*, vol. 1, Victoria, BC, 19–21 May 1993, pp. 228–231.

[45] C. M. Rader, and B. Gold, "Digital filter design techniques in the frequency domain," *Proceedings of the IEEE*, vol. 55, no. 2, pp. 149–171, 1967.

[46] C. Q. Li, H. Guo, and Z. X. Qiong, "A fractional differential approach to low contrast image enhancement," *International Journal of Knowledge and Language Processing*, vol. 2, no. 2, pp. 20–29, 2012.

[47] C. Shi, and B. K. Bhargava, "An efficient MPEG video encryption algorithm," *Seventeenth IEEE Symposium on Reliable Distributed Systems*, West Lafayette, 20–23 October 1998, pp. 381–386.

[48] D. A. Waldman, and J. Joseph, "Method and apparatus for phase–encoded homogenized Fourier transform holographic data storage and recovery," U.S. Patent 7 411 708 B2,

August 12, 2008.

[49] D. Chen, Y. Q. Chen, and D. Xue, "Digital fractional order Savitzky–Golay differentiator," *IEEE Transactions on Circuits and Systems–II: Express Briefs*, vol. 58, no. 11, pp. 758–762, 2011.

[50] D. H. Bailey, and P. N. Swarztrauber, "The fractional Fourier transform and applications," *SIAM Review*, vol. 33, no. 3, pp. 389–404, 1991.

[51] D. Middleton, *An Introduction to Statistical Communication Theory*. Piscataway: Wiley–IEEE Press, 1996.

[52] D. Schlichthärle, *Digital Filters: Basics and Design*. NY: Springer, 2011.

[53] E. Ifeachor, and B. W. Jervis, *Digital Signal Processing: A Practical Approach*. Prentice Hall, 2002.

[54] E. Sejdić, I. Djurović, and L. Stanković, "Fractional Fourier transform as a signal processing tool: An overview of recent developments," *Signal Processing*, vol. 91, no. 6, pp. 1351–1369, 2011.

[55] F. J. Harris, "On the use of windows for harmonic analysis with discrete Fourier transform," *Proceedings of the IEEE*, vol. 66, no. 1, pp. 51–83, 1978.

[56] F. Pisoni, "Fractional Fourier transform convolver arrangement," U.S. Patent 7 543 009 B2, June 2, 2009.

[57] F. Yang, and K. Q. Zhu, "A note on the definition of fractional derivatives applied in rheology," *Acta Mechanica Sinica*, vol. 27, no. 6, pp. 866–876, 2011.

[58] G. Bi, and Y. Zeng, *Transforms and Fast Algorithms for Signal Analysis and Representations*. Boston: Birkhäuser, 2004.

[59] G. E. Carlson, and C. A. Halijak, "Approximation of fractional capacitors $(1/s)^{(1/n)}$ by a regular Newton process," *IEEE Transactions on Circuit Theory*, vol. 11, no. 2, pp. 210–213, 1964.

[60] G. Maione, "A digital, noninteger order, differentiator using Laguerre orthogonal sequences," *International Journal of Intelligent Control Systems*, vol. 11, no. 2, pp. 77–81, 2006.

[61] G. Sharma, O. Altun, and M. Bocko, "Informed watermarking in the fractional Fourier domain," *Thirteenth European Signal Processing Conference*, Antalya, Turkey, 4–8 September 2005.

[62] H. A. Jalab, and R. W. Ibrahim, "Texture enhancement based on the Savitzky–Golay fractional differential operator," *Mathematical Problems in Engineering*, vol. 2013, Article ID 149289, 2013.

[63] H. Brunner, L. Ling, and M. Yamamoto, "Numerical simulations of 2D fractional subdiffusion problems," *Journal of Computational Physics*, vol. 229, no. 18, pp. 6613–6622, 2010.

[64] H. K. Mohammed, R. Tripathi, and K. Kant, "Performance of adaptive modulation with multipath diversity technique," *Tenth International Conference on Advanced Communication Technology*, vol. 3, Gangwon–Do, Korea, 17–20 February 2008, pp. 1496–1499.

[65] H. M. Ozaktas, M. A. Kutay, and Z. Zalevsky, *The fractional Fourier transform with Applications in Optics and Signal Processing*. NY: John Wiley and Sons, 2001.

[66] H. M. Ozaktas, O. Arikan, M. A. Kutay, and G. Bozdağı, "Digital computation of the fractional Fourier transform," *IEEE Transactions on Signal Processing*, vol. 44, no. 9, pp. 2141–2150, 1996.

[67] H. S. Li, Y. Luo, and Y. Q. Chen, "A fractional order proportional and derivative (FOPD) motion controller: Tuning rule and experiments," *IEEE Transactions on Control Systems Technology*, vol. 18, no. 2, pp. 516–520, 2010.

[68] H. Sheng, Y. Q. Chen, and T. S. Qiu, *Fractional Processes and Fractional–Order Signal Processing: Techniques and Applications*, Signals and Communication Technology, Heidelberg, NY: Springer, 2012.

[69] H. Yang, Y. Ye, D. Wang, and B. Jiang, "A novel fractional–order signal processing based edge detection method," *Eleventh International Conference on Control, Automation, Robotics and Vision*, Singapore, 7–10 December 2010, pp. 1122–1127.

[70] H. Zhao, G. Qiu, L. Yao, and J. Yu, "Design of fractional order digital FIR differentiators using frequency response approximation," *International Conference on Communications, Circuits and Systems*, vol. 2, China, 27–30 May 2005, pp. 1318–1321.

[71] I. Podlubny, "Geometric and physical interpretation of fractional integration and fractional differentiation," *Fractional Calculus and Applied Analysis*, vol. 5, no. 4, pp. 367–386, 2002.

[72] I. Podlubny, "Fractional–order systems and $PI^{\lambda}D^{\mu}$–controllers," *IEEE Transactions on*

Automatic Control, vol. 44, no. 1, pp. 208–214, 1999.

[73] I. Podlubny, *Fractional Differential Equations*. San Diego: Academic Press, 1999.

[74] I. Podlunby, I. Petráš, B. M. Vinagre, P. O' Leary, and L'. Dorčák, "Analogue realizations of fractional–order controllers," *Nonlinear Dynamics*, vol. 29, no. 1–4, pp. 281–296, 2002.

[75] I. R. Khan, and R. Ohba, "Digital differentiators based on Taylor series," *The Institute of Electronics, Information and Communication Engineers (IEICE) Transactions Fundamentals*, vol. E82–A, no. 12, pp. 2822–2824, 1999.

[76] I. W. Selesnick, "Maximally flat low-pass digital differentiator," *IEEE Transactions on Circuits and Systems–II: Analog and Digital Signal Processing*, vol. 49, no. 3, pp. 219–223, 2002.

[77] J. A. T. Machado, "Analysis and design of fractional–order digital control systems," *Journal of Systems Analysis Modelling Simulation*, vol. 27, no. 2–3, pp. 107–122, 1997.

[78] J. A. T. Machado, "Application of fractional calculus in engineering sciences," *IEEE Sixth International Conference on Computational Cybernetics*, Stará Lesná, Slovakia, 27–28 November 2008, pp. 11–14.

[79] J. C. Trigeassou, N. Maamri, and A. Oustaloup, "Automatic initialization of the Caputo fractional derivative," *Fiftieth IEEE Conference on Decision and Control and European Control Conference*, Orlando, Florida, 12–15 December 2011, pp. 3362–3368.

[80] J. F. Canny, "A computational approach to edge detection," *IEEE Transactions on Pattern Analysis and Machine Intelligence*, vol. 8, no. 6, pp. 679–698, 1986.

[81] J. F. Kaiser, "Digital Filters," in *System Analysis by Digital Computer*, NY: John Wiley and Sons, 1966, Chapter 7.

[82] J. J. Shyu, S. C. Pei, and C. H. Chan, "An iterative method for the design of variable fractional order FIR differintegrators," *Signal Processing*, vol. 89, no. 3, pp. 320–327, 2009.

[83] J. K. Wu, "Numerical differentiation and digital FIR filter based algorithm for power system measurement," *IEEE Power Engineering Society General Meeting*, vol. 2, 12–16 June 2005, pp. 1367–1374.

[84] J. Lang, R. Tao, and Y. Wang, "The discrete multiple–parameter fractional Fourier transform," *Science China Information Sciences*, vol. 53, no. 11, pp. 2287–2299, 2010.

[85] J. M. De Freitas, *Digital Filter Design Solutions*. Artech House Microwave Library, 2005.

[86] J. Sabatier, O. P. Agrawal, and J. A. T. Machado, *Advances in Fractional Calculus: Theoretical Developments and Applications in Physics and Engineering*, Springer, 2007.

[87] J. Zhang, Z. Wei, and L. Xiao, "Adaptive fractional–order multi–scale method for image denoising," *Journal of Mathematical Imaging and Vision*, vol. 43, no. 1, pp. 39–49, 2012.

[88] K. Assaleh, and W. M. Ahmad, "Modeling of speech signals using fractional calculus," *Ninth International Symposium on Signal Processing and Its Applications*, Sharjah, United Arab Emirates, 12–15 February 2007, pp. 1–4.

[89] K. B. Oldham and J. Spanier, *The Fractional Calculus: Theory and Applications of Differentiation and Integration to Arbitrary Order*. NY: Academic Press, 1974.

[90] K. Diethelm, *The Analysis of Fractional Differential Equations*. Lecture Notes in Mathematics, Springer Berlin Heidelberg, vol. 2004, 2010.

[91] K. Diethelm, N. J. Ford, A. D. Freed, and Y. Luchko, "Algorithms for the fractional calculus: a selection of numerical methods," *Computational Methods in Applied Mechanics Engineering*, vol. 194, no. 6–8, pp. 743–773, 2005.

[92] K. E. Atkinson, *An Introduction to Numerical Analysis*. Second Edition, NY: Wiley, 1989.

[93] K. Huang, Z. Wang, and R. Tao, "Study of incoherent demodulation technique in chirp spread spectrum communication systems," *Ninth International Conference on Signal Processing*, Beijing, China, 26–29 October 2008, pp. 1926–1929.

[94] K. Matsuda and H. Fujii, "H_∞ optimized wave–absorbing control: Analytical and experimental results," *Journal of Guidance, Control, and Dynamics*, vol. 16, no. 6, pp. 1146–1153, 1993.

[95] L. B. Almeida, "The fractional Fourier transform and time-frequency representation," *IEEE Transactions on Signal Processing*, vol. 42, no. 11, pp. 3084–3091, 1994.

[96] L. B. Jackson, *Digital Filters and Signal Processing*. NY: Kluwer Academic Publishers, 1986.

[97] L. B. Michael, M. Ghavami, and R. Kohno, "Multiple pulse generator for ultra–wideband communication using Hermite polynomial based orthogonal pulses," *IEEE Conference*

on Ultra Wideband Systems and Technologies, Baltimore, Maryland, 21–23 May 2002, pp. 47–51.

[98] L. Di, W. X. Li, and S. X. Jun, "Fractional Fourier transform based transmitted reference scheme for UWB communications," *Science China Information Sciences*, vol. 54, no. 8, pp. 1712–1722, 2011.

[99] L. R. Rabiner, and B. Gold, *Theory and Application of Digital Signal Processing*. Prentice–Hall, 1986.

[100] L. R. Rabiner, and K. Steiglitz, "The design of wide-band recursive and nonrecursive digital differentiatiors," *IEEE Transactions on Audio and Electroacoustics*, vol. 18, no. 2, pp. 204–209, 1970.

[101] L. R. Rabiner, J. H. McClellan, and T. W. Parks, "FIR digital filter design techniques using weighted Chebyshev approximation," *Proceedings of the IEEE*, vol. 63, no. 4, pp. 595–610, 1975.

[102] L. Stanković, T. Alieva, and M. J. Bastiaans, "Time–frequency signal analysis based on the windowed fractional Fourier transform," *Signal Processing*, vol. 83, no. 11, pp. 2459–2468, 2003.

[103] L. Yaroslavsky, *Fast Transform Methods in Digital Signal Processing: Theory, Applications, Efficient Algorithms*. Bentham Science Publishers, 2011.

[104] M. A. Al-Alaoui, "Novel digital integrator and differentiator," *Electronics Letters*, vol. 29, no. 4, pp. 376–378, 1993.

[105] M. A. Al-Alaoui, "Novel approach to designing digital differentiators," *Electronics Letters*, vol. 28, no. 15, pp. 1376–1378, 1992.

[106] M. A. Al–Alaoui, "Novel IIR differentiator from the Simpson integration rule," *IEEE Transactions on Circuits and Systems–I: Fundamental Theory and Applications*, vol. 41, no. 2, pp. 186–187, 1994.

[107] M. Abramowitz, and I. A. Stegun, *Handbook of Mathematical Functions with Formulas, Graphs and Mathematical Tables*. NY: Dover, vol. 55, 1964.

[108] M. Benmalek, and A. Charef, "Digital fractional order operators for R–wave detection in electrocardiogram signal," *IET Signal Processing*, vol. 3, no. 5, pp. 381–391, 2009.

[109] M. Caputo, "Linear models of dissipation whose Q is almost frequency independent–II," *Geophysical Journal of the Royal Astronomical Society*, vol. 13, no. 5, pp. 529–539,

1967.

[110] M. D. Ortigueira, *Fractional Calculus for Scientists and Engineers*. Lecture Notes in Electrical Engineering, Springer, vol. 84, 2011.

[111] M. D. Ortigueira, "A coherent approach to noninteger order derivatives," *Signal Processing*, vol. 86, no. 10, pp. 2505–2515, 2006.

[112] M. Deriche, and A. H. Tewfik, "Signal modeling with filtered discrete fractional noise processes," *IEEE Transactions on Signal Processing*, vol. 41, no. 9, pp. 2839–2849, 1993.

[113] M. H. Er, "Designing notch filter with controlled null width," *Signal Processing*, vol. 24, no. 3, pp. 319–329, 1991.

[114] M. Martone, "A multicarrier system based on the fractional Fourier transform for time–frequency–selective channels," *IEEE Transactions on Communications*, vol. 49, no. 6, pp. 1011–1020, 2001.

[115] M. Petrou, and P. Bosdogianni, *Image Processing: The Fundamentals*. John Wiley and Sons, 1991.

[116] N. K. Nishchal, "Optical image watermarking using fractional Fourier transform," *Journal of Optics*, vol. 38, no. 1, pp. 22–28, 2009.

[117] N. Laskin, "Fractional quantum mechanics," *Physical Review E*, vol. 62, no. 3, pp. 3135–3145, 2000.

[118] N. Q. Ngo, "A new approach for the design of wideband digital integrator and differentiator," *IEEE Transactions on Circuits and Systems–II: Express Briefs*, vol. 53, no. 9, pp. 936–940, 2006.

[119] N. Q. Ngo, S. F. Yu, S. C. Tjin, and C. H. Kam, "A new theoretical basis of higher–derivative optical differentiators," *Optics Communications*, vol. 230, no. 1–3, pp. 115–129, 2004.

[120] N. Shrivastava, and A. Trivedi, "Iterative random beamforming for MIMO–OFDM systems," *National Conference on Communications*, Kharagpur, India, 3–5 February 2012, pp. 1–5.

[121] O. Akay, and G. F. B. Bartels, "Fractional convolution and correlation via operator methods and an application to detection of linear FM signals," *IEEE Transactions on Signal Processing*, vol. 49, no. 5, pp. 979–993, 2001.

[122] O. Viano, M. Renfors and T. Saramaki, "Recursive implementation of FIR differentiators with optimum noise attenuation," *IEEE Transactions on Instrumentation and Measurement*, vol. 46, no. 5, pp. 1202–1207, 1997.

[123] R. C. Gonzalez, and R. E. Woods, *Digital Image Processing*. Englewood Cliffs, NJ: Prentice–Hall, 2008.

[124] R. G. Dorsch, A. W. Lohmann, Y. Bitran, D. Mendlovic and H. M. Ozaktas, "Chirp filtering in the fractional Fourier domain," *Applied Optics*, vol. 33, no. 32, pp.7599–7602, 1994.

[125] R. G. Lyons, *Understanding Digital Signal Processing*. Third Edition, Prentice–Hall, 1997.

[126] R. Jacob, T. Thomas, and A. Unnikrishnan, "Applications of fractional Fourier transform in sonar signal processing," *The Institution of Electronics and Telecommunication Engineering (IETE) Journal of Research*, vol. 55, no. 1, pp. 16–27, 2009.

[127] R. Tao, X. M. Li, Y. L. Li, and W. Yue, "Time–delay estimation of chirp signals in the fractional Fourier domain," *IEEE Transactions on Signal Processing*, vol. 57, no. 7, pp. 2852–2855, 2009.

[128] S. A. Elgamel, C. Clemente, and J. J. Soraghan, "Radar matched filtering using the fractional Fourier transform," *Sensor Signal Processing for Defence*, London, 29–30 September 2010, pp. 1–5.

[129] S. C Pei, and M. H. Yeh, Two dimensional discrete fractional Fourier transform, *Signal Processing*, vol. 67, no. 1, pp. 99–108, 1998.

[130] S. C. Dutta Roy, "On the realization of a constant–argument immittance or fractional operator," *IEEE Transactions on Circuit Theory*, vol. 14, no. 3, pp. 264–274, 1967.

[131] S. C. Dutta Roy, and B. Kumar, "Digital Differentiators," in *Handbook of Statistics: Signal Processing and Its Applications*, N. K. Bose and C. R. Rao, Editors North Holland, Amsterdam, The Netherlands: Elsevier, 1993, Chapter 10.

[132] S. C. Pei, and C. C. Tseng, "A new eigenfilter based on total least squares error criterion," *IEEE Transactions on Circuits and Systems–I: Fundamental Theory and Applications*, vol. 48, no. 6, pp. 699–709, 2001.

[133] S. C. Pei, and J. J. Ding, "Closed–form discrete fractional and affine Fourier transforms," *IEEE Transactions on Signal Processing*, vol. 48, no. 5, pp. 1338–1353, 2000.

[134] S. C. Pei, and J. J. Shyu, "Design of FIR Hilbert transformers and differentiators by eigenfilter," *IEEE Transactions on Circuits and Systems*, vol. 35, no. 11, pp. 1457–1461, 1988.

[135] S. C. Pei, and M. H. Yeh, "Improved discrete fractional Fourier transform," *Optics Letters*, vol. 22, no. 14, pp. 1047–1049, 1997.

[136] S. C. Pei, and P. H. Wang, "Closed-form design of maximally flat FIR Hilbert transformers, differentiators, and fractional delayers by power series expansion," *IEEE Transactions on Circuits and Systems–I: Fundamental Theory and Applications*, vol. 48, no. 4, pp. 389–398, 2001.

[137] S. C. Pei, and Y. C. Lai, "Signal scaling by centered discrete dilated Hermite functions," *IEEE Transactions on Signal Processing*, vol. 60, no. 1, pp. 498–503, 2012.

[138] S. C. Pei, C. C. Tseng, and W. S. Yang, "FIR filter designs with linear constraints using the eigenfilter approach," *IEEE Transactions on Circuits and Systems–II: Analog and Digital Signal Processing*, vol. 45, no. 2, pp. 232–237, 1998.

[139] S. C. Pei, C. C. Tseng, M. H. Yeh, and J. J. Shyu, "Discrete fractional Hartley and Fourier transforms," *IEEE Transactions on Circuits and Systems–II: Analog and Digital Signal Processing*, vol. 45, no. 6, pp. 665–675, 1998.

[140] S. Das, and I. Pan, *Fractional Order Signal Processing: Introductory Concepts and Applications*. Springer Briefs in Applied Sciences and Technology, NY: Springer, 2012.

[141] S. E. Dobbs, N. M. Schmitt, and H. S. Ozemek, "QRS detection by template matching using real–time correlation on a microcomputer," *Journal of Clinical Engineering*, vol. 9, no. 3, pp. 197–212, 1984.

[142] S. G. Osgouei, and M. Geravanchizadeh, "Speech enhancement using convex combination of fractional least–mean–squares algorithm," *Fifth International Symposium on Telecommunications*, Tehran, Iran, 4–6 December 2010, pp. 869–872.

[143] S. Ganesan, R. Shah, and A. Agarwal, "Frequency domain real time digital image watermarking," *IEEE International Conference on Electro Information Technology*, Lincoln, Nebraska, 22–25 May 2005, pp. 1–6.

[144] S. M. Salih, *Fourier Transform–Signal Processing*, InTech, 2012.

[145] S. N. Sharma, R. Saxena, and S. C. Saxena, "Tuning of FIR filter transition bandwidth using fractional Fourier transform," *Signal Processing*, vol. 87, no. 12, pp. 3147–3154,

2007.

[146] S. Samadi, M. O. Ahmad, and M. N. S. Swamy, "Exact fractional–order differentiators for polynomial signals," *IEEE Signal Processing Letters*, vol. 11, no. 6, pp. 529–532, 2004.

[147] S. Shinde, and V. M. Gadre, "An uncertainty principle for real signals in the fractional Fourier transform domain," *IEEE Transactions on Signal Processing*, vol. 49, no. 11, pp. 2545–2548, 2001.

[148] S. Sunder, and V. Ramachandran, "Design of equiripple nonrecursive digital differentiators and Hilbert transformers using a weighted least-squares technique," *IEEE Transactions on Signal Processing*, vol. 42, no. 9, pp. 2504–2509, 1994.

[149] S. T. Tzeng, and H. C. Lu, "Genetic algorithm approach for designing higher–order digital differentiators," *Signal Processing*, vol. 79, no. 2, pp. 175–186, 1999.

[150] S. Usui, and I. Amidror, "Digital Low–Pass Differentiation for Biological Signal Processing," *IEEE Transactions on Biomedical Engineering*, vol. 29, no. 10, pp. 686–693, 1982.

[151] T. Odzijewicz, A. B. Malinowska, and D. F. M. Torres, "Fractional variational calculus with classical and combined Caputo derivatives," *Nonlinear Analysis*, vol. 75, no. 3, pp. 1507–1515, 2012.

[152] T. Wysocki, H. Razavi, and B. Honary, *Digital Signal Processing for Communication Systems*. The Springer International Series in Engineering and Computer Science, vol. 403, Springer, 1997.

[153] V. Devabhaktuni, K. Rajasekhar and M. O. Ahmad, "Finding specific RNA sequence motifs using digital filters," *Twenty–fifth IEEE Canadian Conference on Electrical and Computer Engineering*, Montreal, Quebec, 29 April–2 May 2012, pp. 1–4.

[154] V. Namias, "The fractional order Fourier transform and its applications to quantum mechanics," *IMA Journal Applied Mathematics*, vol. 25, no. 3, pp. 241–265, 1980.

[155] W. Burger, and M. J. Burge, *Principles of Digital Image Processing–Fundamental Techniques*. Fundamental Techniques Series: Undergraduate Topics in Computer Science, Springer, 2009.

[156] W. G. Medlin, and J. F. Kaiser, "Bandpass digital differentiator design using quadratic programming," *International Conference on Acoustics, Speech, and Signal Processing*,

vol. 3, Toronto, Ontario, 14–17 May 1991, pp. 1977–1980.

[157] W. Utschick, H. Boche, and R. Mathar, *Robust Signal Processing for Wireless Communications*, Foundations in Signal Processing, Communications and Networking, vol. 2, Springer, 2008.

[158] X. H. Chen, and X. D. Fei, "Improved edge detection algorithm based on fractional differential approach," *International Conference on Image, Vision, and Computing*, vol. 50, Singapore, 2012.

[159] Y. F. Pu, J. L. Zhou and X. Yuan, "Fractional differential mask: a fractional differential–based approach for multiscale texture enhancement," *IEEE Transactions on Image Processing*, vol. 19, no. 2, pp. 491–511, 2010.

[160] Y. Ferdi, J. P. Herbeuval, A. Charef, and B. Boucheham, "R wave detection using fractional digital differentiation," *ITBM–RBM*, vol. 24, no. 5–6, pp. 273–280, 2003.

[161] Y. H. Ha, and J. A. Pearce, "A new window and comparison to standard windows," *IEEE Transactions on Acoustics, Speech and Signal Processing*, vol. 37, no. 2, pp. 298–301, 1989.

[162] Y. Li, J. Lu, and Y. Wang, "A novel chirp based modulation and detection scheme using fractional Fourier transform," *First International Conference on Wireless Communication, Vehicular Technology, Information Theory and Aerospace and Electronic Systems Technology*, Aalborg, Denmark, 17–20 May 2009, pp. 872–874.

[163] Z. Gan, and H. Yang, "Texture enhancement through multiscale mask based on RL fractional differential," *International Conference on Information, Networking and Automation*, vol. 1, Kunming, China, 18–19 October 2010, pp. 333–337.

[164] Z. U. Sheikh, A. Eghbali, and H. Johansson, "Linear–phase FIR digital differentiator order estimation," *Twentieth European Conference on Circuit Theory and Design*, Linköping, Sweden, 29–31 August 2011, pp. 310–313.

VITA

SANJAY KUMAR was born in Dehradun, Uttarakhand, India, in 1981. He received the B.E. degree in Electronics and Communication Engineering from Meerut University, Meerut, India, in 2003, and the M.Tech. degree in VLSI Design from Thapar University, Patiala, Punjab, India, in 2009. He is currently working towards the Ph.D. degree in the Department of Electronics and Communication Engineering, Thapar University, Patiala, Punjab, India. He has worked as Scientist with Indian Space Research Organization (ISRO), Bangalore, India, working toward India's Moon Mission "Chandrayaan—I" before joining Thapar University as an Assistant Professor in the Department of Electronics and Communication Engineering. His current research interests include fractional order transforms, signal processing, implementation and application of fractional order circuits, orthogonal polynomials, and radar signal processing. He has published research papers in peer–reviewed international journals and international conferences. He has in his credit an *h*–index of 2 and an *i*–10 index of 1, since 2009. His email–ID is: er.sanjaykumar@gmail.com and sanjay.kumar@thapar.edu. His google scholar profile is by the name Sanjay Kumar (Shri Hari).

हरे कृष्ण हरे कृष्ण, कृष्ण कृष्ण हरे हरे !
हरे राम हरे राम, राम राम हरे हरे !!

सर्वधर्मान्परित्यज्य मामेकं शरणं व्रज ।
अहं त्वां सर्वपापेभ्यो मोक्षयिष्यामि मा शुचः ॥१८- ६६॥

Relinquishing everything else and all ideas of righteousness surrender unto me (Krishna) exclusively.

I (Krishna) will deliver you from all sins (sinful reactions), do not despair.
[Gītā 18/66]